Role of Human Fractalkine Receptor Variant in Mouse Brain Development

by

Sana Bibi

A thesis submitted in partial fulfillment of the requirements for the degree of

Master of Science

Medical Sciences - Medical Genetics

University of Alberta

Abstract

Multiple sclerosis (MS) is a degenerative disorder of the central nervous system that is triggered in genetically predisposed individuals by environmental insults. In MS, the body's own immune cells attack and damage myelin and the myelin-producing cells, oligodendrocytes. Genetic factors contribute to both the triggers (susceptibility risk) and drivers (severity risk) of MS. Genetic variants associated with MS severity cluster into the central nervous system development category. However, to date, there are no functional studies on MS severity risk genetic variants in central nervous system development. C-X3-C motif chemokine receptor 1 (CX3CR1), a receptor for chemokine fractalkine (FKN), variants are associated with MS severity. Our lab has shown that FKN-CX3CR1 signaling is important for developmental oligodendrocyte formation. However, whether MS-associated CX3CR1 variants affect brain development and function is unknown.

To address this knowledge gap, I analyze brains from developing and adult mice that express human MS-associated CX3CR1$^{I249/M280}$ variant in place of the mouse CX3CR1. These mice are compared to wild type and CX3CR1 knockout (KO) mice. This study shows that in comparison to WT mice, CX3CR1$^{I249/M280}$ variant brains display i) decreased myelin protein abundance and proportion of oligodendrocytes; ii) altered astrocytes; iii) increased activation of microglia (brain immune cells); and iv) aberrant levels of cytokines. Finally, the CX3CR1$^{I249/M280}$ variant mice exhibit aberrant behaviour in adulthood, such as increased anxiety.

In summary, I show that mice expressing the MS-associated human CX3CR1 variant have delayed myelination and aberrant immune environment during CNS development. These transient developmental defects may lead to aberrant brain function in adulthood. These results suggest that

individuals with MS-associated variants may display aberrant brain development, which may contribute to mechanisms of neurodegeneration later in life.

Preface

This thesis is an original work by Sana Bibi. The research project, of which this thesis is a part, received ethics approval from the University of Alberta Research Ethics Board, Project Name "Molecular mechanisms of brain development and regeneration", No. AUP00002527, 2018. This project approval was for the duration of all thesis work and beyond.

Western blot experiments (Fig. 1) were performed in collaboration with Tim Footz. *In vitro* experiments (Fig. 8) were all performed in collaboration with Dr. Monique Marylin Alves de Almeida. All behavioral data presented in Fig. 12 were generated by Yana Kibalnyk.

Acknowledgments

I would like to express my sincere gratitude to all those who have supported me throughout my academic journey, including the completion of this thesis.

First and foremost, I am deeply grateful to my supervisor, Dr. Anastassia Voronova, for providing me with the opportunity to work in her lab where I have had the privilege to grow both academically and personally. Her guidance and unwavering support have been instrumental in shaping the direction and quality of my research. I am truly fortunate to have had her mentorship. I would also like to thank the current and past Voronova lab members for supporting me with my project, especially, Yana Kibalnyk, Monique Marylin Alves de Almeida, and Tim Footz for their contributions to my thesis. Thank you to Adrianne Watson for editing and providing feedback on my writing.

I also want to thank Dr. Bradley J Kerr and Dr. Qiumin Tan for serving as my committee members and for providing feedback and insight to guide my project.

I am grateful to MatCH program and MS Canada (endMS Master's Studentship Award) for providing me with financial assistance, which allowed me to pursue my research.

Thank you to Dr. Astrid E. Cardona from the University of Texas at San Antonio, USA for giving us the hCX3CR1$^{I249/M280}$ (hM280) mice. Thank you to Dr. Qiumin Tan for access to behaviour equipment and Dr. Sarah Hughes for access to confocal microscope. Also, I want to thank the support staff at HSLAS and the department of Medical Genetics at the University of Alberta for their assistance throughout my degree.

And finally, I would like to thank my family and friends, especially my mom, for supporting me throughout my journey.

Table of Contents

List of Figures

List of Abbreviations

AD	Alzheimer's disease
AEP	Entopeduncular area
ALDH1L1	Aldehyde dehydrogenase family 1, member L1
ALS	Amyotrophic lateral sclerosis
AP-1	Activator protein
Arg1	Arginase 1
BBB	Blood-brain barrier
BMP	Bone morphogenetic proteins
BrdU	5-Bromo-2'-deoxyuridine
CA	Cornu ammonis
CC	Corpus callosum
CC1	Adenomatous polyposis coli
CC3	Cleaved caspase-3
CD16/32	Fc gamma III and II receptors
CFTR	Cystic fibrosis transmembrane conductance regulator
CGE	Caudal ganglionic eminence
CH	Cortical hem
CLC	Cardiotrophin-like cytokine
CNPase	2',3'-cyclic-nucleotide 3'-phosphodiesterase
CNS	Central nervous system
CNTF	Ciliary neurotrophic factor
CP	Cortical plate
CPZ	Cuprizone
CREB	cAMP response element-binding protein
CSF	Colony stimulating factor-1
CSF-1R	Colony stimulating factor-1 receptor
CT-1	Cardiotrophin-1
CX3CL1	Fractalkine ligand
CX3CR1	C-X3-C motif chemokine receptor 1
DG	Dentate gyrus
E	Embryonic day
EAE	Experimental autoimmune encephalomyelitis
EBV	Epstein Barr Virus
EC	Entorhinal cortex
EDSS	Expanded Disability Status Scale
EdU	5-ethynyl-2'-deoxyuridine
ELISA	Enzyme-linked immunoassay
EPM	Elevated plus maze
FTD	Frontotemporal dementia
FKN	Fractalkine ligand
GABA	gamma-aminobutyric acid

GalC	Galacto cerebroside
GAPDH	Glyceraldehyde-3-phosphate dehydrogenase
GDNF	Glial-derived neurotrophic factor
GFAP	Glial fibrillary acidic protein
GLAST	astrocyte-specific glutamate transporter
GM	Grey matter
GPCR	G-protein coupled receptors
GWAS	Genome Wide Association Studies
HD	Huntington's disease
hM280	$CX3CR1^{I249/M280}$
HPC	Hippocampus
IBA1	Ionized calcium-binding adapter molecule 1
ICC	Immunocytochemistry
IFN-β	Interferon beta
IFNγ	Interferon gamma
IHC	Immunohistochemistry
IL	Interleukin
IZ	Intermediate zone
KO	Knockout, $CX3CR1^{fl/fl}$
LGE	Lateral ganglionic eminence
LIF	Leukemia inhibitory factor
MAG	Myelin associated glycoprotein
MAZ	Multipolar cell accumulation zone
MBP	Myelin basic protein
MCP-1	Monocyte chemoattractant protein-1, CCL2
MFI	Mean fluorescence intensity
MGE	Medial ganglionic eminence
MHC	Major histocompatibility complex
MIP-1α	Macrophage inflammatory protein 1 alpha, CCL3
MOG	Myelin-oligodendrocyte glycoprotein
MS	Multiple sclerosis
MZ	Marginal zone
NF-κB	Nuclear factor kappa-light-chain-enhancer of activated B cells
NFL	Neurofilament light chain
NG2	Proteoglycan neural-glia antigen 2
NP	Neuropoietin
NPC	Neural progenitor cell
Nrp1	Neuropilin-1
Nrtn	Neurturin
OFT	Open field test

Olig1/2	Oligodendrocyte lineage transcription factor 1/2
OPC	Oligodendrocyte progenitor cell
OSM	Oncostatin M
P	Postnatal day
PAP	Perisynaptic astrocytic process
PAX6	paired box protein 6
PD	Parkinson's disease
PDGFRα	Latelet-derived growth factor receptor alpha
PPMS	Primary progressive MS
ROS	Reactive oxygen species
RGC	Radial glia progenitor cell
PCR	Polymerase chain reaction
PLP	Proteolipid protein
P2YR12	Purinergic receptor
SDF-1	Stromal cell-derived factor 1, CXCL12
SGZ	Subgranular zone
SLM	Stratum lacunosum-moleculare
SOX2	SRY-box transcription factor 2
SP	Subplate
SPMS	Secondary progressive MS
STAT	Signal transducer and activator of transcription
SVZ	Subventricular zone
TGF-β	Transforming growth factor beta
TI	Transformation index
TMEM119	Transmembrane protein 119
TNFα	Tumor necrosis factor alpha
UVB	Ultraviolet B light
VD	Vascular dementia
VEGF	Vascular endothelial growth factor
VZ	Ventricular zone
WT	Wild type

1 Introduction

1.1 How the mouse brain develops

1.1.1 Neural progenitor cells (NPCs)

During mouse embryogenesis, a flat layer of ectodermal origin cells called neuroepithelial cells fold and begin to fuse anteriorly by ~embryonic day (E) 9 to form a structure called the neural tube (reviewed in: (Adnani et al., 2018)). During this process, the neuroepithelial cells undergo proliferation, elongation, apicobasal polarization, and apical constriction via the formation of tight junctions. The neuroepithelial cells give rise to a population of neural progenitor cells (NPCs) called radial glia progenitor cells (RGCs) that line the neural tube (Jinnou et al., 2018; Kriegstein and Alvarez-Buylla, 2009; Levitt and Rakic, 1980; Zhao and Moore, 2018). These NPCs express markers such as nestin, SRY-box transcription factor 2 (SOX2), vimentin, paired box protein 6 (PAX6), glial fibrillary acidic protein (GFAP), and astrocyte-specific glutamate transporter (GLAST) (reviewed in: (Adnani et al., 2018)).

Stem cells are able to self-renew and differentiate to give rise to other cell types with specific functions (Li and Zhao, 2008; Ramalho-Santos and Willenbring, 2007). NPCs are stem cells that undergo both symmetric division to increase the NPC pool and asymmetric division to give rise to intermediate progenitors cells or neurons directly (Zhao and Moore, 2018). The intermediate progenitors can differentiate and give rise to neurons or continue to proliferate, although they have limited proliferative potential compared to NPCs. In addition, NPCs generate macroglia (astrocytes and oligodendrocytes) by first giving rise to glial progenitor and oligodendrocyte progenitor cells (OPCs). NPC differentiation is tightly controlled in a spatial and temporal fashion (Miller and Gauthier, 2007; Okano and Temple, 2009; Temple, 2001).

The anterior folded neural tube divides into three distinct regions called prosencephalon, mesencephalon and rhombencephalon that gives rise to the forebrain, midbrain, and hindbrain, respectively (reviewed in: (Adnani et al., 2018)). The forebrain includes the cerebral cortex, corpus callosum, hippocampus, thalamus, and hypothalamus. The midbrain forms the colliculi, tegmentum, and cerebral peduncles while the hindbrain gives rise to the pons, cerebellum, and

medulla. The prosencephalon further divides into the distinct regions called telencephalon and diencephalon. The telencephalon is further organized in a dorsoventral axis such that the dorsal (top, pallium) region will give rise to cortical structures like the cerebral cortex and the hippocampus while the ventral (bottom, subpallium) region ultimately gives rise to other structures like the basal ganglia (Dale et al., 1997). However, during development, the ventral telencephalon forms transient germinal zones called the medial, caudal and lateral ganglionic eminences (MGE, CGE, and LGE, respectively) (reviewed in: (Bandler et al., 2017)). The ganglionic eminences are proliferative zones, which give rise to interneurons that migrate to various regions in the brain. For example, the MGE and CGE both produce interneurons that travel tangentially in the cortex and hippocampus. The cerebral cortex has six distinct neuronal layers that are formed by NPCs in the ventricular zone (VZ) and subventricular zone (SVZ) in a sequential manner as described in section 1.1.2 below.

A small pool of embryonic NPCs divide more slowly and are set aside at around embryonic day (E) 15 to generate two adult neural stem cell pools in specific niches: the subventricular zone (SVZ) of the lateral ventricles that can give rise to all three neural cell types, and the subgranular zone (SGZ) of the dentate gyrus (DG) of the hippocampus, which can give rise to neurons and astrocytes throughout lifetime (Doetsch, 2003; Göritz and Frisén, 2012; Kempermann et al., 2015).

1.1.2 Neurogenesis

During early murine embryonic cortical neurogenesis, NPCs occupy the layer directly adjacent to the ventricle called the VZ. As proliferation continues, a second layer is formed above the VZ called the SVZ (Angevine et al., 1970; Bayer and Altman, 1991). The NPCs in the cortical VZ and SVZ give rise to excitatory neurons that form the cortex layers in a sequential manner from E11.5 to E17.5 in mice (Angevine and Sidman, 1961; Caviness and Takahashi, 1995; Rakic, 1974). The neurons migrate both radially and tangentially to form the different layers of the cortex (Angevine and Sidman, 1961; Rakic, 1972). Specifically, the VZ and SVZ first give rise to a layer of neurons called the pre-plate, which is divided into the marginal zone (MZ, becomes layer 1 later on) on top and subplate (SP) at the bottom (Bayer and Altman, 1991). A new layer called the cortical plate (CP) appears between the MZ and SP. Newly differentiated

neurons from the VZ and SVZ migrate to the CP to form the six layers of the neocortex in an "inside-first outside-last" fashion (Angevine and Sidman, 1961; Molyneaux et al., 2007; Rakic, 1974). This means that the deeper layers, such as layer five and six are formed before the outer layers two to four, and the latter neurons must migrate past the deeper layers in the CP (MuhChyi et al., 2013). While cortical NPCs generate these excitatory glutamatergic projection neurons, inhibitory gamma-aminobutyric acid (GABA)ergic interneurons are formed by progenitors in the transient ganglionic eminences of the ventral telencephalon that travel tangentially into the cortex (described in section 1.1.1 above and reviewed in: (Adnani et al., 2018; Shin et al., 2019)). Moreover, interneurons that arrive at the intermediate zone (IZ) via tangential migration will then move tangentially or radially towards cortical plate or SVZ region (Yokota et al., 2007).

The excitatory cortical neurons secrete factors that regulate neurogenesis and astrogliogenesis in the developing mouse brain. Cortical neurons secrete factors such as glial-derived neurotrophic factor (GDNF), neurturin (Nrtn), and interferon gamma (IFNγ) that promote the differentiation of NPCs into neurons (Yuzwa et al., 2016). Previous research shows that both intrinsic and extrinsic factors regulate NPC switch from neurogenesis to astrogliogenesis. The cell-intrinsic mechanisms found that overtime, the NPCs become less biased towards producing neurons and switch over to astrocyte production, which is prompted by internal signals like expression of a key transcription factor or key receptor gene, or even an epigenetic change like demethylation of a key promoter (Barnabe-Heider et al., 2005). Other studies found that NPCs are competent at producing glia; however, they require an external signal such as cytokines to switch to astrogliogenesis. Various studies found that the gp130 cytokine family (also called interleukin-6 [IL-6] family), including leukemia inhibitory factor (LIF), ciliary neurotrophic factor (CNTF), and cardiotrophin-1 (CT-1), induce NPCs to produce astrocytes (reviewed in: (Barnabe-Heider et al., 2005; Miller and Gauthier, 2007)). Specifically, newly-formed neurons secrete CT-1, which provides feedback to NPCs to start making astrocytes at ~E18 (Barnabe-Heider et al., 2005). Similar to excitatory neuronal regulation of gliogenesis, migrating interneurons regulate oligodendrocyte progenitor cell (OPC) generation from NPCs by secreting a chemokine called fractalkine (CX3CL1) (Voronova et al., 2017).

During embryogenesis, the hippocampus develops on the caudomedial side of the dorsal telencephalon (Pang et al., 2019). At E12.5, the cortical hem (CH) is formed at the medial border

of the pallium and secretes morphogens such as bone morphogenetic proteins (BMPs) and WNTs (Furuta et al., 1997). These signaling molecules induce the hippocampal formation in the medial pallium beginning with the appearance of the dentate gyrus and hippocampal neuroepithelium at E13.5-14.5 (Pang et al., 2019). By P0, the hippocampal formation folds into an "S shape" and is patterned into the dentate gyrus, cornu ammonis 1-3 (CA1-3), and the subiculum (Chauhan et al., 2021). Pyramidal neurons that occupy CA1 region are generated by the VZ at E12-16 and they migrate to the hippocampal multipolar cell accumulation zone (MAZ) where they transform into multipolar cells with multiple processes (Kitazawa et al., 2014). Late forming (E14-16) CA1 pyramidal neurons transform into bipolar cells in the MAZ that migrate in a zig-zag manner (termed "climbing mode") towards the hippocampal plate that later becomes the stratum pyramidal (layer in the CA1 region). In adulthood, NPC of glutamatergic neurons in the dentate gyrus migrate tangentially along blood vessels, followed by radial migration (Sun et al., 2015).

Neurogenesis in the hippocampus varies by regions: neurons in the CA regions are generated embryonically until birth while neurons in the dentate gyrus (DG) continue to be formed postnatally (Angevine, 1965). A more recent study used 5-ethynyl-2'-deoxyuridine (EdU) birth-dating and confirmed that neurons are generated embryonically with a peak at E15.5 (~9% of neurons are EdU-labeled by P30 when EdU is injected at E15.5) in the CA regions of the hippocampus while DG neurogenesis continues postnatally with a peak at P1 (~6% of neurons are EdU-labeled by P30) (Bond et al., 2020). These proportions of EdU+ neurons were significant as they were the highest obtained in each respective region. In addition, the DG maintains SGZ NPCs that continue to generate neurons in adulthood (reviewed in: (Bond et al., 2015)).

The hippocampus plays a role in memory processing, learning and navigation as well as emotional integration. The hippocampus receives inputs from the rest of the brain via the entorhinal cortex (EC) which projects axons from layer II and III onto all subfields including the dentate gyrus (Witter et al., 2000). The major output of the hippocampus occurs via CA1 projecting to the subiculum (region between the CA1 and EC) and layer V of EC. From layer V, the information is sent to the appropriate structures in the rest of the brain. Specifically, a layer above the dentate gyrus called the stratum lacunosum-moleculare (SLM) acts as a connecting hub between the hippocampus and EC (Chauhan et al., 2021). The hippocampus and cortex are

affected in several neurodegenerative diseases. These include Alzheimer's disease (AD) (Frisoni et al., 1999; Laakso et al., 2000; Sampath et al., 2017), Parkinson's disease (PD) (Connolly and Fox, 2014), Huntington's disease (HD) (Ransome et al., 2012), multiple sclerosis (MS) (Prakash et al., 2019), vascular dementia (VD) (Zhu et al., 2021), frontotemporal dementia (FTD) (Frisoni et al., 1999; Laakso et al., 2000), and amyotrophic lateral sclerosis (ALS) (Beeldman et al., 2015; Christidi et al., 2018).

1.1.3 Astrogliogenesis

After neurogenesis is completed in the developing cortex, NPCs in the VZ and SVZ region begin gliogenesis at E18 by first generating glial progenitor cells, which differentiate into astrocytes (Bayraktar et al., 2015; Burns et al., 2009; Su Akdemir et al., 2020). In addition, terminally differentiated astrocytes in the cortex can also symmetrically divide to expand the pool of astrocytes in the mouse postnatal brain (Burns et al., 2009; Moroni et al., 2018). This proliferative capacity is unique to astrocytes as terminally differentiated neurons and oligodendrocytes do not proliferate (Caviness and Sidman, 1973; Mori and Leblond, 1970). In contrast, astrocytes generated post-natally by SVZ NPCs are postmitotic with no proliferative capacity (Sohn et al., 2015). In the hippocampus, GFAP-positive astrocytes proliferation peaks at P8-16 in rats, reaching peak numbers in specific regions of the hippocampus, such as in the stratum lacunosum-moleculare by about P14 (Nixdorf-Bergweiler et al., 1994). Another study looked at astrogenesis in the mouse hippocampus by injecting the thymidine analogue, 5-ethynyl-2′-deoxyuridine (EdU), at various developmental time points and analyzing EdU+ astrocytes at P30 (Bond et al., 2020). They found that astrocytes in the mouse hippocampus are generated starting on embryonic day 17.5, but most are generated during the first postnatal week. Moreover, they discovered temporal dynamics of astrocyte generation by subregions, for example, astrocytes are generated from E17.5 to P5 and E17.5 to P3 in the stratum oriens and stratum lacunosum-moleculare, respectively.

Astrocyte morphology changes with age and it also differs by region. Astrocytes have two main subtypes identified via their region in the brain: protoplasmic astrocytes found in the gray matter and fibrous astrocytes located in the white matter tract (Ben Haim and Rowitch, 2016). Protoplasmic astrocytes have radial morphology and develop small distal processes called

perisynaptic astrocytic process (PAPs) (Su Akdemir et al., 2020). These PAPs contact neural synapses as well as form direct contact with blood vessels. Fibrous astrocytes have a more elongated morphology and form contacts with oligodendrocytes and myelinated axons at nodes of Ranvier (Ben Haim and Rowitch, 2016). In contrast to spatial organization, astrocyte morphology matures in the hippocampus starting from a smaller, overlapping, less ramified state in early post-natal age to more ramified astrocytes that do not overlap with neighboring cells by post-natal day 28 in rats (Bushong et al., 2004). Mature astrocytes can be identified by markers like GFAP, S100b, aldehyde dehydrogenase family 1, member L1 (ALDH1L1), GLAST, (Raponi et al., 2015). Notably, NPCs also express molecules that are characteristic of astrocytes, such as GFAP and GLAST at the onset of neurogenesis (Kriegstein and Götz, 2003). For example, using transgenically targeted cell fate mapping, a study found that all neuroblasts and neurons generated in the adult mouse forebrain are derived from NPCs that express GFAP (Garcia et al., 2004).

Astrocytes are the largest glial population in the CNS, making up 20-40% of the total glial cells that play a role in homeostasis (Herculano-Houzel, 2014). Their end-feet structures play a role in regulating blood flow, and amino acid and neurotransmitter uptake by neurons (Eroglu and Barres, 2010; Su Akdemir et al., 2020). They constantly monitor synapses via synaptic receptors and respond to changes by secreting neuroactive molecules (Allen and Eroglu, 2017; Eroglu and Barres, 2010).

1.1.4 Oligodendrogenesis

NPCs produce oligodendrocytes in the CNS via OPCs. The multipotent NPCs in the VZ produce OPCs in three waves during mouse development, each from a distinct region (Cai et al., 2005; Fogarty et al., 2005; Kessaris et al., 2006; Pringle and Richardson, 1993; Vallstedt et al., 2005; Warf et al., 1991). First, *Nkx2.1*-expressing NPCs in the MGE and entopeduncular area (AEP) begin giving rise to OPCs that travel tangentially into the cortex, arriving by E15 (Kessaris et al., 2006). Next, *Gsh2*-expressing precursor in the caudal and lateral ganglionic eminences (LGE-CGE) gives rise to OPCs at E15.5 that migrate into the rest of the brain. Lastly, *Emx1*-expressing NPCs in the cortical VZ produce a third wave of OPCs at postnatal day (P) 0, that continue to proliferate rapidly. Notably, the *Nkx2.1*-derived OPCs decline after birth and are

eliminated by P10. As the newly formed OPCs migrate, their self-repulsion towards other OPCs allows them to occupy the brain in a uniform fashion.

OPCs either differentiate into oligodendrocytes around P15 or remain as OPCs into adulthood and populate the entire brain tissue (Kessaris et al., 2006). In adulthood, the cortex contains similar proportion of *Gsh2* and *Emx1*-derived OPCs; however, the *Emx1*-derived OPCs are mostly restricted to the dorsal brain. The OPCs in the hippocampus are mainly *Emx1*-derived. OPCs have high proliferative capacity, have bipolar morphology and remain in the CNS throughout life (Clayton and Tesar, 2021; Pfeiffer et al., 1993). Studies show that cell-to-cell interaction with inhibitory neurons, astrocytes and microglia support density and survival of OPCs in the brain (Balia et al., 2017; Hughes and Stockton, 2021). In addition, adult SVZ NPCs continue to be a source for generating oligodendrocytes in adulthood (Aguirre and Gallo, 2007; Delgado et al., 2021; Jablonska et al., 2010; Levison and Goldman, 1993; Menn et al., 2006; Moshinsky, 1994; Nait-Oumesmar et al., 1999; Picard-Riera et al., 2002; Xing et al., 2014).

OPCs express markers such as the proteoglycan neural-glia antigen 2 (NG2), platelet-derived growth factor receptor alpha (PDGFRα) and oligodendrocyte lineage transcription factor (Olig1/2) (Kuhn et al., 2019; Lin and Bergles, 2002; Nishiyama et al., 1999, 1997, 1996; Zhu et al., 2014). Following birth, OPCs gradually differentiate into immature oligodendrocytes that have not started producing myelin yet (Butts et al., 2008; Hughes and Stockton, 2021). These intermediate cells continue to mature into post-mitotic oligodendrocytes that myelinate axons in the CNS. Mature, myelinating oligodendrocytes are present in the murine brain after ~2 post-natal weeks and the process continues until ~6 post-natal weeks when most oligodendrocytes are formed (Barres et al., 1992; McCarthy and Leblond, 1988; Tripathi et al., 2017). Moreover, oligodendrocytes are actively replaced in specific regions of the brain throughout life, such as in the optic nerve (Zhi et al., 2023).

Oligodendrocyte apoptosis during early brain development is a known process that occurs to ensure that the number of oligodendrocytes match the number of axons that need to be myelinated (reviewed in: (Simons and Nave, 2016)). Initially, oligodendrocytes are produced in excess, and some are later eliminated by apoptosis. For example, 50% of oligodendrocytes die in the developing (P8 to P12) rat optic nerve (Barres et al., 1992). Another study found that between

P7 and P21, approximately 20% of premyelinating oligodendrocytes in the cerebral cortex were degenerating (Trapp et al., 1997).

However, not all OPCs differentiate into mature oligodendrocytes. Recent studies have discovered that OPCs are a heterogenous population and they are involved in other roles besides myelination, such as the fine-tuning of neural circuits (Xiao et al., 2022). In addition, OPCs in adulthood respond to cellular signals by migrating, proliferating, and differentiating into mature oligodendrocytes that remyelinate in response to myelin injury (Carroll et al., 1998; Gensert and Goldman, 1997; Göttle et al., 2019; Kuhn et al., 2019; Tepavčević and Lubetzki, 2022).

In the postnatal murine brain, oligodendrocytes myelinate axons by making contacts with neuron membranes using their processes (reviewed in: (Gil and Gama, 2022; Simons and Nave, 2016)). To initiate myelination, the cells undergo a stabilization period where myelin sheaths are either elongated or retracted (Stadelmann et al., 2019). Once the contact is stabilized, lipids and proteins are delivered to the growing myelin sheath (Nave and Werner, 2014). Each oligodendrocyte can myelinate multiple axons in the CNS.

Mature, myelinating oligodendrocytes are post-mitotic and can be identified by the presence of proteins such as proteolipid protein (PLP), 2',3'-cyclic-nucleotide 3'-phosphodiesterase (CNPase), myelin basic protein (MBP), myelin associated glycoprotein (MAG), myelin-oligodendrocyte glycoprotein (MOG), galacto cerebroside (GalC) in addition to a cell linage transcription factor like Olig2 (Bhat et al., 1996; Kuhn et al., 2019; Scherer et al., 1994). Myelinating oligodendrocytes wrap myelin sheaths, which are composed of lipids and proteins including MBP, CNPase, and PLP, around axons. Myelin sheaths are not continuous along the entirety of axons, but are interspersed with unmyelinated gaps called nodes of Ranvier that are enriched in ion channels ((Huxley and Stampfli, 1949), reviewed in: (Rasband and Peles, 2021)). Myelination and nodes of Ranvier allow the signal to propagate in a fast manner, where electrical signals "jump" from node to node. Myelin also serves an additional role, where myelin sheaths form a tight barrier between the axon and the surrounding nutrient-rich environment to prevent ion leakage (Stadelmann et al., 2019). Therefore, oligodendrocytes also provide metabolic support to neurons via cytoplasmic channels and transport proteins. Astrocytes may also support this metabolic coupling by transferring metabolites to oligodendrocytes via gap junctions (Stadelmann et al., 2019).

1.1.5 Microglia development

Unlike neurons and macroglia (astrocytes and oligodendrocytes), microglia are derived from a different pool of cells. Microglia have a hemopoietic origin and display macrophage markers (Gordon et al., 1992; Lawson et al., 1990; Perry et al., 1985). As well, an *in vitro* experiment showed that microglial progenitors from both embryonic and adult mouse brains have high proliferative capacity (Alliot et al., 1991). Microglia progenitors expressing hematopoietic markers migrate from the yolk sac to the brain via blood vessels between E8.5 and E9.5 (Alliot et al., 1999; Ginhoux et al., 2010). There, these progenitors proliferate and give rise to microglia cells which are maintained throughout life without further contribution from hematopoietic progenitors (Ajami et al., 2007). During embryonic development, the microglia pool expands rapidly; however, they comprise only 1.7% of all brain cells by E18. After birth, microglia proliferate further and account for 10% of all brain cells (Alliot et al., 1999; Gordon et al., 1992; Lawson et al., 1990). Therefore, the majority of microglia cells are born postnatally during the first two weeks of murine development (Alliot et al., 1999; Cossmann et al., 1997).

Previously, it was known that colony stimulating factor-1 (CSF-1) and its receptor (CSF-1R) are responsible for the differentiation of most macrophage populations in adult mice (Chitu and Stanley, 2006). Ginhoux et al. 2010 discovered that CSF-1R was also expressed on yolk sac macrophages and microglia at E9.5 and that their development is dependent on this receptor (Ginhoux et al., 2010). On the contrary, circulating monocyte numbers are not affected by the absence of CSF-1R. Microglia in the murine brain can be labeled with antibodies against cytoplasmic protein marker like ionized calcium-binding adapter molecule 1 (IBA1) that plays a role in phagocytosis, and surface protein markers like purinergic receptor (P2YR12) that plays a role in chemotaxis, transmembrane protein 119 (TMEM119), or CSF-1R (Paolicelli et al., 2022).

As the resident CNS macrophage, microglia continuously survey their environment for foreign material, such as pathogens (Gosselin et al., 2017, 2014; Lavin et al., 2014; Matcovitch-Natan et al., 2016). Microglia play a role in brain homeostasis as well as in host defense against pathogens and in neurodegenerative diseases (El Khoury et al., 2007). In the adult brain during homeostasis, microglia are highly dynamic while surveying their environment and rapidly become activated in response to injury (Nimmerjahn et al., 2005). They sense the environment

via receptors and signaling molecules called the sensome (Hickman et al., 2013). Microglia exhibit plasticity and can be neuroprotective or neurotoxic. For example, in advanced stages of several neurological disorders such as AD, MS, and ALS, microglia takes on a neurotoxic phenotype (Block et al., 2007; Gomes-Leal, 2012; Hickman et al., 2008; Liao et al., 2012; Muzio et al., 2007). Microglia exist on a spectrum between pro-inflammatory (formally classified as M1) and alternatively activated microglia (formally classified as M2) (Michelucci et al., 2009; Paolicelli et al., 2022). Pro-inflammatory microglia secrete reactive oxygen species (ROS) and proinflammatory cytokines, whereas alternatively activated microglia secrete anti-inflammatory cytokines and molecules that promote OPC differentiation into oligodendrocytes (Miron, 2017; Miron et al., 2013). Pro-inflammatory microglia can be identified by markers such as CD16/32 and alternatively activated microglia can marked with arginase 1 (Arg1) (Raes et al., 2002).

Microglia play roles in various processes during development such as refining synaptic networks (Fields et al., 2014; Schafer et al., 2012; Tremblay et al., 2011; Wake et al., 2009), promoting of and the removal of developmental apoptotic cells (Wakselman et al., 2008), positioning neurons in the developing cortex (Hoshiko et al., 2012), and the secretion of growth factors for neuronal survival (Ueno et al., 2013). In the adult brain, microglia continue to monitor synapses and secrete neuromodulatory factors that support synaptic plasticity and learning (Parkhurst et al., 2013).

1.1.6 Crosstalk between microglia and oligodendrocyte progenitor cells (OPCs)

Microglia interact with OPCs during development and in adulthood, resulting in proper myelination of the CNS. For example, alternatively activated microglia that secrete anti-inflammatory cytokines appear at the start of remyelination and are essential for efficient CNS myelin regeneration (Miron et al., 2013). During murine development, ameboid microglia contact and phagocytose viable OPCs at ~P7 that express pre-myelinating stage markers of maturation (Nemes-Baran et al., 2020). In CX3CR1 knockout (KO) mice, microglia do not engulf these OPCs, leading to thinner myelin at P30. Moreover, the presence of neuropilin-1 (Nrp1) receptor on microglia in the corpus callosum promotes OPC proliferation during development as well as OPC response to CNS demyelination (Sherafat et al., 2021). This shows the importance of microglia-OPC interactions in myelination. In multiple sclerosis, microglia have been associated

with inflammation and negative effects on oligodendrocyte production in demyelinating lesions (Heß et al., 2020; Lassmann, 2014). Moreover, phagocytosis of myelin debris by microglia is essential for remyelination after cuprizone induced demyelination in mice (Lampron et al., 2015).

1.2 Multiple Sclerosis (MS)

1.2.1 What is MS?

Multiple sclerosis (MS) is a chronic neuroinflammatory and neurodegenerative disease of the CNS (Cotsapas et al., 2012). MS is highly prevalent in Canada with about 77,000 individuals living with the disease. In MS, the protective myelin sheath around nerve axons is damaged. This is done via two main pathways: 1) immune cell recruitment to the CNS that attacks the myelin and myelin-producing cells oligodendrocytes causing inflammation and demyelination (Karussis, 2014; Trapp et al., 1998); and 2) the inability of the CNS to replace the damaged myelin. More specifically, the infiltrating immune cells targeting myelin in the CNS cause an acute inflammatory, demyelinating lesion which can occur in both the white matter (Raine, 1994) and gray matter (Geurts et al., 2005).

Four main categories of MS lesions have been identified based on histopathology: (1) early active; (2) chronic active; (3) inactive and (4) remyelinated shadow plaques [reviewed in: (Calvi et al., 2022; Frohman et al., 2006)]. Early active lesions appear in the beginning stage of MS diagnosis, which are identified by the loss of myelin and oligodendrocytes, axonal damage, hypertrophic astrocytes, lymphocytes, and the presence of myelin in macrophages. Chronic active lesions are similar to an early active lesion around the border regarding the cellular activity, and expansion of the demyelinated region; however, they have an inactive, hypocellular center with naked axons. Inactive lesions do not have ongoing degradation of myelin at the their border and they show a decrease in the number of immune cell infiltration (Kornek et al., 2000). In contrast, remyelinated shadow plaques are identified by the thin myelin, although some inflammation remains in both of the latter lesions.

MS is a dynamic disease with heterogenous demyelinating lesions that appear unpredictably, for example, new lesions may appear in both acute and chronic cases (Frohman et

al., 2006). However, as the disease progresses, a hallmark is the appearance of the silent lesions without the presence of active inflammation.

Ultimately, demyelination affects the axons and leads to their degeneration that disrupts neuronal signaling and communication, leading to motor, cognitive, and/or neuropsychiatric decline in patients (Niino, 2016). There are two major stages of MS disease: relapsing remitting MS (RRMS) and secondary or primary progressive MS (SPMS and PPMS) (Ghasemi et al., 2017). RRMS is characterized by sudden attacks on the CNS followed by recovery. People with RRMS usually develop SPMS later in life, which is characterized by a steady increase in severity of symptoms. In contrast, PPMS is more severe with rapid decline and no recovery phases. Patients with SPMS and PPMS have a higher proportion of chronic active lesions and it is associated with a more severe disease course (Kornek et al., 2000). Both genetics and environmental factors play a role in the onset and progression of MS; however, more research is needed to decipher these interactions.

1.2.2 MS pathogenesis

1.2.2.1 Hippocampus in MS

In addition to motor and sensory decline, up to 65% of patients with MS experience cognitive decline such as memory impairment (Geurts et al., 2005; Rao, 1995). Extensive demyelination of the hippocampus occurs in many patients such as demyelinated lesions 53-79% postmortem MS hippocampi in addition to neuronal damage and synaptic abnormalities (Geurts et al., 2007; Papadopoulos et al., 2009; Rocca et al., 2018; Vercellino et al., 2005). In contrast, a separate study showed extensive demyelination in patients with MS with minimal neuronal loss; however, a significant decrease in synaptic density was observed (Dutta et al., 2011). Overall, this study found a decreased abundance of proteins involved in axonal transport, synaptic plasticity, memory learning, and neuronal survival in demyelinated hippocampi.

1.2.2.2 MS genetics

The risk of developing MS for relatives of people with MS is higher than the risk for the general population (Dyment et al., 1997; Nielsen et al., 2005; Sadovnick et al., 1988). Genome

Wide Association Studies (GWAS) have been implemented to study the genetics of people with MS compared to the general population to identify risk genes. Through these studies, over 200 MS genetic risk loci have been identified (Baranzini and Oksenberg, 2017). The majority of these risk alleles are detected in genes responsible for inflammation such as the major histocompatibility complex (*MHC*) (Baranzini and Oksenberg, 2017).

An earlier GWAS study collected data from 1000 prospective case series of individuals with MS and matched controls to identify the genomic variants that influence MS susceptibility and severity in addition to other phenotypes (Baranzini et al., 2009). Gene ontology analysis of gene variants enriched in individuals with MS indicates that in addition to immune genes, CNS developmental gene variants are enriched in genes associated with MS susceptibility. Moreover, both CNS and embryonic developmental gene variants are over-represented in MS severity. Therefore, genes that regulate development likely play a role in both MS susceptibility and severity.

1.2.2.3 Environmental factors

Environmental factors are important for MS development and progression (reviewed in: (Dobson and Giovannoni, 2019; Michel, 2018; Pantazou et al., 2015; Zarghami et al., 2021)). Some of these environmental factors are: smoking tobacco, low vitamin D levels or ultraviolet B light (UVB) exposure, Epstein Barr Virus (EBV) infection and obesity (Alfredsson and Olsson, 2019; Bjornevik et al., 2022; Marrodan et al., 2019). The former two environmental factors are also associated with MS progression such as relapse and disability progression. Although these environmental factors play a role, none of them alone can explain MS onset. However, EBV is the leading candidate thus far and is likely a prerequisite for the disease as a recent study showed that the risk of developing MS increased 32-fold after infection with EBV (Bjornevik et al., 2022).

Studies have also found an interaction between genetics and the environment in the risk of developing MS. For example, carrying the HLA-DRB1*15 risk allele and the absence of the HLA-A*02 protective allele increases the risk of developing MS by 4.9-fold while smoking alone in the absence of these alleles increases risk by 1.4-fold. However, the interaction of these alleles with smoking increases this risk from 4.9 to 13.5-fold (Hedström et al., 2011). This represents an

example where carrying a specific gene variant combined with a lifestyle choice increases the risk of developing MS.

1.3 Cytokine and chemokine signaling in the brain

Cytokines and chemokines are small, secreted proteins that act as signaling molecules via binding and activating their cognate receptors on target cells. In short, cytokines and chemokines allow different cells to communicate with each other via autocrine, paracrine, and endocrine action.

1.3.1 Cytokine and chemokine signaling during brain development

Cytokines play a role in the CNS development by regulating various processes including embryonic NPC fates such as neurogenesis and gliogenesis. In particular, the glycoprotein 130 (gp130) cytokine family, that uses gp130 as a common signal transducer in their receptor, regulate embryonic RGCs that generate neurons, astrocytes and OPCs in the CNS by promoting self-renewal and expansion (reviewed in: (Deverman and Patterson, 2009; Taga, 1997)). The gp130 cytokine family, also known as the IL-6 family, include Interleukin-6 (IL-6), IL-11, IL-27, leukemia inhibitory factor (LIF), oncostatin M (OSM), ciliary neurotrophic factor (CNTF), cardiotrophin-1 (CT-1), novel neurotrophin-1/B cell stimulating factor-3 or cardiotrophin-like cytokine (CLC), and neuropoietin (NP) (reviewed in: (Fasnacht and Müller, 2008)). Several of these cytokines are expressed in the embryonic brain such as CT-1 in neurons, NP in neuroepithelium and LIF and CNTF in the choroid plexus (Barnabe-Heider et al., 2005; Derouet et al., 2004; Gregg and Weiss, 2005). IL-6 is produced by NPCs and directly regulates their proliferation and differentiation (Gallagher et al., 2013; Storer et al., 2018). In addition, LIF, CNTF, and IL-11 have been shown to promote oligodendrocyte differentiation and survival (Barres et al., 1993).

Chemotactic cytokines called chemokines are a group of secreted, small 8-10 kilodalton (kDa) proteins with cysteine (Cys) residues that induce changes in the behaviour of target cells (Walz et al., 1987; Yoshimura et al., 1987). Chemokines are categorized into several groups: CC, CXC, and XC to CX3C, where the X represents the number of amino acids between the Cys residues at their N-terminus (reviewed in: (Watson et al., 2020)). More specifically, when a chemokine ligand binds and activates its cognate receptor on target cell, a signaling cascade that

results in cellular changes such as: cell adhesion, migration, phagocytosis, additional cytokine secretion, proliferation, survival and/or apoptosis (Ambrosini and Aloisi, 2004; Deverman and Patterson, 2009; Ramesh et al., 2013; Tran and Miller, 2003).

Chemokines bind and activate G-protein coupled receptors (GPCR) with seven transmembrane domains that were initially discovered to play a role in immune cell recruitment to injury sites (Ambrosini and Aloisi, 2004). However, later research shows the importance of chemokines and GPCRs in CNS development, homeostasis, and response to injury or insult. Within the CNS, different cells such as neurons, glia (microglia, OPCs, oligodendrocytes, astrocytes) and endothelial cells secrete chemokines as well as express their receptors to communicate with each other during homeostasis and disease (Ambrosini and Aloisi, 2004; Gallagher et al., 2013; Ji et al., 2004; Kim et al., 2014; Omari et al., 2005; Storer et al., 2018; Stuart et al., 2015; Tran and Miller, 2003; Williams et al., 2014). Generally, chemokines involved in homeostasis are expressed constitutively whereas those involved in inflammation are produced in response to injury or disease (Moser and Loetscher, 2001).

An example of a chemokine that plays a role in development is CXCL12 (stromal cell-derived factor 1, SDF-1) and its receptors CXCR4 and CXCR7 (reviewed in: (Deverman and Patterson, 2009; Watson et al., 2020). They have critical roles in neuronal migration, proliferation, and axon organization as well as OPC survival, migration, proliferation, and differentiation in the CNS. CXCL12 is expressed in the meninges embryonically, which decreases in adulthood, and in microglia, astrocytes and neurons postnatally (Tham et al., 2001). Interaction of CXCL12 with CXCR4 expressed in OPCs during early development regulates their migration and interaction of CXCL12 with CXCR7 enhances oligodendrocyte production (Dziembowska et al., 2005; Göttle et al., 2010).

1.3.2 Cytokine and chemokine signaling during inflammation.

Some chemokines such as CXCL9, CXCL10, and CXCL11 are induced by interferon-gamma (IFN-γ). They are expressed by neurons in response to CNS infection and inflammation (Campanella et al., 2008; Klein et al., 2005). CXCL9, CXCL10, and CXCL11 and IFN-γ are inflammatory cytokines that are upregulated during inflammation such as experimental autoimmune encephalomyelitis (EAE) (reviewed in: (Watson et al., 2020)).

In addition, reactive microglia can secrete CCL2 (monocyte chemoattractant protein-1, MCP-1), CCL3 (macrophage inflammatory protein 1 alpha, MIP-1α) and CCL5 as well as various cytokines like IL-1β, IL-6, IL-12, IL-23, IL-33, tumour necrosis factor alpha (TNF-α), interferon beta (IFN-β), and transforming growth factor beta (TGF-β) to promote inflammation and the recruitment of immune cells to the site of injury (Lampron et al., 2013; Negi and Das, 2018). In contrast, IL-4 and IL-10 stimulated microglia secrete a different set of cytokines and chemokines like vascular endothelial growth factor (VEGF) to promote tissue repair (Lampron et al., 2013). Similar to microglia, activated astrocytes also secrete a variety of cytokines in response to inflammation, such as CCL2 (MCP-1), CCL5, IL-1β, IL-6, IL-8, IL-10, IFNα, IFNβ, TNFα, and TGF-β (Kigerl et al., 2014; Klein et al., 2017; Lampron et al., 2013)

1.4 C-X3-C motif chemokine receptor 1 (CX3CR1)

CX3CR1 is a GPCR with seven transmembrane helices that was initially discovered in 1994 in rat CNS (Harrison et al., 1994) while its ligand, the chemokine CX3CL1 (fractalkine, FKN), was discovered in 1997 in both humans and mice (Bazan et al., 1997; Pan et al., 1997). The FKN ligand is secreted by neurons in the CNS (Harrison et al., 1998) and it exists as both a soluble and membrane-bound signaling molecule with roles in adhesion and chemoattraction, respectively (Luo et al., 2019; Paolicelli et al., 2014). FKN is constitutively expressed in the neurons of the cerebral cortex, hippocampus, caudate putamen, thalamus, and the olfactory bulb (reviewed in (Watson et al., 2020)).

Imai et al. first described the CX3CR1-FKN signaling axis connection in 1998 using leukocyte migration and adhesion assays (Imai et al., 1997). Intracellular signal transmission via CX3CR1 occurs through the heterotrimeric G proteins that activates different secondary messengers and transcription factors such as nuclear factor kappa-light-chain-enhancer of activated B cells (NF-κB), cAMP response element-binding protein (CREB), signal transducer and activator of transcription (STAT), and activator protein 1 (AP-1) (reviewed in: (Poniatowski et al., 2017)). These downstream activators and transcription factors may play a role in cytoskeletal reorganization, migration, proliferation, and apoptosis. FKN binds to the CX3CR1 receptor, which was previously thought to be exclusively expressed on microglia, leading to studies on the signaling axis in neuron-microglia interactions (Jung et al., 2000; Sheridan and

Murphy, 2013). However, further studies have shown that CX3CR1 is also expressed by OPCs (de Almeida et al., 2023; Voronova et al., 2017; Watson et al., 2021), NPCs (Ji et al., 2004; Watson et al., 2021), and neurons (Dworzak et al., 2015). During development, postnatal OPCs express elevated CX3CR1 compared to embryonic OPCs (Voronova et al., 2017). A second independent study using RNA-sequencing confirmed that *CX3CR1* mRNA in OPCs from the brain is highest on postnatal day 7 (Marques et al., 2018; Watson et al., 2020).

In vitro experiments show that soluble FKN ligand directly binds to its receptor on NPCs and OPCs and increases their differentiation to oligodendrocytes (de Almeida et al., 2023; Voronova et al., 2017; Watson et al., 2021). In addition, mice lacking the FKN receptor constitutively or specifically in embryonic cortical NPCs show a decrease in oligodendrocyte density postnatally due to a decrease in differentiation (Voronova et al. 2017). In agreement, infusion of soluble FKN into normal adult brain increases SVZ NPC to OPC commitment, and OPC differentiation into oligodendrocytes (Watson et al., 2021). Furthermore, infusion of FKN into cuprizone demyelinated murine brain enhances remyelination by increasing cortical grey matter OPC proliferation as well as white and grey matter OPC differentiation into oligodendrocytes (de Almeida et al., 2023).

FKN-CX3CR1 signaling likely plays a role in human disease as CX3CR1 KO mice have more severe outcomes when subjected to cuprizone-induced demyelination, such as reduced oligodendrocyte regeneration, aberrant myelin morphology, reduced OPC density and proliferation, as well as decreased phagocytic function of microglia (Lampron et al., 2015; Mendiola et al., 2022). In addition, single-nuclei RNA sequencing data show that CX3CR1 is expressed in committed OPCs, immune oligodendroglia and microglia/macrophages in MS patient brain lesions (de Almeida et al., 2023; Jäkel et al., 2019; Watson et al., 2020).

Together, these studies suggest FKN-CX3CR1 signaling axis is important for proper brain development, homeostasis, and regeneration. As outlined below, *CX3CR1* variants contribute to demyelinating disease mechanisms. The focus of my thesis are developmental changes due to a *CX3CR1* variant that may contribute to the severity of demyelinating disorders.

1.5 Rationale for thesis

Both genetic and environmental factors contribute to the development and progression of MS. While over 200 MS genetic risk loci have been identified (Baranzini and Oksenberg, 2017), we understand very little about the burden of these genetic variants on affected individual's brain development, function, susceptibility to neurodegeneration and the ability to regenerate. The majority of MS susceptibility variants are detected in genes responsible for inflammation (Baranzini and Oksenberg, 2017). In contrast, majority of MS severity variants are detected in genes responsible for CNS development (Baranzini et al., 2009). Whether neurodevelopment is linked to neurodegeneration in MS is not known.

One of such severity risk genes is *CX3CR1* (reviewed in: (Watson et al., 2020)). Namely, two single nucleotide polymorphisms have been shown to associate with worsened disease progression in MS, ALS and AD (Arli et al., 2013; Cardona et al., 2018; Lopez-Lopez et al., 2014; López-López et al., 2018; McDermott et al., 2003; Stojković et al., 2012; Thompson and Gilbert, 2017). These two polymorphic changes are a valine to isoleucine at position 249 and a threonine to methionine at position 280, which makes the CX3CR1 receptor less responsive to FKN stimulation (McDermott et al., 2003). Notably, patients with MS who are homozygous V249I carriers have higher Expanded Disability Status Scale (EDSS) score compared to heterozygous carriers with MS (Arli et al., 2013). In addition, homozygous T280M patients have a non-significant increasing trend in EDSS. A carrier is traditionally defined as an individual who has one specific allele of a gene associated with a disease or a trait that is inherited in an autosomal-recessive manner; therefore, a carrier does not show symptoms or features of the trait. However, in the context of risk genes in MS, individuals are referred to as carriers when they have at least one copy of the risk allele; however, they may or may not develop MS. To better understand the influence of these variants on brain physiology, knock in mice were created that express the human *CX3CR1* gene with both amino acid changes (hCX3CR1$^{I249/M280}$, hM280) (Cardona et al., 2018). Mice expressing hCX3CR1$^{I249/M280}$ develop more severe demyelination when subjected to EAE or cuprizone demyelination (Cardona et al., 2018; Mendiola et al., 2022). The majority of observed phenotypes are attributed to aberrant function of microglia, which express high levels of CX3CR1 (Limatola and Ransohoff, 2014). However, CX3CR1 is also expressed in OPCs, both in the

developing and the adult murine central nervous system (CNS) as well as healthy and demyelinated human brains (reviewed in (Watson et al., 2020)).

Our lab showed that constitutive CX3CR1 KO or CX3CR1 knockdown in cortical progenitors leads to decreased oligodendrocyte formation in the developing brain (Voronova et al., 2017). This raises the possibility that individuals carrying MS-associated variants in CX3CR1 may display aberrant brain development that may predispose them to faster disease onset and/or poor progression. This is a critical question to address as genetic perturbations in other neurodegenerative disorders, like Huntington's disease (HD), have shown aberrant early brain development preceding the appearance of a degenerative phenotype, leading to a novel postulate that neurodegenerative diseases may have a neurodevelopmental component (Barnat et al., 2020). This is an important consideration for MS community as an abnormally developed and functioning CNS may react differently to an environment, resulting in a more severe neurodegeneration upon an environmental insult. Indeed, murine studies show inducing oligodendrocyte cell death in the postnatal developing CNS leads to worse outcomes when challenged with a demyelination injury later in life (Caprariello et al., 2015). However, how genetic variants detected in MS patients impact developmental myelination is not known. To address this gap, I ask whether MS-associated CX3CR1$^{I249/M280}$ variant impairs CNS development.

1.6 Hypothesis and objectives

Hypothesis: Human disease associated CX3CR1 variant (CX3CR1$^{I249/M280}$) affects brain development by altering OPC and microglia fates.

This hypothesis was addressed via three objectives:

Objective 1: Identify the effect of the hM280 variant on oligodendrocyte and myelin formation.

Objective 2: Identify the effect of the hM280 variant on microglia cell fates.

Objective 3: Determine the effect of the hM280 variant on CNS function.

To achieve these aims, I analyzed brain tissue, including the cerebrum, from developing and adult wild type, CX3CR1 KO and hM280 homozygous mice. Through a collaboration with Yana Kibalnyk, we also started to determine the behavioral phenotypes of these mice.

2 Material and Methods

2.1 Animal models

2.1.1 Mice: C57BL/6 (wild type), CX3CR1$^{fl/fl}$ (KO), CX3CR1$^{I249/M280}$ (hM280)

Animal use protocol was approved by the Research Ethics Office at the University of Alberta in accordance with the Canadian Council of Animal Care Policies. C57BL/6J (wild type, WT) mouse line was obtained from Jackson Laboratory (JAX, 000664). CX3CR1$^{fl/fl}$ and CX3CR1$^{I249/M280}$ mouse lines were a kind gift from Dr. Astrid Cardona (University of Texas San Antonio). The CX3CR1$^{fl/fl}$ mice have the human MS specific hCX3CR1$^{I249/M280}$ variant knocked into the endogenous mouse CX3CR1 locus (Cardona et al., 2018). This knocked-in human variant is under the control of the endogenous mouse CX3CR1 promoter; however, it contains a neomycin gene flanked by lox P sites, so it acts as a knockout (herein referred as KO) (Cardona et al., 2018). Any cells that normally expresses the CX3CR1 protein, including microglia and OPCs, are not expressing the receptor in KO (Cardona et al., 2018). To generate the CX3CR1$^{I249/M280}$ mouse line, Dr. Cardona's lab crossed the CX3CR1$^{fl/fl}$ mouse with B6.FVB-Tg(EIIa-cre)C5379Lmgd/J (The Jackson Laboratory, Stock No. 003724), which is germline E2ACre recombinase expressing mouse line (Cardona et al., 2018). In the germline cells, cre-mediated recombination of the floxed neomycin resistance gene caused removal of the stop cassette and the loss of the SA-15/SA-16 1,004 base pair fragment. Subsequently, this results in the expression of the human *CX3CR1$^{I249/M280}$* variant gene in all cells that normally express this gene (herein referred as hM280). To generate wild type, heterozygous and homozygous hM280 mice, a heterozygous male and female are crossed. For the current study, KO mice were set-up to generate KO progeny, WT mice generated WT progeny, and hM280 homozygous mice generated hM280 homozygous progeny.

Mice were housed in normal 12-hour light: 12-hour dark cycles at average temperatures of 68-70ºF and 54-58% humidity. Food was provided *ad libitum*. Mice from both sexes were used in all *in vivo* and *in vitro* experiments. No sex differences were observed in this study. For *in vivo* experiments, mice were collected at postnatal day (P) 15, 30 and 70. For behavioural assays, mice were used at 2-3 months of age. For *in vitro* experiments, P0-P2 pups were used.

For genotyping, the following primers were used for CX3CR1$^{fl/fl}$ and recombined CX3CR1$^{I249/M280}$ to identify the genotypes of each animal using polymerase chain reaction (PCR).

CX3CR1$^{fl/fl}$: TACCTGGCCATCGTCCTGGCCGCCA (5'-3', forward), ACGAGACTAGTGAGACGTGCTACTT (5'-3', reverse), GTCTTCACGTTCGGTCTGGT (5'-3', control forward), CCCAGACACTCGTTGTCCTT (5'-3', control reverse). Samples were identified by the presence of DNA bands as follows in base pairs (bp): 1) homozygous: 1004 bp, 2) heterozygous: 1004 bp and 410 bp, and 3) control/WT: 410 bp.

Recombined CX3CR1$^{I249/M280}$: CCAAGACAGAATTTCACTGTGTAGC (5'-3', forward), CAACAAATTTCCCACCAGGCCAATG (5'-3', reverse), GTCTTCACGTTCGGTCTGGT (5'-3', control forward), CCCAGACACTCGTTGTCCTT (5'-3', control reverse). Samples were identified by the presence of DNA bands as follows: 1) homozygous: 1245 bp, 2) heterozygous: 1245 bp and 410 bp, and 3) control/WT: 410 bp.

2.1.2 Behaviour assays

2.1.2.1 Open field test (OFT)

Mice had not undergone any prior behavioural tests. 2-3-month-old WT, KO and hM280 mice were habituated in the experiment room in their home cage for at least 1 hour before the experiment. Experiment was set up in the EthoVision XT 17 tracking software (Noldus) and the arena (40x40 cm) was cleaned with 70% ethanol before each trial. Each mouse was placed in the arena to move freely for 10 minutes. The center was designated in the tracking software as a 20x20 cm^2 in the middle of the arena.

2.1.2.2 Elevated plus maze (EPM)

The EPM experiment was performed on the same mice the day after the OFT. Mice were habituated in the experiment room in their home cage for at least 1 hour before starting the test. Each mouse was placed in the center of the EPM, facing an open arm and allowed to move freely for 10 minutes. The mice were returned to their home cage at the end of the experiment.

2.2 5-Bromo-2'-deoxyuridine (BrdU) injections

A solution of 8mg/ml of 5-Bromo-2'-deoxyuridine (BrdU, Sigma-Aldrich) in sterile 1x phosphate buffered saline (PBS) was prepared fresh before injections. BrdU was dissolved in the 1x PBS by heating the solution at 95°C for 15 seconds, then vortexing. Each P14 mouse was weighted and injected with the BrdU solution at 100 mg/kg using intraperitoneal (IP) injection method. Brain tissue was collected 24 hours later at P15 following the method outlined in 2.5 below.

2.3 Cuprizone-induced demyelination

For cuprizone-induced demyelination, 10-week-old WT mice were subjected to nutragel (Bio-Serv) containing 0.2% cuprizone (bis-cyclohexanone oxaldihydrazone, Sigma) for 6 weeks as described in (de Almeida et al., 2023; Saito et al., 2021). Animals were monitored weekly for weight and apparent behaviour changes. If mice lost more than 20% of their weight, lost mobility and/or exhibited obvious pain symptoms or stopped moving, then they were immediately euthanized.

2.4 Tissue dissection and collection

P15 mice were euthanized with CO_2 using a 2.5 flow rate with a fill rate of 30% of the chamber volume per minute. Mice at one month of age or over (P30, P70) were anesthetized with 102 mg/kg of body weight Euthansol (WDDC) and perfused transcardially with ice-cold ~30 ml of HBSS (Hank's balance salt solution, Invitrogen).

Brains were dissected and cut in sagittal. One hemisphere with the cerebellum was placed in 4% PFA (paraformaldehyde, Thermo Scientific, Cat# 50980487) at 4°C for 24 hours. Then, the tissue was cryopreserved for 72 hours in 30% sucrose (Thermo Fisher Scientific, Cat# BP220-10) in 1x PBS. After 72 hours, the specimens were embedded in optimal cutting temperature (O.C.T) compound (Thermo Scientific™ Shandon™ Cryomatrix™, Cat# 67-690-06), flash frozen, and stored at -80°C.

The other hemisphere was used to generate lysates for western blot and multiplex-ELISA (enzyme-linked immunoassay, Meso Scale Discovery). The cerebellum was removed from the cerebrum. The cerebrum was cut into smaller pieces with a clean scalpel and lysed in 500 µl of

Levin Lysis Buffer (0.1% Sodium dodecyl sulfate, Bio-Rad, Cat# 161-0322; 0.2% sodium deoxycholate, Sigma-Aldrich, Cat# D6750 and 1% IGEPAL CA-630, Sigma-Aldrich, Cat# I-3021 in 1x PBS) supplemented with 0.001M phenylmethylsulfonyl fluoride, PMSF (Thermo Scientific, Cat# 36978), 1x protease inhibitor cocktail, PIC (Sigma-Aldrich, Cat# P8340), and 1x phosphatase inhibitor, PhosSTOP (Sigma-Aldrich, Cat# 406845001). The samples were sonicated with a Thermo Fisher Scientific Sonic Dismembrator at 4-5W for 10 sec, and centrifugated at 20800g at 4°C for 5 minutes to remove cell debris. The supernatant was transferred to a clean tube. The samples were stored at -80°C for downstream assays.

2.5 Primary microglia cultures

Cerebral cortices and hippocampi from P0-P2 WT, KO and hM280 mice were cultured as described in (de Almeida et al., 2023). P0-P2 brains were dissected and meninges from the cortex were removed in HBSS solution containing 1% penicillin/streptomycin (Pen/Strep, Lonza) in a petri dish. While holding the cerebellum with tweezers, the cortex including the hippocampus was unfolded and removed in a spoon-like shape using a spatula. The inside of the cortex was cleaned from remaining meninges and blood vessels, and the tissue was kept in hibernate A (Gibco, Cat# A1247501) with 1% Pen/Strep (penicillin-streptomycin, Gibco, Cat# 15140122). Next, the solution was replaced with 0.025% trypsin (Sigma-Aldrich, Cat# T2011) at 1ml per cortex and incubated at 37°C for 15 minutes to enzymatically digest the cortices. The trypsin was replaced with DMEM/F12 (Dulbecco's Modified Eagle Medium, Ham's F-12, Gibco, Cat# 13320033) with 10% FBS (Fetal Bovine Serum, Sigma-Aldrich, Cat# F1051), 1% Pen/Strep, 1% sodium pyruvate (Gibco, Cat# 11360070) and 50 μM β-mercaptoethanol (Sigma-Aldrich, Cat# AAJ6674230) (herein referred to as **microglia media**). The solution was titrated with 5ml serological pipette until a homogenous solution was obtained and centrifuged at 1500 rpm for 2 minutes to remove the supernatant. The pellet was resuspended in fresh microglia media, filtered through a 70 μm cell strainer (Thermo Fisher Scientific, Cat# 22-363-548), and cells were counted via trypan blue (Sigma-Aldrich, Cat# T0887) by mixing cell culture with trypan blue in a 1:1 ratio to assess viability. The cells were seeded in 15ml microglia media at $1x10^6$ live cells/ml in a T75 flask (Falcon, Cat# 13-680-65).

Media was replaced twice a week. To increase microglia density, the cultures were treated with 5 ng/ml GM-CSF (Granulocyte Macrophage Colony Stimulating Factor, Sigma-Aldrich, Cat# SRP3201) on days 8-11. Media was replaced on day 11 with microglia media. Media was replaced on day 13 again to generate conditioned media on day 14, which was collected and filtered through a 0.22µm filtration unit (Starstedt, Cat# 83.1826.001). Microglia were isolated using 15 mM lidocaine hydrochloride monohydrate (Sigma-Aldrich, Cat# L5647) and shaking the plate at 100 rpm for 10 min. Isolated cells were plated at 47,000-52,000 cells/cm^2 density for 24h in 50% conditioned media and 50% microglia media without β-mercaptoethanol. After 24h, media was replaced with microglia media without β-mercaptoethanol and FBS. The cells were processed for immunocytochemistry (ICC) as per below at the 3-day *in vitro* timepoint.

2.6 Antibodies

Primary antibodies: mouse anti-CNPase (WB: 1:800, Sigma-Aldrich, Cat# AMAB91072), rat anti-MBP (a. a. 82-87) (WB: 1:300, IHC:1:500, Millipore, RRID: AB_94975), rabbit anti-PLP (WB: 1:500, Abcam, RRID:AB_776593), rabbit anti-GFAP (WB: 1:800, Agilent, RRID:AB_10013382), rat anti-GFAP (WB: 1:800, IHC: 1:1000, Thermo Fisher Scientific, RRID:AB_2532994), mouse anti-GAPDH (WB: 1:5000, Sigma-Aldrich, RRID:AB_1078991), chicken anti-NFL (IHC: 1:500, EnCor Biotechnology, RRID:AB_2149931), goat anti-PDGFRα (IHC: 1:300, R&D Systems, RRID: AB_2236897), mouse anti-APC/CC1 (IHC: 1:150, Calbiochem, RRID:AB_2057371), rabbit anti-Olig2 (IHC: 1:1000, Millipore, RRID: AB_570666), mouse anti-Olig2 (IHC: 1:1000, Millipore, RRID: AB_10807410), rabbit anti-IBA1 (IHC: 1:1000, ICC: 1:1000, Wako, RRID: AB_839504), rat anti-CD16/32 (ICC: 1:400, Tonbo Biosciences, RRID:AB_2621487), goat anti-arginase1 (ICC: 1:500, Novus Biologicals, #NB100-59740), sheep anti-BrdU (IHC: 1:1000, Abcam, RRID:AB_302659), rabbit anti-CC3 (IHC: 1:250, Abcam, AB_91556).

Fluorescently labeled highly cross-absorbed secondary antibodies raised in donkey were used at 1:500 dilution in phosphate buffered saline (PBS). The following secondary antibodies were used: anti-chicken-Alexa647 (Jackson ImmunoResearch, Cat# 703-605-155), anti-goat-Alexa488 (Invitrogen, Cat# A11055), anti-rabbit-Alexa488 (Jackson ImmunoResearch, Cat# 711-545-152), anti-rabbit-Cy3 (Jackson ImmunoResearch, Cat# 711-165-152), anti-rabbit-Alexa647 (Jackson ImmunoResearch, Cat# 711-605-152), anti-rat-Alexa488 (Jackson

ImmunoResearch, Cat# 712-545-150), anti-rat-Cy3 (Jackson ImmunoResearch, Cat# 712-165-153), anti-rat-Cy5 (Jackson ImmunoResearch, Cat# 712-175-153), and anti-sheep-Alexa647 (Jackson ImmunoResearch, Cat# 713-175-147). If primary antibodies were raised in mouse for IHC, mouse on mouse (MOM) kit (MJS BioLynx, Cat# VECTBMK2202) was used, where Alexa488 (Cat# 016-010-084), Cy3 (Cat# 016-160-084), or Cy5 (Cat# 016-170-084) conjugated streptavidin secondaries (Jackson ImmunoResearch) were used at 1:500 dilution in PBS. For western blot protein detection using enhanced chemiluminescence (ECL), the horse-radish peroxidase (HRP) conjugated secondary antibodies used were anti-rat and anti-rabbit (Thermo Fisher Scientific).

2.7 Western blot

Protein concentrations in brain lysates were measured via Bradford assay (Bio-rad, Cat# 5000006) using Biochem GeneQuant Spectrophotometer (Beckman). Lysates were thawed on ice and 25 μg of protein from each sample was loaded onto 10% sodium dodecyl sulfate (SDS)-polyacrylamide gel by boiling the samples in 1x SDS-PAGE loading buffer [0.06M Tris (Thermo Fisher Scientific, Cat# BP152), 2.05% SDS (Bio-Rad, Cat# 161-0322), 1% β-mercaptoethanol, 0.1M dithiothreitol (DTT, Thermo Fisher Scientific, Cat# BP172), 0.05% bromophenol blue (Bio-Rad, Cat# 161-0404), and 5-10% glycerol (Gibco, Cat# 15514-011)] at 95 °C for 5 minutes. Resolved proteins were transferred to a 0.2 μm nitrocellulose membrane (Bio-Rad, Cat# 162-0112), blocked in 5% milk or PBS blocking buffer (LI-COR, Cat# 927-70001) for 1 hour at room temperature and reacted with antibodies raised against CNPase, MBP, PLP, GFAP and GAPDH at 4 ºC overnight. The membrane was then incubated with HRP-conjugated secondary antibodies or fluorescently labeled secondary antibodies for 1 hour at room temperature. HRP signal was detected using ECL substrates (Thermo Fisher Scientific) while the fluorescently labeled antibodies were detected with the Odyssey LI-COR imager (LI-COR). Up to two antibodies were detected with ECL reagent while up to three were detected with LI-COR. For additional protein detection, the membranes were stripped with 5M NaCl (Sigma-Aldrich, Cat# 746398) and 1M TrisHCl for 10 minutes before the process was repeated beginning with blocking for 1 hour at room temperature.

2.8 Multiplex-ELISA (enzyme-linked immunoassay)

Ultrasensitive MSD U-PLEX assay kit (Meso Scale Discovery, MSD, Cat# K15069L-1) using monoclonal antibodies and ECL detection with MESO QuickPlex SQ 120MM were used by ordering a custom plate and processing it according to manufacturer's instructions. Cerebrum protein lysates prepared and used for western blot analysis were used here as well. 10 µl (~100-500 µg of protein) of each sample was loaded into each well during the experiment. The precise concentration of each sample was inputted into the manufacturer's analysis software (MSD, Discovery Workbench 4.0) to normalize the data output. The custom plate allowed testing for IFN-γ, IL-1β, IL-6, IL-10, MCP-1, MIP-1α, SDF-1α, TNF-α, and VEGF-A.

2.9 Immunohistochemistry (IHC)

Cryopreserved brains were sectioned in sagittal plane at 18 µm, starting near the midline when the hippocampus appeared. Five sections were collected per slide for a total of eight slides that were stored at -80°C until IHC.

The sections were stained as described in (Watson et al., 2021). Slides were first dried at 37°C for 10 minutes, then rehydrated in 1x PBS. Next, the tissue was permeabilized and blocked with 5% BSA and 0.3% Triton-X100 in 1x PBS for 1 hour at room temperature followed by incubation with primary antibodies at 4°C overnight. The primary antibodies were incubated with slides in 5% BSA in 1x PBS for 24 hours at 4C, after which the sections were incubated with appropriate secondary antibodies for 1 hour at room temperature in the dark. Nuclei were counterstained with Hoechst 33258 (Riodel-De Haen Ag, Cat# 33217) for 2 minutes at room temperature. Sections were mounted with Fluoromount-G (Thermo Fisher Scientific, Cat# 5018788). Primary and secondary antibodies are listed in section 2.6.

BrdU staining was performed as described in (Li et al., 2022). Briefly, the sections were post-fixed in 4% PFA for 10 minutes after the initial primary and secondary antibodies. Then, the sections were treated with 1M hydrochloric acid (HCl) for 10 minutes at room temperature followed by 2M HCl for 10 minutes at room temperature, then 20 minutes at 37°C. Next, the tissue was blocked with 5% normal donkey serum (Jackson ImmunoResearch, Cat# 017-000-121) with 1% Triton X-100 (Bio Basic, Cat# TB0198) and 1M glycine (Sigma-Aldrich, Cat# G7126) in 1x PBS for 1 hour at room temperature and anti-sheep BrdU antibody was added for

overnight at 4°C. After ~24 hours, appropriate secondary antibody was added for 1 hour in the dark, followed by Hoechst and mounting as described above.

2.10 Immunocytochemistry (ICC)

Cell cultures were fixed and stained as described in (Watson et al., 2021). Microglia cell cultures were fixed with 4% PFA for 10 minutes at room temperature, permeabilized with 0.2% NP-40 (Thermo Fisher Scientific, Cat# 28324) in 1xPBS for 5 min and blocked with 6% donkey serum and 0.5% BSA in 1x PBS. Cells were incubated with primary antibodies overnight at 4°C. After ~24 hours, secondary antibodies were added in 1xPBS for 1 hour at room temperature. Nuclei were counterstained with Hoechst 33258. Sections were mounted with Fluoromount-G.

2.11 Microscopy

In vivo and *in vitro* images were captured using Zeiss Axio Imager M2 fluorescence widefield microscope equipped with ORCA-Flash LT sCMOS Camera (Hamamatsu), LED light source (Module 385nm, 475nm, 567nm and 630nm), and Zen software (Zeiss). The objective lenses were EC Plan-Neofluar 10x/0.30 M27 (Zeiss) and Plan-Apochromat 20x/0.8 M27 (Zeiss). Cultured cells and *in vivo* sections were imaged in a single plane, except images for microglia transformation index analysis and mean fluorescence intensity (MFI), which were captured using Z-stacks with optical thickness of 0.5-1.2 µm spanning 10-18 µm. *In vitro* images were captured with the 20x objective. Composite *in vivo* images were tiled from images taken with 10x or 20x objective. DAPI was detected with an excitation wavelength of 353nm (channel 1). Secondary antibodies were detected through three different channels with excitation wavelengths of 488nm, 590nm, and 650nm (channels 2-4). The excitation filter wavelengths for channels 1 to 4 were 370-410nm, 450-490nm, 533-558nm, and 625-655nm, respectively. The emission filter wavelengths for channels 1 to 4 were 430-470nm, 500-550nm, 570-640nm, and 665-715nm, respectively.

Exposure time varied for each objective and target. Slides containing tissue from WT, KO, and hM280 were imaged using same settings for each marker. DAPI was detected with an exposure time of 7-12 ms. In *in vitro* experiments, Arg1, CD16/32, and IBA1 were detected with channel 2 to 4 with an exposure time of 200 ms, 400 ms, and 70 ms, respectively. In *in vivo* experiments, PDGFRα, CC1, and Olig2 were detected with channel 2 to 4 with an exposure time

of 150 ms, 200 ms, and 400 ms, respectively, using both the 10x and 20x objective. GFAP and NFL were both detected with channel 4 with an exposure time of 300 ms and 70 ms, respectively. MBP was detected using channel 2 or 3 with an exposure time of 150 ms and 400 ms, respectively. IBA1 was detected with channel 4 with an exposure time of 250 ms for both single-plane images and Z-stacks.

2.12 Quantifications and statistical analysis

Images from western blot experiments were processed with ImageJ. The pixel intensity of each band from a control and protein of interest was quantified using a constant-sized box. The pixel intensity of the protein of interest was normalized to the pixel intensity of the control (GAPDH). The value was then normalized to the WT samples by dividing the two numbers. Each blot contained WT controls. The data was obtained from n=3-9, where n is the number of animals from each genotype and shown in figure 1 as individual data points.

In vivo experiment images were tiled to include the hippocampus (HPC), corpus callosum (CC) and cortical grey matter (GM) above the HPC if possible. Otherwise, these three regions were imaged separately. Areas of interest were identified with Hoechst or MBP staining. For the CC and GM data, the cortical column was identified above the hippocampus with a consistent width by using a rectangle aligned with the edge of the pia layer. The CC and GM were further defined by using Hoechst staining and nuclei morphology. Data was obtained from n=3-5, where n is the number of animals from each genotype and indicated as individual data points in the figures. Data was collected from 3-5 anatomically matched sections per each animal. Data is presented as (1) marker MFI (mean fluorescence intensity), (2) average # of marker+ cells per area (density), or (3) %marker1+marker2+/marker2+ cells (index).

For microglia transformation index (TI) in the SLM and MFI in the cortical GM, one z-stack was captured using 20X objective in the SLM of CA1 of HPC and a second z-stack was captured in the cortical GM above the CC using IBA1 marker. For TI, five images were analysed per animal and 1-5 IBA1+ microglia were traced in each image for a total of 13-25 IBA1+ microglia per animal. The perimeter and area of the IBA1 stain were calculated by ImageJ and recorded. Data was obtained from n=3-4, where n is the number of animals from each genotype. Each data point in figure 6E represents an IBA1+ cell. The following formula was used to calculate TI for each cell:

$TI = \frac{P^2}{4*3.14*A}$ where P is perimeter and A is area of each cell.

Due to technical limitations of tracing IBA1+ cells in the GM, MFI of each IBA1+ cell body in the GM was used instead. Using the z-stack images in the GM explained above, 10-16 IBA1+ microglia cell bodies were outlined in each image for a total of 40-79 IBA1+ microglia per animal from 5 sections. The MFI was recorded and presented in figure 7C as individual dots. Data was obtained from n=3-4, where n is the number of animals from each genotype.

For *in vitro* experiments, each n represents dissected cerebrums including the hippocampus from 2-3 P0-P2 pups. The data is from at least 3 independent experimental replicates. During each experiment, at least two technical replicates were produced, stained, and 5-10 field of view images were taken with a 20X objective. At least 5 images were analyzed per experiment from each genotype. Data is presented as (1) %marker+/nuclei, (2) average marker+ cells per field of view, or (3) %marker1+ marker2+/ marker2+ cells (index).

For the Meso Scale cytokine assay, data was analyzed in the Discovery Workbench 4.0 Analysis Software provided by the Meso Scale Discovery manufacturer. Data was obtained from n=2-4, where n is the number of animals from each genotype.

MFI and cell counting data analysis was completed in ImageJ software V1.53c in a blinded fashion (Schindelin et al., 2012). Representative images were processed in Photoshop CC 2015 and figures were created in Adobe Illustrator CC 2015. Biorender was used to generate brain schematics.

For behaviour analysis, EthoVision XT 17 tracking software was used to quantify the distance traveled and the time spent in the open arms. The grooming time was scored manually by an observer in the software. Data was obtained from n=8-17, where n is the number of animals from each genotype.

All data analysis was performed with GraphPad Prism version 8. Data was tested for normality using Shapiro-Wilk and Kolmogorov test. If data passed the normality tests, it was analyzed with 1-way ANOVA followed by Tukey or the Dunnett's multiple comparison's tests (indicated in the figure legends). If the data did not pass the normality tests, it was analyzed using non-parametric Dunn's multiple comparison's test and Kruskal-Wallis test. All data is presented as a mean +/- standard error of the mean (SEM).

3 Results

3.1 Myelin protein abundance is perturbed in the developing cerebrum of CX3CR1 knockout (KO) and CX3CR1$^{I249/M280}$ (hM280) mice.

To determine whether there were any changes in myelin in the developing or adult brain, cerebrum lysates were collected from postnatal days 15 (P15), when myelin is just starting to form (Kessaris et al., 2006), and 70 (P70), when myelination is largely complete (Baumann and Pham-Dinh, 2001). WT, KO, and hM280 mice were subjected to western blot analysis using myelin-specific antibodies (Fig. 1A). It is important to note that the lysate contained both dorsal (cortex, striatum, hippocampus) and ventral (thalamus, hypothalamus, etc.) brain areas and excluded cerebellum and olfactory bulb.

In comparison to WT, the P15 hM280 cerebra, but not CX3CR1 KO cerebra had a ~2.6-fold ($p=0.0312$) decrease in the abundance of 2',3'-Cyclic-nucleotide 3'-phosphodiesterase (CNPase) and a trending decrease in myelin basic protein (MBP) (Fig. 1B-D). CNPase makes up 4% of total myelin protein, whereas MBP forms 30-40% of total CNS myelin protein (Pfeiffer et al., 1993). Surprisingly, the myelin proteolipid protein (PLP), the most abundant myelin-associated protein making up 50% of the protein mass of CNS myelin (Pfeiffer et al., 1993; Timsit et al., 1995), was ~1.7-fold ($p=0.0208$) and ~1.5-fold ($p=0.0424$) increased in the KO compared to WT and hM280, respectively, at P15 (Fig. 1E). In contrast to early development, both the KO and hM280 did not show altered CNPase and MBP protein levels at P70 (Fig. 1G, H). Moreover, these mice did not show any significant changes in the abundance of glial fibrillary acidic protein (GFAP), an astrocyte marker (Raponi et al., 2015), at either age (Fig. 1F, I). These results demonstrate that mice that express the hM280 variant display a decrease in the abundance of CNPase protein and a trending decrease in MBP protein during brain development, but not in adulthood. Together, these data demonstrate that the hM280 mice have a transient developmental myelin phenotype that is distinct from WT and KO mice.

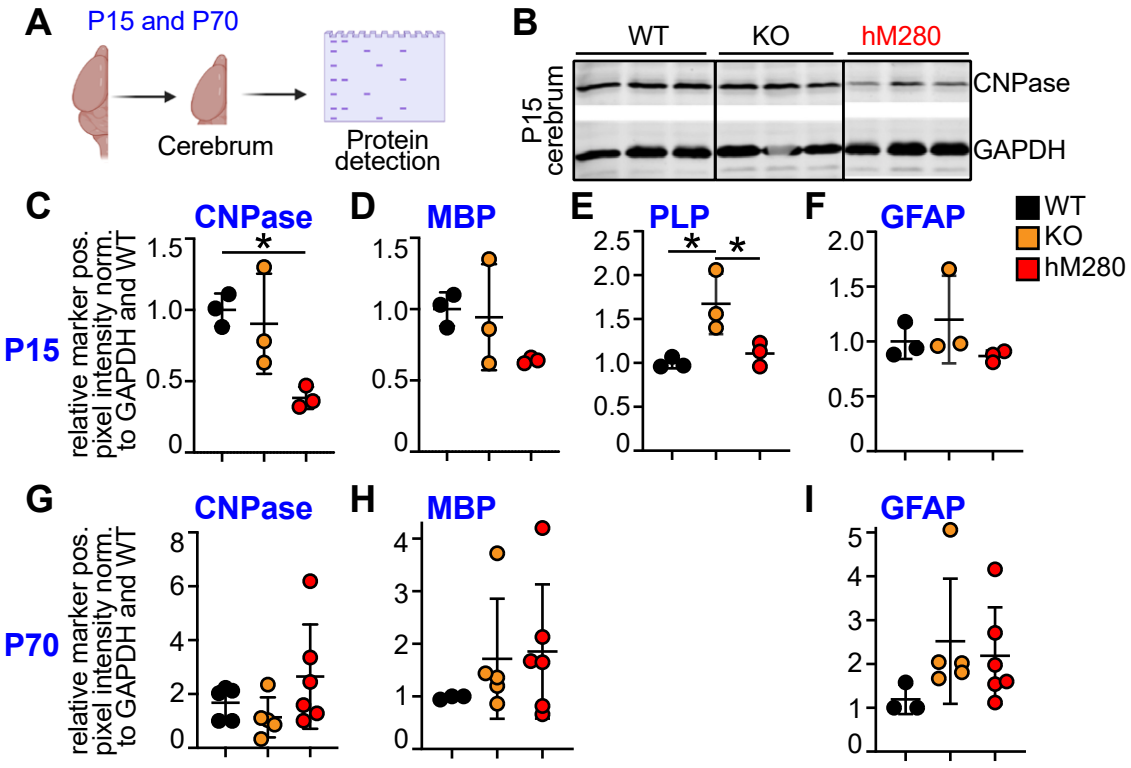
A
P15 and P70
Cerebrum
Protein detection
B
WT
KO
hM280
P15 cerebrum
CNPase
GAPDH
C
CNPase
D
MBP
E
PLP
F
GFAP
WT
KO
hM280
P15
relative marker pos. pixel intensity norm. to GAPDH and WT
G
CNPase
H
MBP
I
GFAP
P70
relative marker pos. pixel intensity norm. to GAPDH and WT

Fig. 1: Myelin protein abundance is perturbed in the developing cerebrum of CX3CR1 knockout (KO) and CX3CR1$^{I249/M280}$ (hM280) mice. A Schematic diagram of the experimental design. P = postnatal day (BioRender). Briefly, P15 and P70 cerebrum lysates were analyzed via western blot in B-I. **B** A representative western blot image from P15 cerebrum total protein lysates probed for CNPase and GAPDH. Lanes were spliced out from the same autoradiogram as indicated by black vertical lines. **C-I** Quantification of B from P15 **(C-F)** and P70 **(G-I)** cerebrum total protein lysates for relative abundance of CNPase, MBP, PLP and GFAP proteins. Each marker+ pixel intensity was normalized to GAPDH and calibrated to WT at respective age. WT=Wild type, KO=Knockout, hM280=CX3CR1$^{I249/M280}$ homozygous, CNPase=2',3'-cyclic-nucleotide 3'-phosphodiesterase, MBP=myelin basic protein, PLP=proteolipid protein, GFAP=glial fibrillary acidic protein, GAPDH=glyceraldehyde-3-phosphate dehydrogenase. All graphs analyzed with 1-way ANOVA followed by Tukey's multiple comparison's test. *$p<0.05$, **$p<0.01$. n=3-9 animals for each genotype. Data are mean +/- SEM.

3.2 hM280 mice have delayed myelination in the stratum lacunosum-moleculare (SLM) of the Cornu Ammonis 1 (CA1) region in the hippocampus at postnatal day 15 (P15).

To confirm my findings from cerebral lysates, and to expand the analysis spatially, thin sagittal brain sections were immunostained for MBP (Fig. 2A-A'). Qualitative analysis of the sections revealed that there were differences in MBP staining between the genotypes in the hippocampus, specifically, in the SLM region which acts as a connecting hub. Within the hippocampus, this connecting region between the entorhinal cortex and CA1 of hippocampus called stratum lacunosum-molecular (SLM), has the highest density of mature oligodendrocytes at P15 (DeFlitch et al., 2022). MBP staining between the WT, KO, and hM280 brains differed in this region; therefore, the hippocampus analysis was focused on the SLM.

Analysis of the MBP mean fluorescence intensity (MFI) showed a ~1.1-fold decrease ($p=0.0317$) in the KO SLM and ~1.3-fold ($p=0.0005$) decrease in the hM280 SLM compared to WT at P15 (Fig. 2B). MBP MFI also showed a ~1.2-fold ($p=0.0339$) decrease in the hM280 SLM compared to KO (Fig. 2B). By P30, the level of MBP abundance in this area was comparable to WT (Fig. 2C). Moreover, at P70, MBP MFI showed no significant changes between WT, KO and hM280 (Fig. 2D). The observed deficit in MBP protein presence at P15 could be a defect in myelination or a secondary response to the absence or reduction in axons. To test the latter, MFI for neurofilament light chain (NFL), a marker of axons (Julien et al., 1986), was measured in the SLM of WT, KO and hM280 brains at P15, 30 and 70 (Fig. 2A'). Fig. 2E-G showed NFL MFI was not altered between the genotypes at any timepoints examined. This suggests that mice that express the hM280 variant display a developmental delay in MBP abundance and that this delay is not due to an absence or decrease in neuronal axons, as measured by NFL.

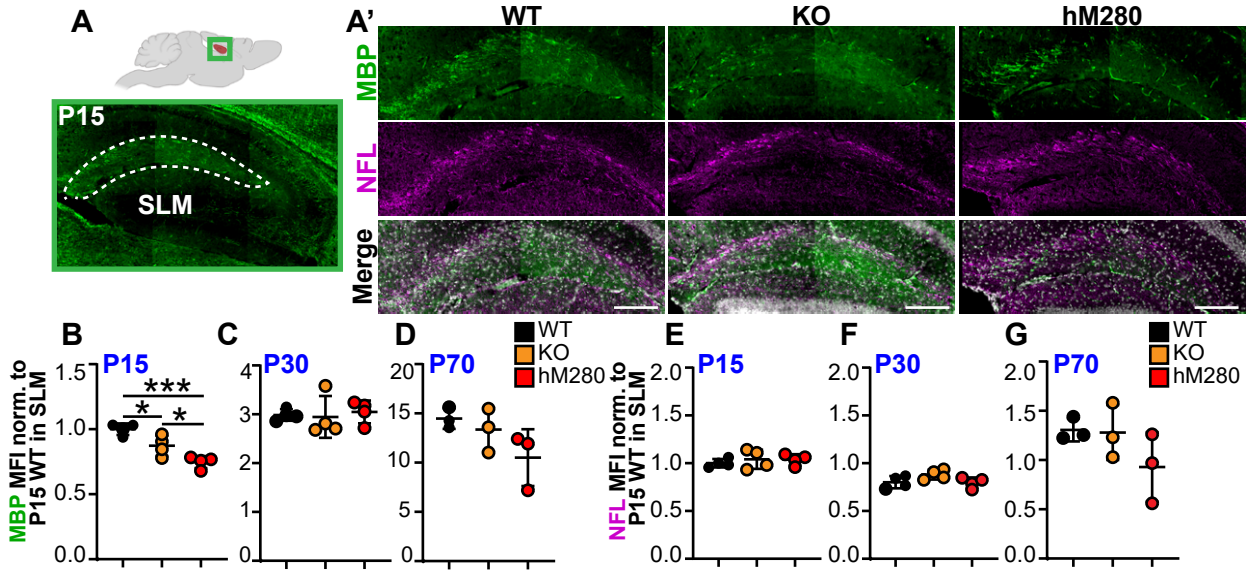
A
P15
SLM
A'
WT
KO
hM280
MBP
NFL
Merge
B
C
D
E
F
G
P15
P30
P70
WT
KO
hM280
MBP MFI norm. to P15 WT in SLM
NFL MFI norm. to P15 WT in SLM
***
*
*

Fig. 2: hM280 mice have delayed myelination in the stratum lacunosum-moleculare (SLM) of the Cornu Ammonis 1 (CA1) region in the hippocampus at postnatal day 15 (P15). A Schematic of the sagittal brain section. Hippocampus is highlighted in red. Representative image of hippocampus immunostained for MBP (green). Region of interest is outlined in white dashed line (SLM) and shown at higher magnification in A' (BioRender). **A'** Representative images of SLM from WT, KO and hM280 P15 samples immunostained for MBP (green), NFL (magenta) and counterstained with Hoechst (white in merge). Scale bars are 200 μm. **B-G** Quantification of MBP **(B-D)** and NFL **(E-G)** mean fluorescence intensity (MFI) in SLM region at P15, P30 and P70. MFI is normalized to P15 WT samples. SLM=stratum-lacunosum moleculare, MBP=myelin basic protein, NFL= neurofilament light chain. All graphs analyzed with 1-way ANOVA followed by Tukey's multiple comparison's test. *$p<0.05$, **$p<0.01$. n=3-4 animals for each genotype. Data are mean +/- SEM.

3.3 hM280 and KO mice have decreased oligodendrocytes in the developing hippocampus.

Neural stem and progenitor cells (NPCs) give rise to oligodendrocyte precursor cells (OPCs). Some OPCs will populate brain parenchyma to establish a pool of adult OPCs and others will differentiate into oligodendrocytes that produce myelin and myelinate the central nervous system axons (Kessaris et al., 2006). To determine whether the decrease in SLM MBP fluorescence at P15 was due to altered levels of oligodendroglia cells, thin sagittal brain sections were immunostained for Olig2 (oligodendrocyte lineage transcription factor 2), which is expressed in OPCs and oligodendrocytes, PDGFRα (platelet-derived growth factor receptor alpha), a marker of OPCs (Kuhn et al., 2019; Nishiyama et al., 1996; Zhu et al., 2014) and CC1 (adenomatous polyposis coli, also known as APC), a marker of oligodendrocytes (Bhat et al., 1996) (Fig. 3A-A').

There was a ~1.3-fold ($p=0.0007$) and a ~1.5-fold ($p<0.0001$) decrease in the proportion of OPCs (% PDGFRα+Olig2+/Olig2+ cells) in the KO compared to WT and hM280 at P15, respectively (Fig. 3B). With regard to oligodendrocytes, there was a statistically significant decrease in the proportion of mature oligodendrocytes (% CC1+Olig2+/Olig2+ cells) in both the KO (a ~1.8-fold [$p<0.001$]) and hM280 (a ~2.3-fold [$p<0.0001$]) compared to WT at P15 (Fig. 3E). Notably, these changes in OPCs and oligodendrocytes were not present at P30 or P70 (Fig. 3C-D, F-G). Thus, mice that express the hM280 variant have delayed formation of oligodendrocytes in the SLM of CA1 in hippocampus at P15.

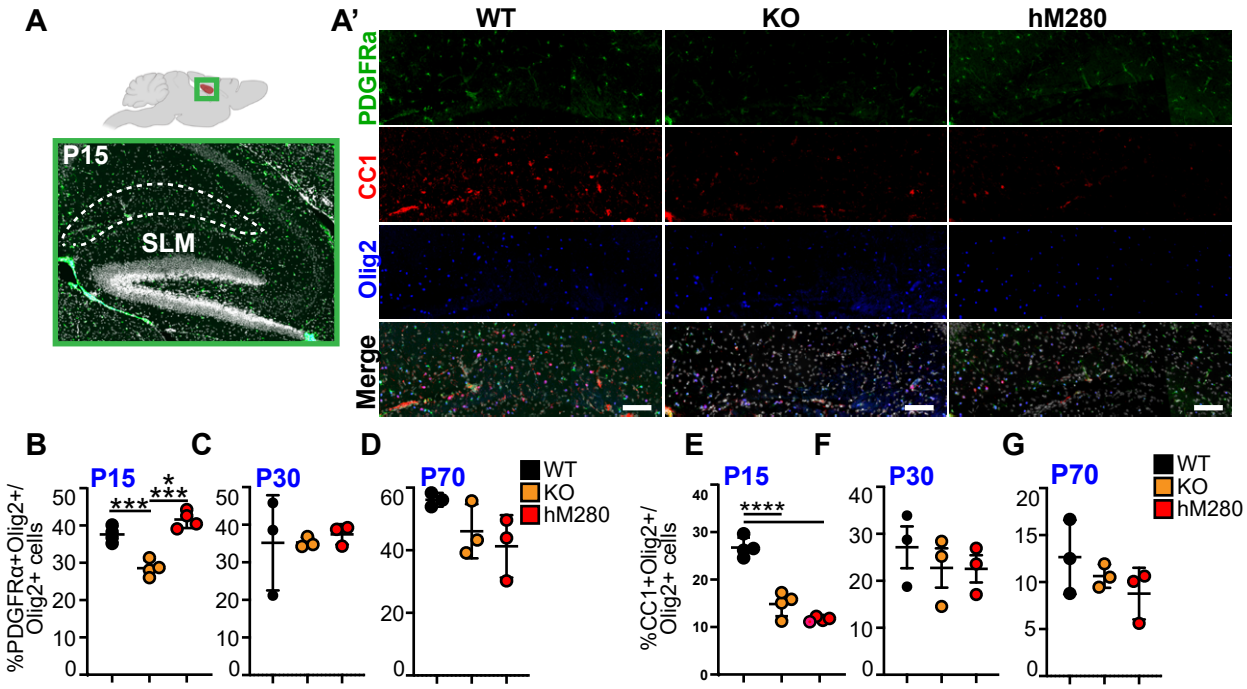
A
A'
WT
KO
hM280
PDGFRa
CC1
Olig2
Merge
P15
SLM
B
C
D
E
F
G
P15
P30
P70
WT
KO
hM280
%PDGFRα+Olig2+/ Olig2+ cells
%CC1+Olig2+/ Olig2+ cells
***
***
*
****

Fig. 3: hM280 and KO mice have decreased oligodendrocytes in the developing hippocampus. A Schematic of the sagittal brain section. Hippocampus is highlighted in red. Representative image of hippocampus immunostained for PDGFRα (green) and Hoechst (white). Region of interest is outlined in white dashed line (SLM) and shown at higher magnification in A' (BioRender). **A'** Representative images of SLM from WT, KO and hM280 P15 samples immunostained for PDGFRα (green), CC1 (red), Olig2 (blue), and counterstained with Hoechst (white in merge). Scale bars are 50 μm. **B-G** Quantification of the proportion of PDGFRα+ OPCs (% PDGFRα+Olig2+/Olig2+ cells) **(B-D)** and CC1+ mature oligodendrocytes (% CC1+Olig2+/Olig2+ cells) **(E-G)** in the SLM region at P15, P30 and P70. All graphs analyzed with 1-way ANOVA followed by Tukey's multiple comparison's test. *p<0.05, **p<0.01, ***p<0.001, ****p<0.0001. n=3-4 animals for each genotype. Data are mean +/- SEM.

3.4 hM280 mice have reduced mature oligodendrocytes in the developing cortical gray matter.

A decrease in both OPCs and oligodendrocytes was observed previously in the cortical regions of the CX3CR1 KO mice at P15 (Voronova et al., 2017). I subsequently expanded the oligodendroglia analysis to P15 corpus callosum (CC, white matter tracts) and cortical grey matter (GM) of WT, KO and hM280 mice as demarcated in Fig. 4A. There were no differences in the proportion of OPCs in the CC and cortical GM between WT, KO, and hM280 mice (Fig. 4B, D). There was a trending decrease in the proportion of oligodendrocytes in the CC of KO and hM280 compared to WT mice that did not reach statistical significance (Fig. 4C). However, there was a ~2-fold ($p=0.0009$) and ~1.7-fold ($p=0.0143$) decrease in the proportion of mature oligodendrocytes in the cortical GM of hM280 mice when compared to WT and KO, respectively, and a trending decrease in the KO mice compared to WT that did not reach statistical significance (Fig. 4E). Thus, mice that express the hM280 variant have decreased proportion of mature oligodendrocytes in both the GM of the hippocampus and the cortex, but not the white matter tracts (CC). The difference between my results showing no statistical differences for OPCs or oligodendrocytes in the developing cortex of the KO mice and a previous report (Voronova et al., 2017) could be due to how data were expressed.

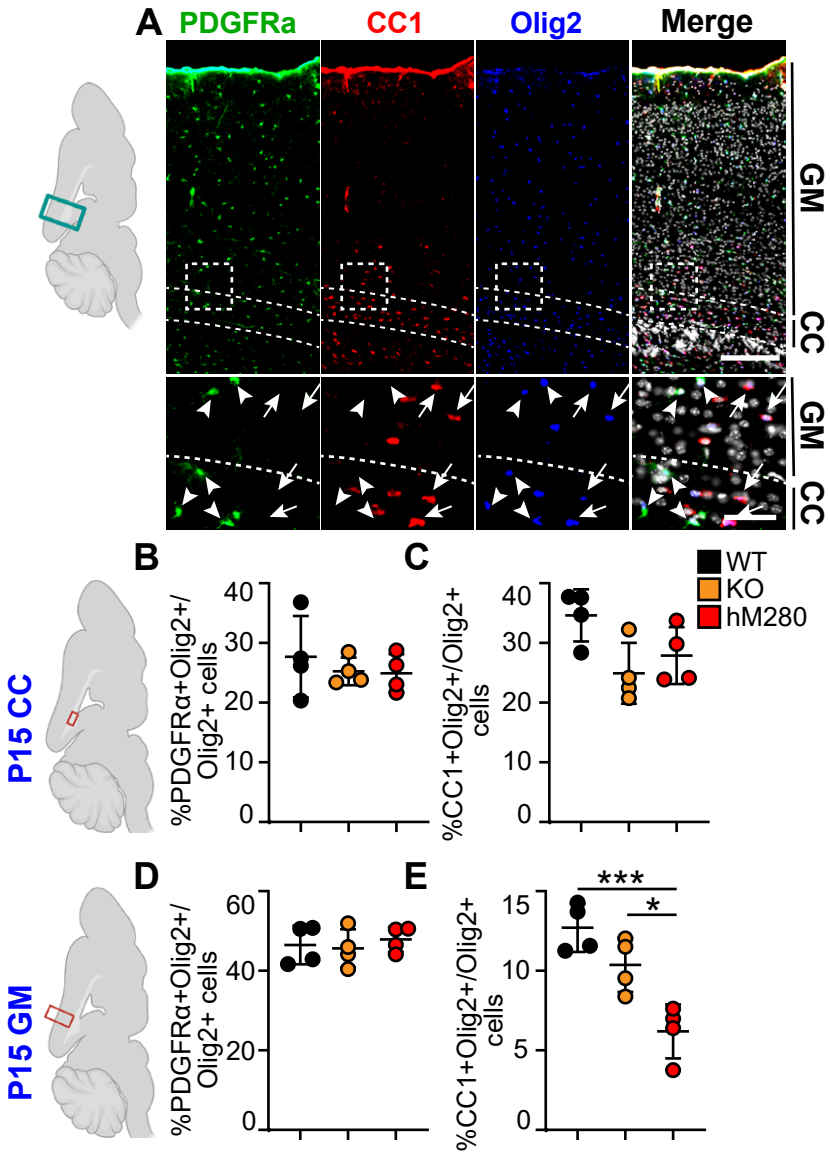
A
PDGFRa
CC1
Olig2
Merge
GM
CC
GM
CC
B
C
WT
KO
hM280
P15 CC
%PDGFRα+Olig2+/ Olig2+ cells
%CC1+Olig2+/Olig2+ cells
D
E
P15 GM
%PDGFRα+Olig2+/ Olig2+ cells
%CC1+Olig2+/Olig2+ cells
***
*

Fig. 4: hM280 mice have reduced mature oligodendrocytes in the developing cortical gray matter. A Schematic of the sagittal brain section on the left with cortical column highlighted in green box. Representative images of the WT cortical column (right, top) showing cortical gray matter (GM) and corpus callosum (CC) immunostained for PDGFRα (green), CC1 (red), Olig2 (blue), and counterstained with Hoechst (white in merge). GM and CC border were identified using Hoechst and MBP staining (not shown). Insets outlined in white dashed boxes are shown at the bottom at higher magnification. Arrow heads are pointing to PDGFRα+Olig2+ OPCs and full arrows are pointing to CC1+Olig2+ mature oligodendrocytes. Scale bars for cortical columns are 200 μm and for insets are50 μm. **B-E** Quantification of the proportion of PDGFRα+ OPCs (% PDGFRα+Olig2+/Olig2+ cells) in CC **(B)** and GM **(D)** and CC1+ mature oligodendrocytes (% CC1+Olig2+/Olig2+ cells) in CC **(C)** and GM **(E)** at P15. All graphs analyzed with 1-way ANOVA followed by Tukey's multiple comparison's test. **$p<0.01$. n=4 animals for each genotype. Data are mean +/- SEM.

3.5 hM280 mice show increased abundance of astrocyte marker glial fibrillary acidic protein (GFAP) in the developing brain.

NPCs also differentiate into another macroglia cell type called astrocytes, starting at embryonic day 18 (E18) (Bayraktar et al., 2015; Burns et al., 2009; Su Akdemir et al., 2020). Therefore, astrocytes were studied in the cortical GM, white matter (CC), and SLM region of the hippocampus by performing immunostaining for GFAP (Raponi et al., 2015) (Fig. 5A). Surprisingly, GFAP MFI analysis showed hM280 mice had a statistically significant increase in GFAP signal in the P15 SLM (~1.3-fold [p=0.0468]), CC (~1.4-fold [p=0.0184]), and GM (~1.2-fold [p=0.0432]) compared to WT (Fig. 5A-D). In contrast, the KO mice showed a ~1.4-fold (p=0.0139) increase in GFAP signal only in the P15 CC (Fig. 5C), with no changes in the SLM or the cortical GM compared to WT (Fig. 5B, D). Changes in GFAP intensity were likely due to an increase in astrocyte numbers and/or an upregulation of the GFAP protein levels in astrocytes (Fig. 5A). Reactive astrocytes upregulate GFAP (Bignami and Dahl, 1976); therefore, mice that express the hM280 variant may have increased astrocyte activation.

In addition, in comparison to WT, both the hM280 and KO show increased GFAP protein presence near the outer edge of the cortex, where pial layer, a part of the blood-brain barrier (BBB), is located (Fig. 5A, white arrows). Astrocytes extend their terminal processes, also known as endfeet, to contact the brain vasculature and help regulate BBB ionic concentrations by expressing KIR4.1 potassium ion channels and aquaporin 4 (Abbott et al., 2006). Therefore, the hM280 and KO mice may have disrupted ionic concentrations and volume regulation at the BBB.

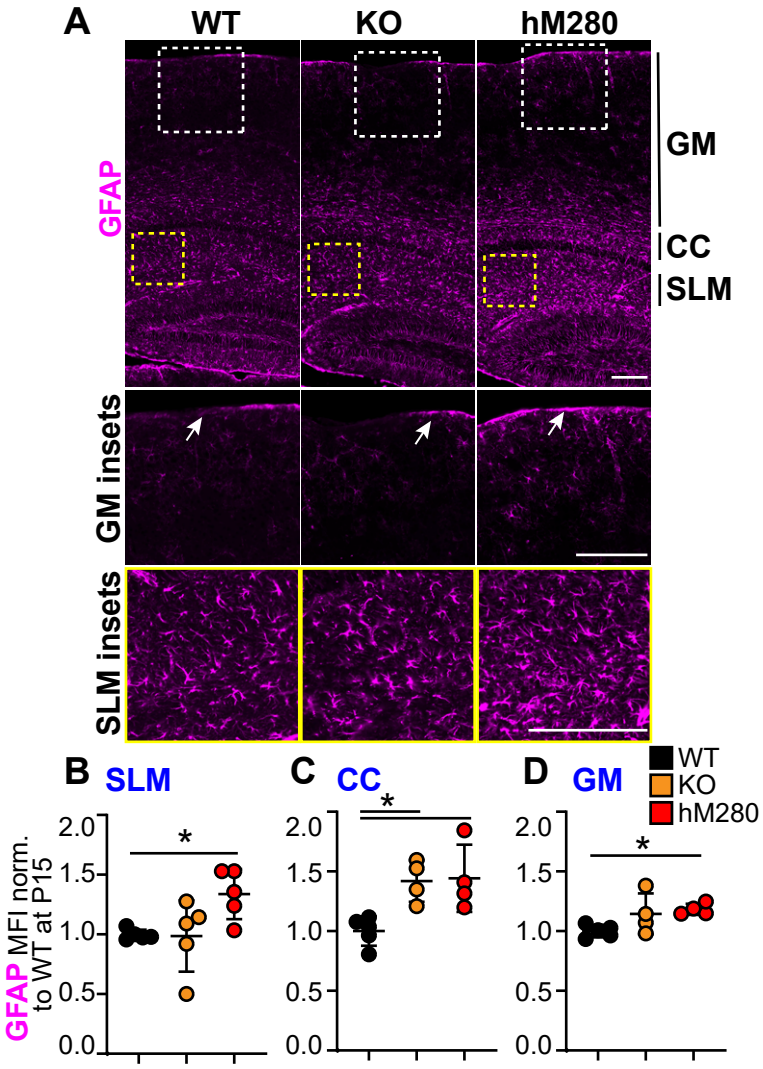
A
WT
KO
hM280
GFAP
GM
CC
SLM
GM insets
SLM insets
B SLM
C CC
D GM
WT
KO
hM280
GFAP MFI norm. to WT at P15
2.0
1.5
1.0
0.5
0.0
*

Fig. 5: hM280 mice show increased abundance of astrocyte marker glial fibrillary acidic protein (GFAP) in the developing brain. A A representative image of the cortical column from WT, KO and hM280 mice with pia layer at the top and hippocampus near the bottom. Images are immunostained for GFAP (magenta). White dashed insets in GM and yellow dashed insets in the SLM are shown at higher magnifications below. White arrows indicate the outer edge of the cortex in the GM insets. Scale bars are 200 μm. **B-D** Quantification of GFAP mean fluorescence intensity (MFI) in the SLM region **(B)**, CC **(C)**, and cortical GM **(D)** at P15. MFI is normalized to WT samples. GFAP=glial fibrillary acidic protein. All graphs analyzed with 1-way ANOVA followed by Dunnett's multiple comparison's test. *$p<0.05$. n=4-5 animals for each genotype. Data are mean +/- SEM.

3.6 hM280 and KO mice show aberrant microglia morphology in the developing hippocampus.

In addition to OPCs, microglia also express CX3CR1 (Harrison et al., 1998). Therefore, microglia were analyzed in the SLM of WT, KO, and hM280 mice using immunostaining for ionized calcium binding adaptor molecule 1 (IBA1), a marker of microglia (Paolicelli et al., 2022). At P15 and P70, the SLM region in both the KO and hM280 mice showed no changes in the density of IBA1+ cells when compared to WT (Fig. 6A-B, D). However, at P30, there was a ~1.5-fold ($p=0.0110$) increase in KO and a ~1.4-fold ($p=0.0302$) increase in hM280 IBA1+ cell density in the SLM region compared to WT (Fig. 6C).

Microglia cells exist on a spectrum between homeostasis and activation (Paolicelli et al., 2022). During homeostasis, microglia display a ramified morphology with many processes (Nimmerjahn et al., 2005). Reactive microglia rapidly replace their resting process with highly motile protrusions and take on a more amoeboid shape (Stence et al., 2001). Thus, microglia activation can be measured indirectly by measuring their transformation index (TI), which uses the perimeter and area of each cell (Torres-Platas et al., 2014). The lower the TI, the more amoeboid the microglia cell and hence, more activated (Fujita et al., 1996; Szabo and Gulya, 2013). The results from Z-stack images of the SLM showed a ~1.6-fold ($p<0.0001$) decrease in KO and a ~1.4-fold ($p<0.0001$) decrease in hM280 microglia TI at P15 compared to WT (Fig. 6E).

These data indicate that both KO and hM280 mice have aberrant microglia morphology, which is indicative of reactive microglia (Kreutzberg, 1996), in the P15 hippocampus without changes in their density. Technical limitations precluded studying microglia ramification in P30 and P70 samples.

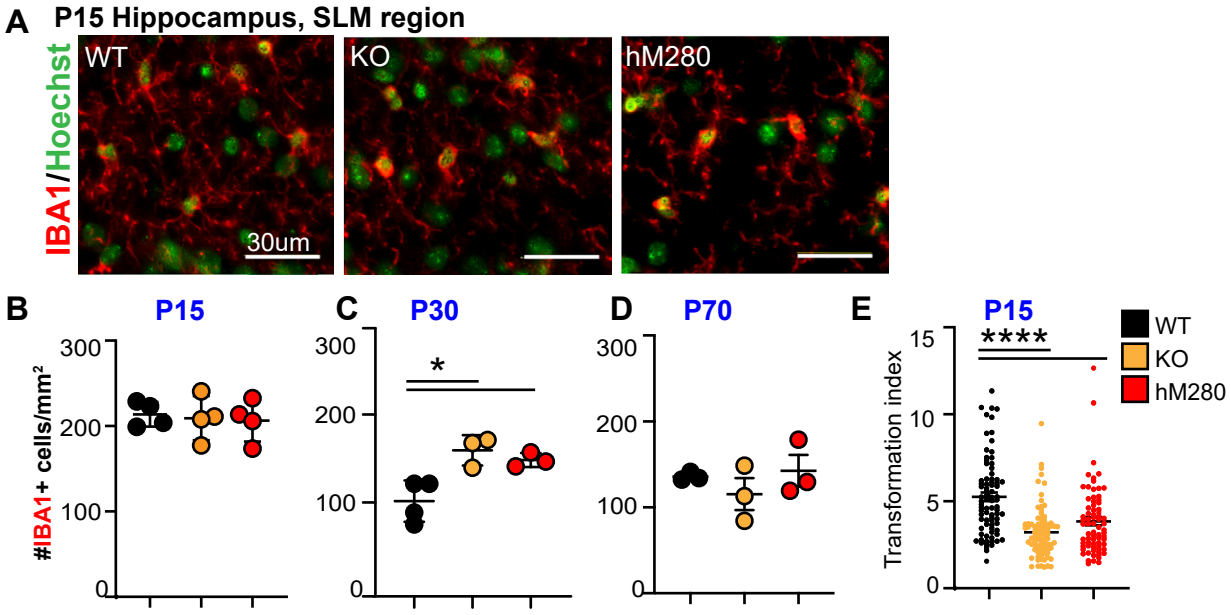
A
P15 Hippocampus, SLM region
IBA1/Hoechst
WT
KO
hM280
30um
B
P15
#IBA1+ cells/mm²
300
200
100
0
C
P30
*
300
200
100
0
D
P70
300
200
100
0
E
P15
****
Transformation index
15
10
5
0
WT
KO
hM280

Fig. 6: hM280 and KO mice show aberrant microglia morphology in the developing hippocampus. A A representative image of P15 SLM region immunostained for IBA1 (red) and counterstained with Hoechst (green). Scale bars are 30 μm. **B-D** Quantification of IBA1+ microglia density in WT, KO, and hM280 SLM at P15 **(B)**, P30 **(C)**, and P70 **(D)**. Each dot represents a mouse. **E** IBA1+ microglia transformation index in WT, KO, and hM280 SLM at P15. Each dot represents an IBA1+ cell. IBA1=ionized calcium-binding adapter molecule 1. **B-D** graphs are analyzed with 1-way ANOVA followed by Tukey's multiple comparison's test. Graph in **E** was analyzed with Dunn's multiple comparison's test and Kruskal-Wallis test. *$p<0.05$, ****$p<0.0001$. n=3-4 animals for each genotype. Data are mean +/-SEM.

3.7 hM280 and KO mice have altered microglia morphology in the developing cortical gray matter.

Since microglia populate the entire brain parenchyma (Ginhoux et al., 2013), the microglia analysis was expanded to the CC and cortical GM. The data showed no statistical differences in the density of microglia cells in either CC or GM of P15 KO and hM280 mice compared to WT (Fig. 7A-C). Previous literature has shown that activated microglia increases the level of IBA1 protein (Hopperton et al., 2018). Therefore, IBA1 mean fluorescence intensity (MFI) per each IBA1+ cell body (without processes) was measured (Fig. 7A, white arrows in insets), analyzing at least 5-10 cells per image or about 40 cells per animal. The results showed a ~1.2-fold ($p<0.0001$) decrease in KO and a ~1.2-fold ($p<0.0001$) increase in hM280 IBA1 MFI in the cortical GM at P15 compared to WT (Fig. 7D). There was a ~1.4-fold ($p<0.0001$) increase in hM280 IBA1 MFI compared to KO in the GM at P15. In addition, representative high-magnification images show the KO and hM280 cortical GM microglia have less processes compared to WT (Fig. 7A, insets). Therefore, the KO and hM280 microglia have varying levels of IBA1 protein abundance and are qualitatively more ameboid (activated) compared to the ramified (resting) WT microglia. Together, this data suggests that while the density of microglia in the P15 cortical GM is comparable between WT, KO and hM280 mice, IBA1+ cells display different morphology and IBA1 protein levels in the KO and hM280 mice, which is indicative of aberrant reactive microglia states.

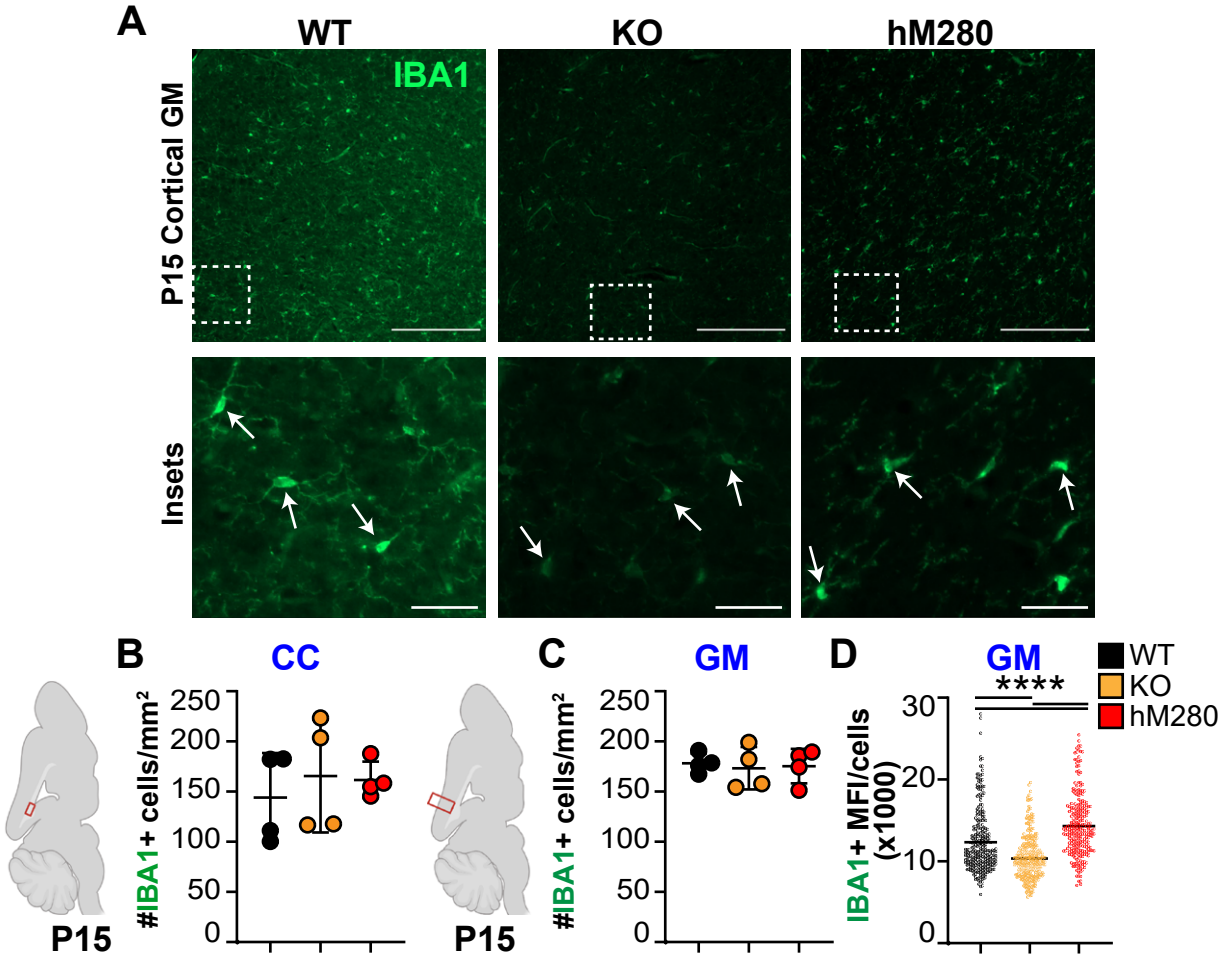
A
WT
KO
hM280
IBA1
P15 Cortical GM
Insets
B
CC
#IBA1+ cells/mm²
250
200
150
100
50
0
P15
C
GM
#IBA1+ cells/mm²
250
200
150
100
50
0
P15
D
GM
****
IBA1+ MFI/cells (x1000)
30
20
10
0
WT
KO
hM280

Fig. 7: hM280 and KO mice have altered microglia morphology in the developing cortical gray matter. A Representative images of P15 WT, KO and hM280 GM immunostained for IBA1 (green). White dashed insets are shown at higher magnification at the bottom. Arrows indicate IBA1+ cell bodies. Scale bars are 200 μm for top images and 50 μm for insets. **B-C** Schematics of the sagittal brain section are on the left side with regions of interest highlighted in red boxes. Quantification of IBA1+ microglia density in WT, KO, and hM280 CC **(B)** and GM **(C)** at P15. Each dot represents a mouse. **D** Quantification of A, where MFI of IBA1 signal in individual cell bodies is analysed in WT, KO, and hM280 GM at P15. Each dot represents an IBA1+ cell body. **B-C** graphs are analyzed with 1-way ANOVA followed by Tukey's multiple comparison's test. Graph in **D** was analyzed with Dunn's multiple comparison's test and Kruskal-Wallis test. ****$p<0.0001$. n=4 animals for each genotype. Data are mean +/- SEM.

3.8 Microglia isolated from hM280 mice display aberrant reactivity *in vitro*.

Microglia can adopt pro-inflammatory (formerly known as M1) or alternatively activated (formerly known as M2) phenotypes (Paolicelli et al., 2022). Pro-inflammatory state can be identified by the presence of specific markers such as Fc gamma III and II receptors (CD16/32) (Ma et al., 2017). Alternatively activated microglia states can be detected by the presence of arginase 1 (Arg1) protein (Ma et al., 2017).

To determine whether KO and hM280 microglia are pro-inflammatory or alternatively activated, P0-2 cerebra including the cortex and hippocampus from WT, KO, and hM280 were dissected and cells were cultured separately. Microglia cells from each genotype were isolated on day 14 and they were stained with antibodies against IBA1, CD16/32, and Arg1 (Fig. 8A-B). The microglia cultures from WT, KO and hM280 were 97-99% enriched in IBA1+ cells (Fig. 8C).

Approximately 10% of all microglia in WT cultures contained CD16/32 or Arg1 (Fig. 8D-E). In comparison to WT cultures, there were no differences in the proportion of CD16/32+IBA1+ cells in the KO and hM280 microglia cultures (Fig. 8D). In contrast, there was a ~1.9-fold ($p=0.0071$) increase in the proportion of Arg1+IBA1+ cells in the hM280, but not KO, cultures compared to WT (Fig. 8E). These data show that the microglia isolated from the hM280 mice have increased Arg1+ microglia, which is indicative of alternatively activated microglia state.

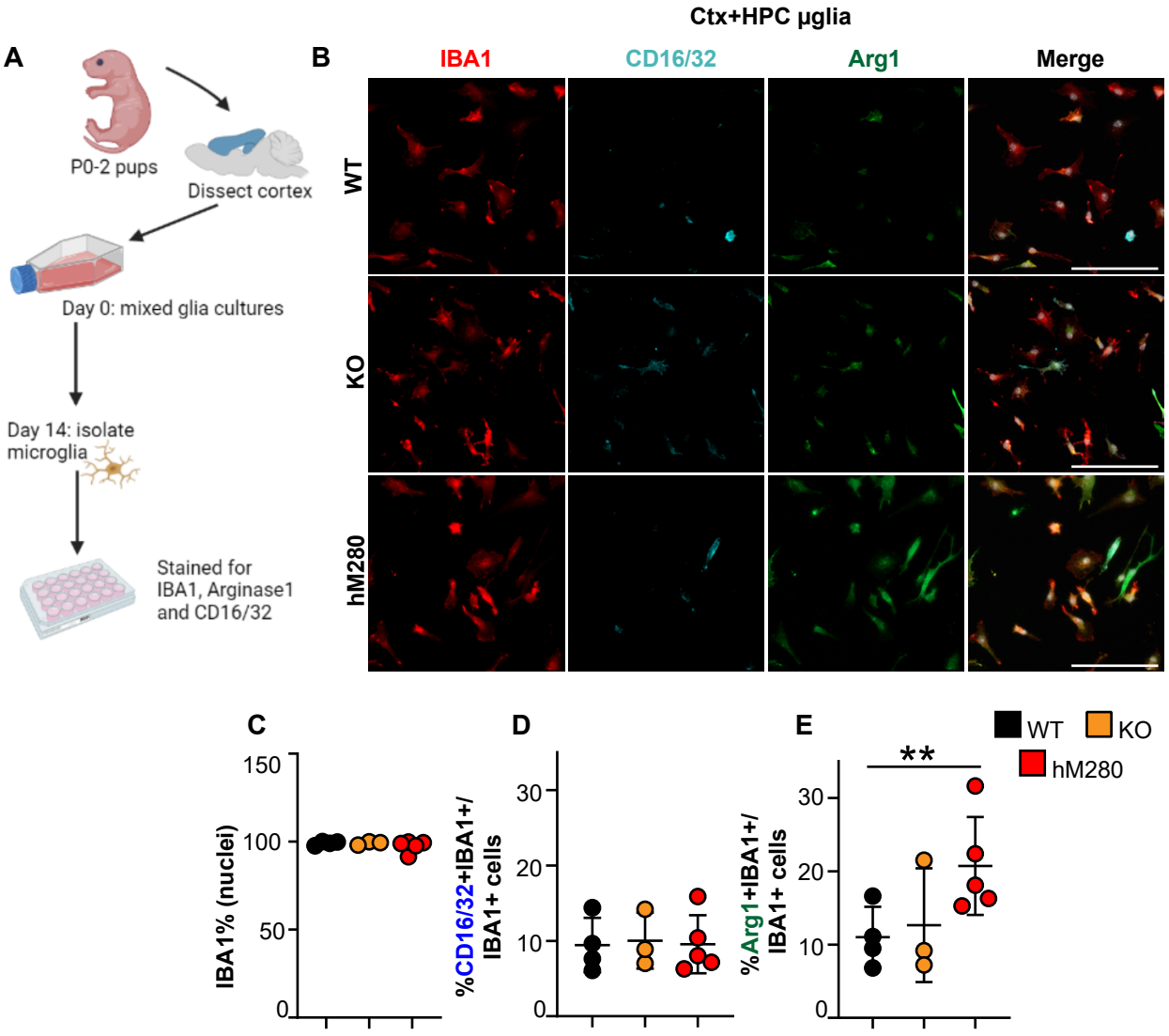
A
P0-2 pups
Dissect cortex
Day 0: mixed glia cultures
Day 14: isolate microglia
Stained for IBA1, Arginase1 and CD16/32
B
Ctx+HPC µglia
IBA1
CD16/32
Arg1
Merge
WT
KO
hM280
C
IBA1% (nuclei)
150
100
50
0
D
%CD16/32+IBA1+/ IBA1+ cells
30
20
10
0
E
%Arg1+IBA1+/ IBA1+ cells
**
30
20
10
0
WT
KO
hM280

Fig. 8: Microglia isolated from hM280 mice display aberrant reactivity *in vitro*. A Schematic diagram of the experimental design (BioRender). **B** Representative images of *in vitro* microglia from WT, KO, and hM280 mice immunostained for IBA1 (red), CD16/32 (cyan), and Arg1 (green). Scale bars are 100 μm. **C-E** Quantification of the proportion of IBA1 (% IBA1+ cells from healthy Hoechst+ cells) **(C)**, CD16/32+IBA1+ (% CD16/32+IBA1+/IBA1+ cells) **(D)**, and Arg1+IBA1+ (% Arg1+IBA1+/IBA1+ cells) **(E)** microglia in WT, KO, and hM280 cultures. CD16/32=Fc gamma II and III, Arg1=arginase1. All graphs analyzed with 1-way ANOVA followed by Dunnett's multiple comparison's test. **p<0.01. n=3-5 replicates for each genotype. Data are mean +/- SEM.

3.9 Tumor necrosis factor alpha (TNFα) and interferon gamma (IFNγ) are decreased in the developing hM280 cerebrum lysates.

Various brain cells secrete and respond to both inflammatory and anti-inflammatory cytokines in the brain (Mousa and Bakhiet, 2013). To identify whether there is altered cytokine protein levels in KO and hM280 mice brain, a multiplex-ELISA experiment was carried out using P15, P30 and P70 cerebrum lysates from WT, KO, and hM280 mice.

Notably, the hM280 brain lysates had a ~3-fold ($p=0.0227$) decrease in the classically defined pro-inflammatory cytokine TNFα (tumor necrosis factor alpha) compared to WT at P15 only (Fig. 9A). In addition, IFNɤ (interferon gamma) was not detected at all in hM280 mice at P15 but was present in WT and KO mice at comparable levels (Fig. 9B). By P70, hM280 mice brains contained TNFα and IFNɤ proteins at comparable levels to WT. In contrast, IL-1β (interleukin-1 beta) and MIP-1α (macrophage inflammatory protein-1 alpha), which are also proinflammatory cytokines, were not altered in KO or hM280 compared to WT (Fig. 9C-D). Other tested cytokines and chemokines were IL-10, IL-6, MCP-1, SDF-1α and VEGF (Fig. 9E-I). They did not show any differences between the genotypes. Brain lysates from cuprizone-demyelinated adult WT brains served as positive controls since this demyelination protocol increases proinflammatory cytokines in the central nervous system (Biancotti et al., 2008; Carlton, 1966; Hiremath et al., 1998; Praet et al., 2014). Specifically, it has been shown that 4-week cuprizone treatment leads to an increase in proinflammatory cytokines TNFα and IL-1β in mice brains (Biancotti et al., 2008). In the current study, an increase in IL-1β but not TNFα was observed in cuprizone treated mice brains (Fig. 9A, C). This conflicting result may be due to the age of the mice at the time of demyelination and the length of cuprizone treatment. The mice in the above study were 25-30 days younger than the ones used here and they were fed cuprizone for 4 weeks while the mice in the current study were fed cuprizone for 6 weeks.

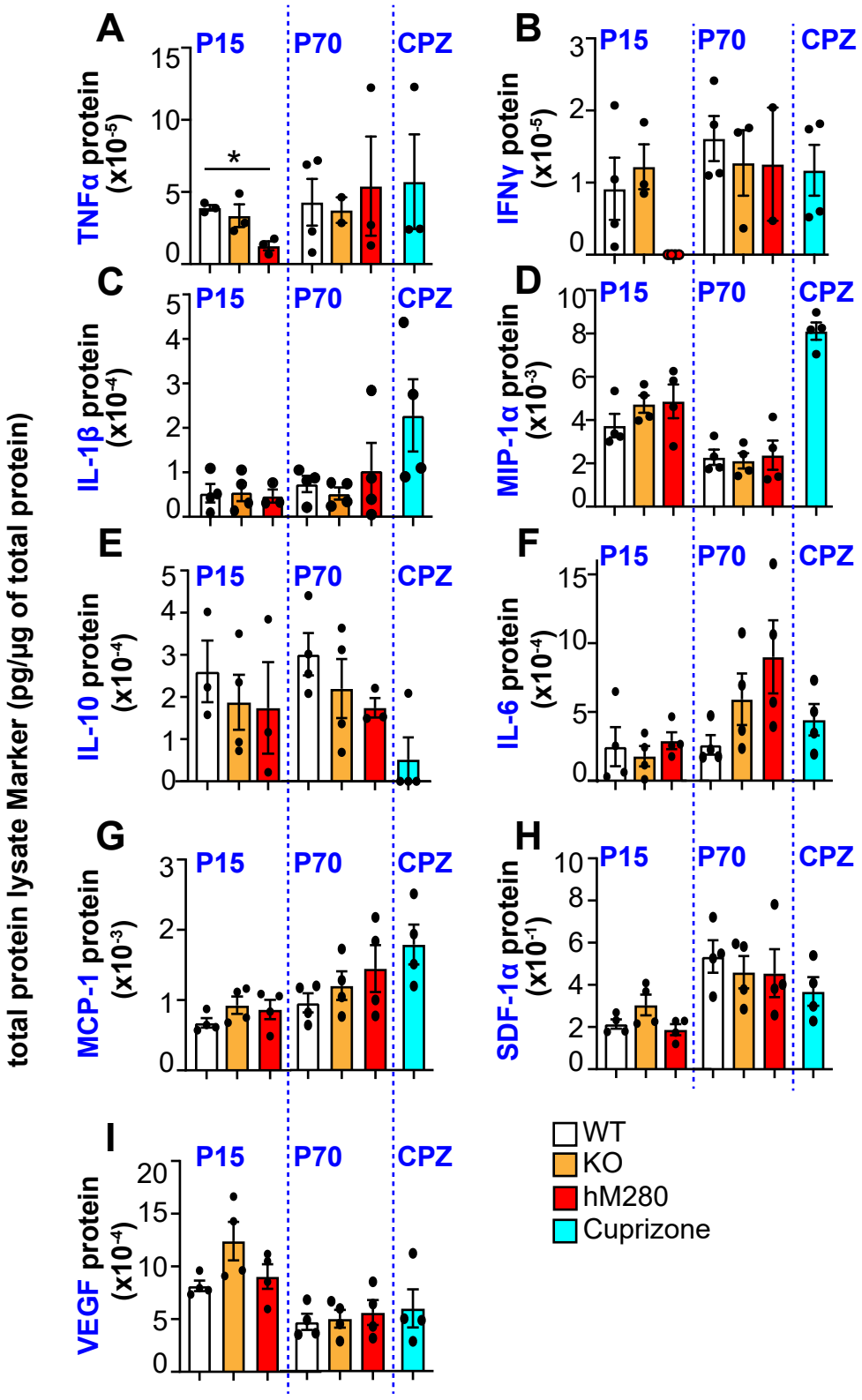
A
TNFα protein (x10-5)
P15
P70
CPZ
*
B
IFNγ potein (x10-5)
C
IL-1β protein (x10-4)
D
MIP-1α protein (x10-3)
E
IL-10 protein (x10-4)
F
IL-6 protein (x10-4)
G
MCP-1 protein (x10-3)
H
SDF-1α protein (x10-1)
I
VEGF protein (x10-4)
total protein lysate Marker (pg/µg of total protein)
WT
KO
hM280
Cuprizone

Fig. 9: Tumor necrosis factor alpha (TNFα) and interferon gamma (IFNγ) are decreased in the developing hM280 cerebrum lysates. A-I Quantification of TNFα **(A)**, IFNγ **(B)**, IL-1β **(C)**, MIP-1α **(D)**, IL-10 **(E)**, IL-6 **(F)**, MCP-1 **(G)**, SDF-1α **(H)**, and VEGF **(I)** cytokines and chemokines in WT, KO, and hM280 P15 and P70 cerebrum lysates per μg of total protein. Cuprizone-demyelinated (CPZ) cerebrum lysates from WT mice served as a positive control. *$p<0.05$. All graphs analyzed with 1-way ANOVA followed by Tukey's multiple comparison's test. n=2-4 animals for each genotype. Data are mean +/- SEM.

3.10 hM280 mice have increased proliferating cells in the developing hippocampus.

To explore whether changes in proliferation exist in KO and hM280 brains compared to WT, P14 mice were injected with 5-bromo-2'-deoxyuridine (BrdU), which is incorporated into proliferating cell's DNA during the S-phase of the cell cycle as a thymidine analogue (Nowakowski et al., 1989). Brains were dissected 24 hours later at P15, and thin, sagittal sections were immunostained for BrdU, Olig2 and IBA1 to identify the density and identity of proliferating cells. Both OPCs and microglia exhibit substantial proliferation in the developing, but none to minimal proliferation in the adult brain (Askew et al., 2017; Rivers et al., 2008). In addition, since most of the oligodendroglia and microglial cellular phenotypes were observed in the developing hM280 and KO brains (Fig. 1C, D, Fig. 2B, Fig. 3B, E, Fig. 4E, Fig. 6E, Fig. 7C), we chose P15 timepoint for analysis of proliferation.

In the P15 SLM, there was a ~6.9-fold ($p=0.0438$) increase in the density of BrdU+ cells in the hM280 samples compared to WT (Fig. 10A-B). When the SLM data were stratified further based on Olig2+ or IBA1+ cells, there was a non-significant increasing trend in the density of Olig2+BrdU+ and IBA1+BrdU+ cells in the hM280 samples when compared to WT (Fig. 10C-D). Next, proliferation analysis was expanded to the CC and cortical GM. There were increasing trends in BrdU+ and Olig2+BrdU+ cells in the hM280 samples compared to WT, which did not reach statistical significance (Fig. 10 E-H). Together, this data indicates that the hM280 mice have an increase in proliferating cells in the SLM but not in the CC and cortical GM.

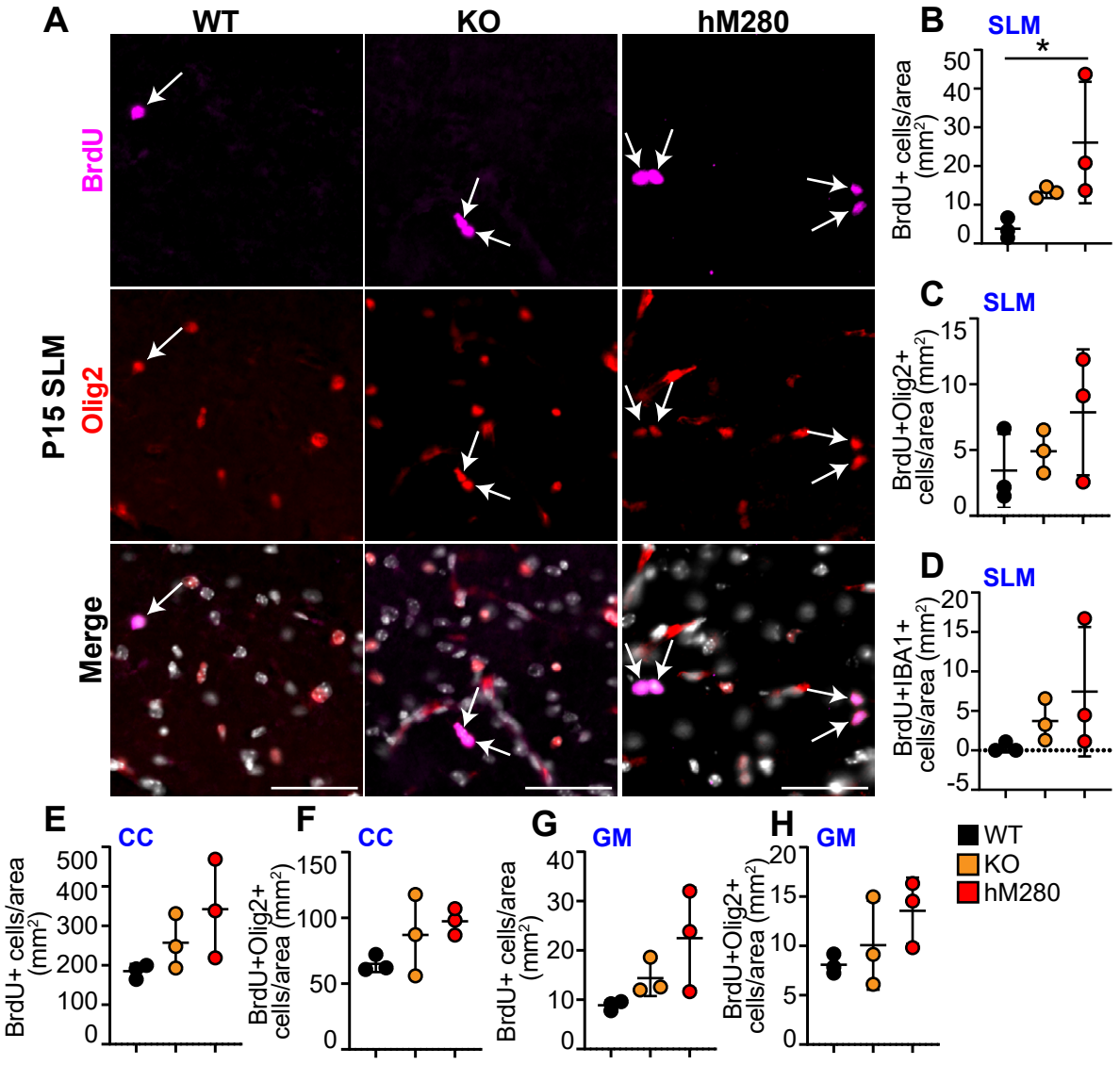
A
WT
KO
hM280
BrdU
Olig2
Merge
P15 SLM
B
SLM
BrdU+ cells/area (mm²)
C
SLM
BrdU+Olig2+ cells/area (mm²)
D
SLM
BrdU+IBA1+ cells/area (mm²)
E
CC
BrdU+ cells/area (mm²)
F
CC
BrdU+Olig2+ cells/area (mm²)
G
GM
BrdU+ cells/area (mm²)
H
GM
BrdU+Olig2+ cells/area (mm²)
WT
KO
hM280

Fig. 10: hM280 mice have increased proliferating cells in the developing hippocampus. A Representative images of P15 WT, KO and hM280 SLM immunostained for BrdU (magenta), Olig2 (red), and counterstained with Hoechst (white in merge). White arrows indicate BrdU+Olig2+ cells. Scale bars are 50 μm. **B-D** Quantification of the density of BrdU+ **(B)**, BrdU+Olig2+ **(C)**, and BrdU+IBA1+ **(D)** cells in the WT, KO and hM280 SLM at P15. **E-H** Quantification of the density of BrdU+ cells in the CC **(E)** and GM **(G)**, and BrdU+Olig2+ cells in the CC **(F)** and GM **(H)** in P15 WT, KO and hM280 mice. BrdU=5-Bromo-2'-deoxyuridine. All graphs analyzed with 1-way ANOVA followed by Dunnett's multiple comparison's test. *$p<0.05$. n=3 animals for each genotype. Data are mean +/- SEM.

3.11 hM280 and KO mice do not have significant changes in apoptosis in the developing brain.

Cell death plays an important role in mammalian brain development (Oppenheim, 1991). In the mouse cerebral cortex, it was discovered that 70% of cortical cells are dying by E14 and 50% by E18; however, very few cells are dying during adulthood (Blaschke et al., 1996). More recently, Mosley et al. 2017 quantified cell apoptosis in various forebrain regions from E17 to P11 using CC3 marker (Mosley et al., 2017). They discovered that in most brain regions, cell death rises and peaks soon after birth followed by a decline to very low levels by P11.

When cells are undergoing a programmed cell death called apoptosis, an enzyme caspase-3 is cleaved in the cytoplasm; thus, activating it (Fernandes-alnemri et al., 1994). The cleaved caspase-3 (CC3) cleaves key proteins such as cell cycle proteins, leading to condensation and cell death (Porter and Jänicke, 1999). To determine changes in cell apoptosis in the developing WT, KO, and hM280 mice, thin brain sections from P15 mice were immunostained for CC3 (Fig. 11A). Fig. 11B-D showed no statistically significant changes in CC3+ cell density in the P15 SLM, CC, and cortical GM of KO and hM280 brains compared to WT.

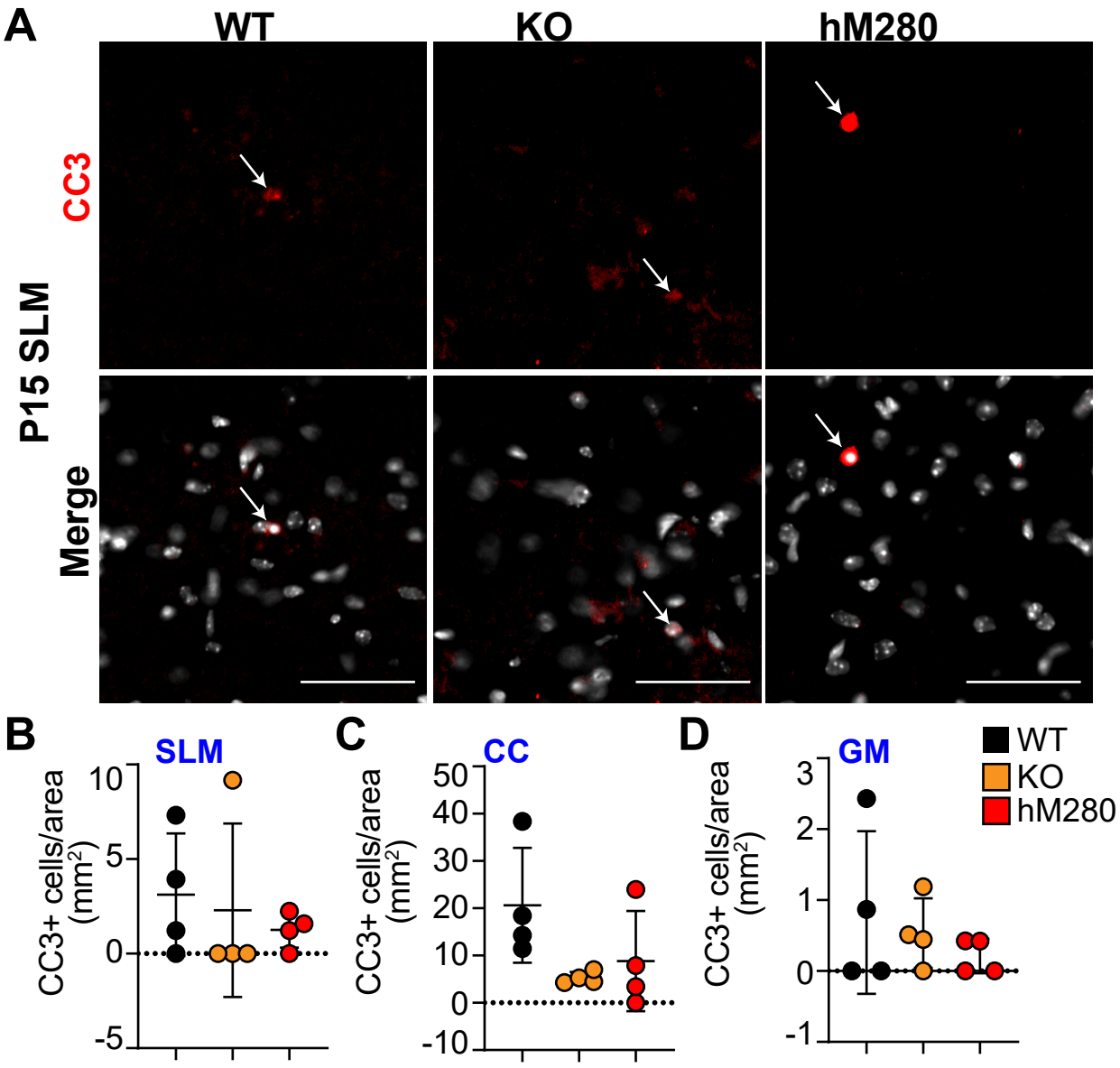
A
WT
KO
hM280
CC3
P15 SLM
Merge
B
SLM
CC3+ cells/area (mm²)
10
5
0
-5
C
CC
CC3+ cells/area (mm²)
50
40
30
20
10
0
-10
D
GM
CC3+ cells/area (mm²)
3
2
1
0
-1
WT
KO
hM280

Fig. 11: hM280 and KO mice do not have significant changes in apoptosis in the developing brain. A Representative image of P15 WT, KO and hM280 SLM immunostained for CC3 (red) and counterstained with Hoechst (white). White arrows indicate CC3+ cells. Scale bars are 50 μm. **B-D** Quantification of the density of CC3+ cells in the SLM **(B)**, CC **(C)**, and GM **(D)** at P15. CC3= cleaved caspase-3. All graphs analyzed with 1-way ANOVA followed by Tukey's multiple comparison's test. n=4 animals for each genotype. Data are mean +/- SEM.

3.12 hM280 and KO mice exhibit increased anxiety in adulthood.

Finally, to ask whether developmental perturbations in brain development affect brain function in adulthood, we subjected 2–3-month-old WT, KO, and hM280 mice to an open field test (OFT) and elevated plus maze (EPM) (Fig. 12A, D). The OFT is a well-accepted measure of locomotion and anxiety (Seibenhener and Wooten, 2015). EPM also tests for anxiety (Walf and Frye, 2007), indicated by a decrease in the amount of time spent in the open arm of the maze (Fig. 12D). The OFT tests showed that KO mice had a ~2-fold ($p<0.0001$) decrease in distance traveled compared to WT and hM280 mice (Fig. 12B), in agreement with previous reports (Méndez-Salcido et al., 2022). In the EPM, both KO and M280 mice had a ~2-fold ($p<0.0001$) decrease and a ~1.4-fold ($p=0.0005$) decrease in distance traveled compared to WT, respectively (Fig. 12E). The KO mice also had a ~1.5-fold ($p=0.004$) decrease in distance traveled compared to hM280 (Fig. 12E). Since KO mice had reduced locomotion, we opted not to measure time spent in center vs periphery of the OFT box. Instead, we measured time spent self-grooming, a well-accepted measure of repetitive behaviour and anxiety (Zhan et al., 2014). The KO mice spent twice as much time self-grooming ($p=0.0009$) compared to WT and 2.5 times as much time self-grooming ($p=0.0007$) compared to hM280 (Fig. 12C). When distance spent in open arms was measured in the EPM, KO mice showed a ~4.7-fold ($p<0.0001$) decrease in the amount of time spent in the open arms compared to WT (Fig. 12F). This is indicative of an anxiety phenotype and is in agreement with previous reports (Méndez-Salcido et al., 2022). While the distance travelled by hM280 mice did not differ from WT in an OFT test (Fig. 12B), it was decreased in an EPM test, but less so when compared to KO (Fig. 12E). In the OFT test, the time spent grooming did not differ between WT and hM280 mice (Fig. 12C). However, hM280 mice spent ~1.6-fold ($p=0.0041$) less time in the open arms compared to WT mice, although this phenotype was less pronounced than in the KO mice (Fig. 12F). These results indicate that mice that express the hM280 variant exhibit an anxiety phenotype in adulthood, but to a lesser extent when compared to KO mice.

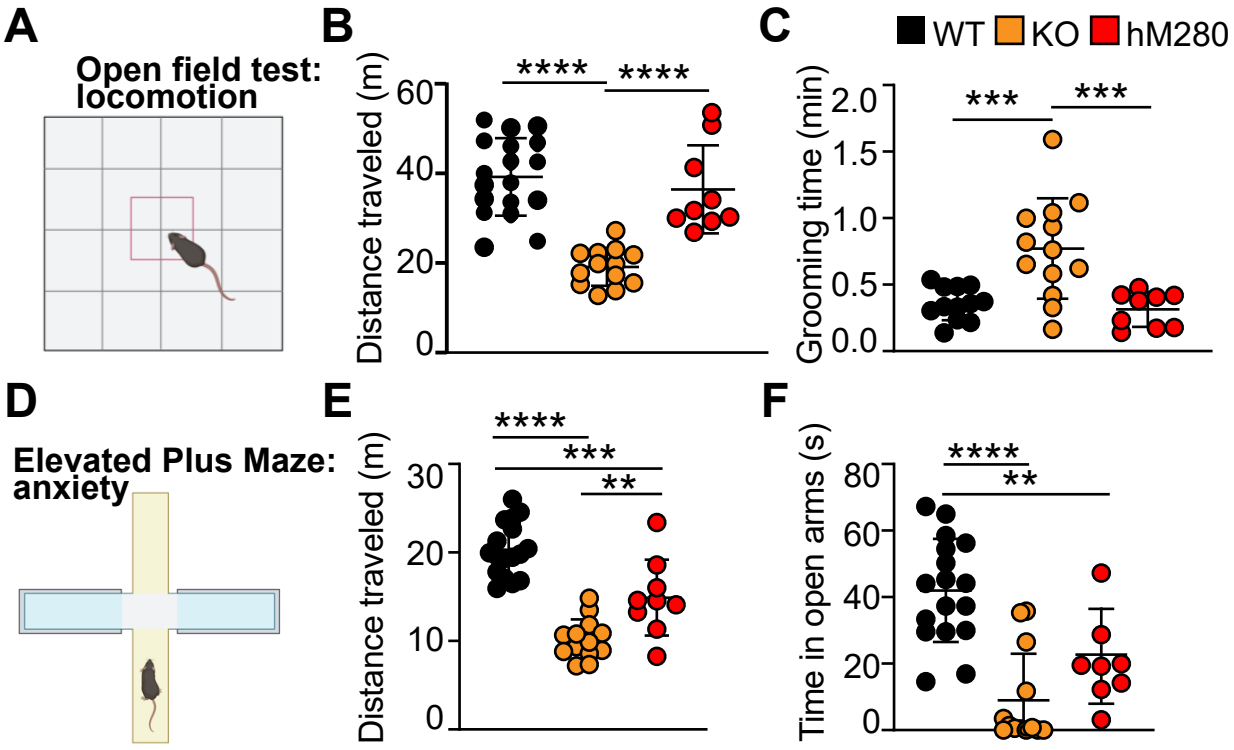
A
Open field test:
locomotion
B
Distance traveled (m)
60
40
20
0
****
****
C
WT
KO
hM280
Grooming time (min)
2.0
1.5
1.0
0.5
0.0
***
***
D
Elevated Plus Maze:
anxiety
E
Distance traveled (m)
30
20
10
0
****
***
**
F
Time in open arms (s)
80
60
40
20
0
****
**

Fig. 12: hM280 and KO mice exhibit increased anxiety in adulthood. A Schematic diagram of the open field test. **B-C** Quantification of the distance traveled **(B)** and grooming time **(C)** of 2-3-month-old WT, KO, and hM280 mice during the 10 minutes spent in the open field test. **D** Schematic diagram of the elevated plus maze. **E-F** Quantification of the distance traveled **(E)** and time spent in the open arms **(F)** of WT, KO, and hM280 mice in the elevated plus maze. All graphs analyzed with 1-way ANOVA followed by Tukey's multiple comparison's test. *$p<0.05$, ***$p<0.001$, ***$p<0.0001$. n=8-17 animals for each genotype. Data are mean +/- SEM.

4 Discussion and conclusions

4.1 Oligodendroglia findings in CX3CR1$^{I249/M280}$ homozygous (hM280) mice

hM280 mice have aberrant myelin protein levels compared to WT mice, specifically during early postnatal development at P15, when oligodendrocytes and myelin first start to develop [reviewed in: (Adnani et al., 2018)]. These changes in myelin protein include a statistically significant decrease in CNPase and a trending decrease in MBP. Notably, these changes in the hM280 brain lysates were not present in the adult cerebrum lysates when compared to WT. When MBP levels was analyzed spatially in sagittal brain sections, the SLM region in the hM280 hippocampus showed decreased MBP staining in the early postnatal, but not adult mice. The change in MBP was not due to the absence of axons as NFL staining was present and comparable to WT. The decrease in MBP in the developing hM280 hippocampus correlated with a decrease in mature oligodendrocytes and not OPCs. Importantly, these changes were not due to altered proliferation or cell death. Therefore, it is likely that the hM280 mice have a decreased OPC differentiation into oligodendrocytes in the early postnatal brain that leads to a developmental delay in myelination. These data from the hippocampus support and extend prior reports that showed decreased oligodendrogenesis in the developing cortex of the CX3CR1 KO mice (Voronova et al. 2017) or in OPCs treated with anti-CX3CR1 function-blocking antibodies *in vitro* (Watson et al., 2021).

However, data presented here on oligodendrogenesis in the developing cortical GM and CC of KO mice differs from a previous study (Voronova et al., 2017). Specifically, the difference between my results showing no statistical differences for OPCs or oligodendrocytes in the developing cortex of the KO mice and a previous report (Voronova et al., 2017) could be due to how data were expressed. My data is expressed as a proportion of OPCs and oligodendrocytes relative to total Olig2+ cells, and the previous report showed average numbers of PDGFRα+ and CC1+ cells. Moreover, the KO mice in my study were generated by inserting the human *CX3CR1* gene with the I249/M280 variants along with a neomycin gene flanked by loxP sites into the endogenous mouse locus; therefore, the variant *CX3CR1* mRNA, but no protein is produced from

the locus. In contrast, the KO mice used in the previous study were generated by knocking in a functional *GFP* gene into the endogenous *CX3CR1* locus; therefore, the *CX3CR1* mRNA and protein were both absent in cells that would normally express the receptor. This may have led to the more severe oligodendroglia decrease observed in both the CC and cortical GM at P15 in the previous study. In addition, the presence of the *GFP* mRNA and protein in cells that normally express the CX3CR1 protein may have negative or off-target effects in the cells, leading to a more pronounced phenotype.

An intriguing question that arises from these data is that while oligodendrocytes are decreased in the hM280 brain at P15, the western blot shows altered changes in the different myelin proteins such as a decrease in CNPase but no change in PLP. It has been recently shown that oligodendrocytes are a heterogenous population in both morphology and transcriptomics [reviewed in: (Floriddia et al., 2020; Lentferink et al., 2018; Marques et al., 2018, 2016; Osanai et al., 2022; Pandey et al., 2022; Valihrach et al., 2022)]. Different oligodendrocytes serve various functions, such as supporting a specific type of axons [reviewed in: (Simons and Nave, 2016)]. Thus, it is possible that the hM280 variant may affect the formation and/or function of a specific group of oligodendrocytes that contain more CNPase and less PLP. Though this specific oligodendrocyte category has not been reported in literature yet, it is known that overexpression of *PLP* gene results in hypomyelination as well as cognitive deficits in mice that include anxiety-like behaviours (Kagawa et al., 1994; Tanaka et al., 2009). On the other hand, hM280 variant may change the protein composition of intact myelin by affecting oligodendrocyte homeostasis. Finally, reduced abundance of myelin-specific proteins can affect myelin biogenesis (Poggi et al., 2016). It is possible that hM280 mice may have aberrant myelin formation and/or changes in axon myelination, which could be investigated by transmission electron microscopy. A limitation of this work is the NFL stain used to mark axons to check for their presence; however, presence may not correlate with function. Active neurons play a role in the proliferation of OPCs and myelination (Barres and Raff, 1993; Gibson et al., 2014; McKenzie et al., 2014; Ortiz et al., 2019; Venkatesh et al., 2015). Moreover, CX3CR1 KO mice show exacerbated axon transport dysfunction in retinal ganglion cells (Breen et al., 2016) that leads to deficits in synaptic pruning, which in turn is associated with weak synaptic transmission and decreased brain connectivity (Zhan et al., 2014). Loss of CX3CR1 results in neurotoxicity in animal models of Parkinson, ALS, and demyelination via lipopolysaccharide injections (Cardona et al. 2006). Therefore, if

axons in CX3CR1 KO and hM280 mice are not functioning properly, it may be affecting myelination in the SLM indirectly. This can be addressed in the future by staining for markers that indicate axon health and by performing electrophysiology.

4.2 Astrocyte findings in hM280 mice

The hM280 mice show increased GFAP marker in the developing grey and white matter compared to WT. This may be due to an increase in astrocyte density and/or an increase in GFAP protein levels by each astrocyte. In contrast, western blot analysis of the whole cerebrum shows that GFAP levels are not altered in hM280 brains compared to WT (Fig. 1F). As cerebrum also contains additional areas, like the thalamus and the striatum, it is possible that the changes in GFAP protein levels are specific to hippocampus and cortex, which were analyzed via IHC. OPCs are known to differentiate into astrocytes and oligodendrocytes (Behar, 2001; Suzuki et al., 2017). My results support and extend a previous publication, where OPCs, differentiated in the presence of anti-FKN or anti-CX3CR1 function blocking antibodies, showed an increase in the formation of astrocytes (Watson et al., 2021). It is possible that hM280 mice display altered OPC fates with increased astrocyte and decreased oligodendrocyte differentiation. In the developing brain, the reduced density of oligodendrocytes leads to less myelination of axons while the increased astrocytes may alter neuronal development. Overall, these displacements from homeostasis may ultimately lead to the anxiety phenotype these mice experience in adulthood.

It is also possible that the elevated GFAP levels in hM280 hippocampus and cortex may indicate astrogliosis, a process during which astrocytes proliferate, increase their cell body as well as GFAP mRNA and protein, and display shorter, stubby processes (Carmignoto et al., 2021). Reactive astrocytes have been observed during regular aging as well as in various diseases, such as AD, MS, and Creutzfeldt-Jakob's disease as well as in EAE (Eng and Ghirnikar, 1994; Verkerke et al., 2021). Therefore, GFAP upregulation in the hM280 mice may indicate an early sign of astrocyte response to a potential injury. Notably, the hM280 cortex had increased GFAP protein levels near the pial layer, where the blood brain barrier (BBB) is located (Fig. 5A, white arrows). This raises questions about whether the BBB may be disrupted in the hM280 mice leading to an "injurious" phenotype. To pursue this question, brain sections can be stained for a specific potassium channel (KIR4.1) or glutamate transporters (EAAT1 and 2) expressed in

astrocyte endfeet in addition to junctional proteins to determine whether the BBB is affected (Carmignoto et al., 2021).

4.3 Microglia findings in hM280 mice

While the density of microglia in the P15 hippocampus and cortex are comparable between WT, KO, and hM280 mice, the KO and hM280 mice displayed altered microglia morphology and/or IBA1 staining. These changes are likely indicative of altered microglia function (Hopperton et al., 2018; Torres-Platas et al., 2014). A previous study showed that microglia in naïve adult hM280 mice cerebellum are more activated (have reduced TI) compared to WT and KO (Cardona et al., 2018). The contrasting results in KO microglia are likely due to the difference in mice age, different housing environments, and/or the region of interest analyzed between the previous study and this work. Moreover, there was an increase in microglia density in KO and hM280 SLM at P30, but not P70 (Fig. 6C, D). At P15, there is a statistically significant increase in BrdU+ cells as well as a trending increase in proliferating microglia in hM280 mice, but not KO. Therefore, the transient increase in hM280 microglia density at P30 could be achieved by compensatory increase in microglia proliferation that occurs sometime between P15 and P30. Altered microglia proliferation in KO mice has been chronicled in literature, including in AD mouse models (Chidambaram et al., 2020; Lee et al., 2010).

Approximately 10% of all *in vitro* WT microglia are positive for CD16/32 or Arg1 protein marker, which is in line with other reports that showed similar levels of pro- and anti-inflammatory marker presence in “naïve” non-polarized microglia cultures (de Almeida et al., 2023; Galleguillos et al., 2022). Further *in vitro* analysis showed an increased proportion of Arg1+IBA1+ cells in the hM280 microglia cultures. This could be indicative of a more protective (alternatively activated) state of microglia (Fig. 8). Recently, it was shown that Arg1+ microglia are found in the brain during early post-natal mouse brain development and that knocking down this population leads to deficits in the hippocampus (Stratoulias et al., 2023). These deficits include deficient neuron innervations and impaired dendritic maturation, which results in impaired cognition in female mice. Since Arg1+ microglia play an important role in post-natal brain development, future experiments identifying Arg1+ microglia in WT, KO and hM280 brains *in vivo* may provide more insight. Moreover, the hM280 brain lysates but not the KO have

reduced concentrations of proinflammatory cytokines TNFα and IFNɤ (Fig. 9). No changes were observed in IL-1β, MIP-1α, IL-10, IL-6, MCP-1, SDF-1α and VEGF. In contrast, a previous study found that CX3CR1 KO mice have increased IL-1β levels in the hippocampus and increased TNFα in the cerebellum at 3-months of age (Rogers et al., 2011). These conflicting results are likely due to the different ages of the mice between the two studies, the different housing facilities where the mice were kept as well as the region analyzed as the current study used whole cerebrum without the cerebellum. Despite the changes in methodology, the hM280 mice have a trending increase in IL-1β protein levels in the brain at P70 (Fig. 9C); however, KO are comparable to WT. This indicates that there may be altered levels of IL-1β protein in KO and hM280 brains at a later time-point, not covered in the current experiment. Future cytokine analysis on older brain lysates may provide more insight into the abundance of these cytokines.

Notably, previous research has found dual roles for TNFα and IFNɤ. Regarding TNFα, the phenotype depends on the TNFα receptor subtype that is activated and the subsequent downstream signaling pathways. An example is in the EAE mouse model, where knocking out TNF receptor 1 has beneficial effects while knocking out TNF receptor 2 exacerbates the disease (Suvannavejh et al., 2000). An additional recent study discovered that exogenous administration of TNF to mice pups from P1 to P5 result in increased locomotor activity two weeks after birth, suggesting that TNF plays a role in early development (Paraschivescu et al., 2022). Similarly, IFNɤ plays a role in processes like adult hippocampal neurogenesis, neuronal connectivity, spatial learning, memory, and social behaviour (Baron et al., 2008; Filiano et al., 2016). Therefore, the TNFα and IFNɤ decrease observed in the hM280 brain lysates at P15 could indicate altered cytokine homeostasis in early development contributing to aberrant developmental myelination and leading to long-term effects in adulthood.

4.4 Comparison of CX3CR1 KO and CX3CR1$^{I249/M280}$ variant

CX3CR1 KO and hM280 mice show similarities and differences at the molecular level in both the hippocampus and cortical gray matter. For example, both genotypes are largely comparable to WT at P70 when analyzing myelin proteins, MBP presence, oligodendroglia, and microglia. Moreover, both genotypes exhibit similar microglia results and astrocyte analysis in the CC at P15 as well as anxiety behaviour in adulthood, though the hM280 anxiety is less severe

than the KO. Notably, when the KO and hM280 phenotypes are similar, the hM280 phenotype appears to be less severe than the KO, such as the microglia density and the transformation index at P30. In contrast, there are differences between the two genotypes that largely occur only at P15. For example, KO mice PLP levels were higher, while hM280 mice had less CNPase compared to WT. Moreover, while KO had a decrease in both OPCs and oligodendrocytes in the SLM at P15, hM280 only had a decrease in oligodendrocytes and MBP protein levels. hM280 mice also show altered abundance of cytokines, which are not observed in the KO at P15. These differences are likely due to the hM280 variant being expressed but with decreased affinity for its ligand fractalkine (Cardona et al., 2018). This result is in line with other animal models, such as the cystic fibrosis mouse models, where null mutations in the cystic fibrosis transmembrane conductance regulator (*CFTR*) gene result in more severe phenotype compared to a variant that decreases the function of the protein instead (reviewed in: (Guilbault et al., 2007)). This suggests that variants with missense mutations and KO mice may not exhibit the same phenotype and therefore, should not be used interchangeably.

4.5 CX3CR1-dependent interaction of microglia and OPCs

In this study, the hM280 and KO mice brains exhibit changes in both oligodendrocyte, and microglia cells during early development. The animal models have either an endogenous expression of the hM280 variant under the CX3CR1 promoter (hM280), or no expression of the *CX3CR1* gene (KO), in all cells that would normally express this gene. Since both OPCs, the precursors to oligodendrocytes, and microglia express CX3CR1, this raises questions about whether the observed results are mainly due to aberrant FKN signaling in microglia or OPCs. According to literature, fractalkine ligand regulates *in vitro* oligodendrocyte formation from NPCs and OPCs in the absence of microglia (Voronova et al., 2017; Watson et al., 2021). Another study treated OPCs and microglia with fractalkine before co-culturing them *in vitro* to discover which cell type largely responded to the ligand, leading to the increase in oligodendrocytes (de Almeida et al., 2023). The results suggest it was necessary to pre-treat both OPCs and microglia with fractalkine to elicit an increase in oligodendrocytes *in vitro*. Pre-treatment of one cell type with fractalkine is not sufficient. However, this and the current study were not able to rule out the contribution of microglia in *in vivo* experiments, where FKN-mediated crosstalk via microglia may also have important biological effects.

Future co-culture experiments are needed to shed more light on the relationship between OPC and microglia in development in the context of the CX3CR1 receptor. A limitation of these experiments is that the cells may change their behaviour due to removing them from their native environment; thus, the results may not be representative of *in vivo* cell behaviour. Alternatively, conditional CX3CR1 KO mice may be developed, where the *CX3CR1* gene can be specifically knocked out in either OPCs or microglia to study its effects *in vivo*.

4.6 Implications of aberrant brain development in adulthood and demyelinating injury

Previous studies show that CX3CR1 KO mice have an anxiety phenotype (Méndez-Salcido et al., 2022; Zhan et al., 2014). Another study also discovered that adult CX3CR1 KO mice have deficits in motor learning; however, their baseline motor skills are comparable to WT as test via an increasing rotarod test (Rogers et al., 2011). The present thesis recapitulates the anxiety phenotype by showing that KO mice do exhibit it in adulthood as measured in an open field test and an elevated plus maze. In addition, these tests were expanded to include the hM280 mice in adulthood, which also show an anxiety phenotype; however, less pronounced than in KO. This may be due to the molecular differences between the KO and the hM280 variant observed in early development as the KO does not express the receptor, but the variant is present with lesser affinity for the ligand. In the future, it will be important to test the baseline motor skills of both CX3CR1 KO and hM280 mice in an increasing rotarod test to ensure that locomotion issues are not a confounding factor in the anxiety phenotype measured by an open field test and elevated plus maze as the measurements depend on movement.

Observing the anxiety phenotype in the hM280 in adulthood raises questions about the influence of early development on later life outcomes. Using the various methods to look at oligodendrocytes and microglia cells, it appears that at P70, the hM280 mice brains are largely comparable to WT whereas there are notable differences at P15, such as oligodendrocyte density in the cortical GM and the SLM of CA1 of the hippocampus. Therefore, despite appearing as comparable to WT by P70, the hM280 mice still exhibit a phenotype in adulthood, raising the possibly that early development may still have implications in adulthood despite the molecular machinery seemingly having caught up to WT.

In addition to the increased anxiety, previous literature shows that CX3CR1 KO and the hM280 variant both exacerbate clinical EAE, induced in adulthood at 8-10 weeks of age) disease in mice (Cardona et al., 2018). Notably, the disease in hM280 mice is less severe than in the KO mice. Moreover, microglia density and activation (decrease in TI) increased in WT, KO and hM280 cerebellum in response to EAE. The FKN ligand protein is increased in naïve KO brain lysates in adulthood compared to WT. Additionally, EAE increases FKN ligand in brain lysates in both WT and KO; however, it remains consistent in hM280 brains. Additional studies show that CX3CR1 KO and hM280 mice have defective clearance of myelin debris by microglia in cuprizone-induced demyelination, leading to more severe demyelination and impaired remyelination (Lampron et al., 2015; Mendiola et al., 2022). These severe outcomes may be attributed to altered KO and hM280 brain development as characterized in this thesis. The CX3CL1-CX3CR1 axis plays a role in communication between neurons, microglia, and OPCs in the brain; therefore, the complete loss (KO) or reduced signaling (hM280) between these cell types in early development has a long-lasting influence. One way that this influence may manifest in adulthood is altered response to external stressor like EAE and cuprizone.

The importance of early development on later life consequences has been shown by others as well. For example, ablating oligodendrocytes during the first postnatal week in mice leads to delayed developmental myelination (Caprariello et al., 2015). While adult CNS in these animals looks comparable to controls, remyelination fails in response to lysolecithin-induced demyelination (Caprariello et al., 2015). The failure occurred despite myelination “catching up” to normal levels in the adult naïve mice. It is tempting to speculate that the exacerbated demyelination and poor remyelination in the hM280 mice may be at least in part due to delayed developmental myelination. This hypothesis is in part supported by the observations that while the oligodendroglial and microglial changes in the developing hM280 mice returns to WT levels by P30 and P70; the behavioral phenotypes are abnormal in adulthood.

During development, embryonic RGCs transition to a quiescent adult NPC during late embryogenesis according to their transcriptional profile (Yuzwa et al., 2017). Therefore, the dormant adult NPCs continue to maintain a core transcriptional identity that is similar to the late embryonic NPCs; however, they are in a non-proliferative state. A recent single-cell profiling study confirmed this finding (Borrett et al., 2020). Moreover, they showed that when adult NPCs

become activated to make neurons, they acquire embryonic RGC-like identity. They concluded that the transition from dormant adult NPC to activated embryonic RGC is a result of the niche environment rather than fundamental changes in cell identity.

A large body of previous research suggests that the re-activation of normal developmental processes are important for repairing CNS damage and injury (reviewed in: (Okano, 2010)). These developmental processes include neurogenesis, gliogenesis, migration, axonal sprouting, and myelination. Re-activating these processes involve both intrinsic factors like expressing a key developmental receptor as well as extrinsic factors like specific embryonic morphogens (Hilton and Bradke, 2017; Tanaka and Ferretti, 2009). Together, this may indicate that regeneration in the brain during adulthood is at least driven in part by the recapitulation of developmental processes. For example, after demyelinating adult mice via cuprizone and allowing them to remyelinate for a week, microglia and oligodendroglia cells largely recapitulated the developmental hippocampus data presented here: no change in KO and hM280 microglia compared to WT, trending decrease in KO and increase in hM280 OPCs compared to WT, and a statistically significant decrease in mature oligodendrocytes in KO and hM280 compared to WT (Mendiola et al., 2022). Specifically, the results presented here from KO and hM280 mice mirror the results in these mice following remyelination after cuprizone-induced demyelination. Therefore, it is possible that the hM280 mice have more severe disease outcomes in response to EAE and cuprizone because their re-activated developmental mechanisms during injury are not effective compared to WT.

References

Abbott, N.J., Rönnbäck, L., Hansson, E., 2006. Astrocyte-endothelial interactions at the blood-brain barrier. Nat. Rev. Neurosci. 7. https://doi.org/10.1038/nrn1824

Adnani, L., Han, S., Li, S., Mattar, P., Schuurmans, C., 2018. Mechanisms of Cortical Differentiation, in: International Review of Cell and Molecular Biology. pp. 223–320. https://doi.org/10.1016/bs.ircmb.2017.07.005

Aguirre, A., Gallo, V., 2007. Reduced EGFR signaling in adult progenitors of the subventricular zone attenuates oligodendrogenesis after demyelination. Neuron Glia Biol. 3, 209–220. https://doi.org/https://doi.org/10.1017/S1740925X08000082

Ajami, B., Bennett, J.L., Krieger, C., Tetzlaff, W., Rossi, F.M.V., 2007. Local self-renewal can sustain CNS microglia maintenance and function throughout adult life. Nat. Neurosci. 10, 1538–1543. https://doi.org/10.1038/nn2014

Alfredsson, L., Olsson, T., 2019. Lifestyle and environmental factors in multiple sclerosis. Cold Spring Harb. Perspect. Med. 9, 1–12. https://doi.org/10.1101/cshperspect.a028944

Allen, N.J., Eroglu, C., 2017. Cell Biology of Astrocyte-Synapse Interactions. Neuron 96, 697–708.

Alliot, F., Godin, I., Pessac, B., 1999. Microglia derive from progenitors, originating from the yolk sac, and which proliferate in the brain. Dev. Brain Res. 117, 145–152. https://doi.org/10.1016/S0165-3806(99)00113-3

Alliot, F., Lecain, E., Grima, B., Pessac, B., 1991. Microglial progenitors with a high proliferative potential in the embryonic and adult mouse brain. Proc. Natl. Acad. Sci. U. S. A. 88, 1541–1545. https://doi.org/10.1073/pnas.88.4.1541

Ambrosini, E., Aloisi, F., 2004. Chemokines and glial cells: A complex network in the central nervous system. Neurochem. Res. 29, 1017–1038. https://doi.org/10.1023/B:NERE.0000021246.96864.89

Angevine, J.B., 1965. Time of neuron origin in the hippocampal region. An autoradiographic study in the mouse. Exp. Neurol. 1–39.

Angevine, J.B., Bodian, D., Coulombre, A.J., Edds, M. V., Hamburger, V., Jacobson, M., Lyser, K.M., Prestige, M.C., Sidman, R.L., Varon, S., Weiss, P.A., 1970. Embryonic vertebrate central nervous system: Revised terminology. Anat. Rec. 166, 257–261. https://doi.org/10.1002/ar.1091660214

Angevine, J.B.J., Sidman, R.L., 1961. Autoradiographic Study of Cell Migration during Histogenesis of Cerebral Cortex in the Mouse. Nature 192, 766–768.

Arli, B., Irkec, C., Menevse, S., Yilmaz, A., Alp, E., 2013. Fractalkine gene receptor polymorphism in patients with multiple sclerosis. Int. J. Neurosci. 123, 31–37.

https://doi.org/10.3109/00207454.2012.723079

Askew, K., Li, K., Olmos-Alonso, A., Garcia-Moreno, F., Liang, Y., Richardson, P., Tipton, T., Chapman, M.A., Riecken, K., Beccari, S., Sierra, A., Molnár, Z., Cragg, M.S., Garaschuk, O., Perry, V.H., Gomez-Nicola, D., 2017. Coupled Proliferation and Apoptosis Maintain the Rapid Turnover of Microglia in the Adult Brain. Cell Rep. https://doi.org/10.1016/j.celrep.2016.12.041

Balia, M., Benamer, N., Angulo, M.C., 2017. A specific GABAergic synapse onto oligodendrocyte precursors does not regulate cortical oligodendrogenesis. Glia 65, 1821–1832.

Bandler, R.C., Mayer, C., Fishell, G., 2017. Cortical interneuron specification: the juncture of genes, time and geometry. Curr. Opin. Neurobiol. 42, 17–24. https://doi.org/10.1016/j.conb.2016.10.003.Cortical

Baranzini, S.E., Oksenberg, J.R., 2017. The genetics of multiple sclerosis: From 0 to 200 in 50 years. Trends Genet. 33, 960–970. https://doi.org/10.1016/j.tig.2017.09.004.The

Baranzini, S.E., Wang, J., Gibson, R.A., Galwey, N., Naegelin, Y., Barkhof, F., Radue, E.-W., Lindberg, R.L.P., Uitdehaag, B.M.G., Johnson, M.R., Angelakopoulou, A., Hall, L., Richardson, J.C., Prinjha, R.K., Gass, A., Geurts, J.J.G., Kragt, J., Sombekke, M., Vrenken, H., Qualley, P., Lincoln, R.R., Gomez, R., Caillier, S.J., George, M.F., Mousavi, H., Guerrero, R., Okuda, D.T., Cree, B.A.C., Green, A.J., Waubant, E., Goodin, D.S., Pelletier, D., Matthews, P.M., Hauser, S.L., Kappos, L., Polman, C.H., Oksenberg, J.R., 2009. Genome-wide association analysis of susceptibility and clinical phenotype in multiple sclerosis. Hum. Mol. Genet. 18, 767–778. https://doi.org/10.1093/hmg/ddn388

Barnabe-Heider, F., Wasylnka, J.A., Fernandes, K.J.L., Porsche, C., Sendtner, M., Kaplan, D.R., Miller, F.D., 2005. Evidence that Embryonic Neurons Regulate the Onset of Cortical Gliogenesis via Cardiotrophin-1. Neuron 48, 253–265.

Barnat, M., Capizzi, M., Aparicio, E., Boluda, S., Wennagel, D., Kacher, R., Kassem, R., Lenoir, S., Agasse, F., Bra, B.Y., Liu, J.P., Ighil, J., Tessier, A., Zeitli, S.O., Duyckaerts, C., Dommergues, M., Durr, A., Humbert, S., 2020. Huntington's disease alters human neurodevelopment. Science (80-.). 369, 787–793. https://doi.org/10.1126/science.aax3338

Baron, R., Nemirovsky, A., Harpaz, I., Cohen, H., Owens, T., Monsonego, A., 2008. IFN-gamma enhances neurogenesis in wild-type mice and in a mouse model of Alzheimer's disease. FASEB J. 8, 2843–2852.

Barres, B.A., Hart, I.K., Coles, H.S.R., Burne, J.F., Voyvodic, J.T., Richardson, W.D., Raff, M.C., 1992. Cell death and control of cell survival in the oligodendrocyte lineage. Cell 70, 31–46. https://doi.org/10.1016/0092-8674(92)90531-G

Barres, B.A., Raff, M.C., 1993. Proliferation of oligodendrocyte precursor cells depends on electrical activity in axons. Nature 361, 258–260. https://doi.org/10.1038/361258a0

Barres, B.A., Schmid, R., Sendnter, M., Raff, M.C., 1993. Multiple extracellular signals are required for long-term oligodendrocyte survival. Development 118, 283–295. https://doi.org/10.1242/dev.118.1.283

Baumann, N., Pham-Dinh, D., 2001. Biology of oligodendrocyte and myelin in the mammalian central nervous system. Physiol. Rev. 81, 871–927. https://doi.org/10.1152/physrev.2001.81.2.871

Bayer, S.A., Altman, J., 1991. Neocortical development. Raven Press, New York.

Bayraktar, O.A., Fuentealba, L.C., Alvarez-Buylla, A., Rowitch, D.H., 2015. Astrocyte development and heterogeneity. Cold Spring Harb. Perspect. Biol. 7. https://doi.org/10.1101/cshperspect.a020362

Bazan, J.F., Bacon, K.B., Hardiman, G., Wang, W., Soo, K., Rossi, D., Greaves, D.R., Zlotnik, A., Schall, T.J., 1997. A new class of membrane-bound chemokine with a CX3C motif. Nature 385, 640–642. https://doi.org/10.1038/385640a0

Beeldman, E., Raaphorst, J., Twennaar, M.K., De Visser, M., Schmand, B.A., De Haan, R.J., 2015. The cognitive profile of ALS: A systematic review and meta-analysis update. J. Neurol. Neurosurg. Psychiatry 87, 1–9. https://doi.org/10.1136/jnnp-2015-310734

Behar, T.N., 2001. Analysis of fractal dimension of 02A glial cells differentiating in vitro. Methods 24, 331–339. https://doi.org/10.1006/meth.2001.1203

Ben Haim, L., Rowitch, D.H., 2016. Functional diversity of astrocytes in neural circuit regulation. Nat. Rev. Neurosci. 18, 31–41. https://doi.org/10.1038/nrn.2016.159

Bhat, R. V., Axt, K.J., Fosnaugh, J.S., Smith, K.J., Johnson, K.A., Hill, D.E., Kinzler, K.W., Baraban, J.M., 1996. Expression of the APC tumor suppressor protein in oligodendroglia. Glia 17, 169–174.

Biancotti, J.C., Kumar, S., Vellis, J. de, 2008. Activation of Inflammatory Response by a Combination of Growth Factors in Cuprizone-Induced Demyelinated Brain Leads to Myelin Repair. Neurochem Res 33, 2615–2628. https://doi.org/10.1007/s11064-008-9792-8

Bignami, A., Dahl, D., 1976. The astroglial response to stabbing. Immunofluorescence studies with antibodies to astrocyte-specific protein (GFA) in mammalian and submammalian vertebrates. Neuropathol. Appl. Neurobiol. 2, 99–110. https://doi.org/10.1111/j.1365-2990.1976.tb00488.x

Bjornevik, K., Cortese, M., Healy, B.C., Kuhle, J., Mina, M.J., Leng, Y., Elledge, S.J., Niebuhr, D.W., Scher, A.I., Munger, K.L., Ascherio, A., 2022. Longitudinal analysis reveals high prevalence of Epstein-Barr virus associated with multiple sclerosis. Science (80-.). 375, 296–301. https://doi.org/10.1126/science.abj8222

Blaschke, A.J., Staley, K., Chun, J., 1996. Widespread programmed cell death in proliferative and postmitotic regions of the fetal cerebral cortex. Development 122, 1165–1174.

https://doi.org/10.1242/dev.122.4.1165

Block, M.L., Zecca, L., Hong, J.S., 2007. Microglia-mediated neurotoxicity: Uncovering the molecular mechanisms. Nat. Rev. Neurosci. 8, 57–69. https://doi.org/10.1038/nrn2038

Bond, A.M., Berg, D.A., Lee, S., Garcia-Epelboim, A.S., Adusumilli, V.S., Ming, G.L., Song, H., 2020. Differential timing and coordination of neurogenesis and astrogenesis in developing mouse hippocampal subregions. Brain Sci. 10, 1–14. https://doi.org/10.3390/brainsci10120909

Bond, A.M., Ming, G.L., Song, H., 2015. Adult Mammalian Neural Stem Cells and Neurogenesis: Five Decades Later. Cell Stem Cell. https://doi.org/10.1016/j.stem.2015.09.003

Borrett, M.J., Innes, B.T., Jeong, D., Tahmasian, N., Storer, M.A., Bader, G.D., Kaplan, D.R., Miller, F.D., 2020. Single-Cell Profiling Shows Murine Forebrain Neural Stem Cells Reacquire a Developmental State when Activated for Adult Neurogenesis. Cell Rep. 32. https://doi.org/10.1016/j.celrep.2020.108022

Breen, K.T., Anderson, S.R., Steele, M.R., Calkins, D.J., Bosco, A., Vetter, M.L., 2016. Loss of fractalkine signaling exacerbates axon transport dysfunction in a chronic model of glaucoma. Front. Neurosci. 10, 1–15. https://doi.org/10.3389/fnins.2016.00526

Burns, K.A., Murphy, B., Danzer, S.C., Kuan, C.Y., 2009. Developmental and post-injury cortical gliogenesis: A genetic fate-mapping study with nestin-CreER mice. Glia 57, 1115–1129. https://doi.org/10.1002/glia.20835

Bushong, E.A., Martone, M.E., Ellisman, M.H., 2004. Maturation of astrocyte morphology and the establishment of astrocyte domains during postnatal hippocampal development. Int. J. Dev. Neurosci. 22, 73–86. https://doi.org/10.1016/j.ijdevneu.2003.12.008

Butts, B.D., Houde, C., Mehmet, H., 2008. Maturation-dependent sensitivity of oligodendrocyte lineage cells to apoptosis: Implications for normal development and disease. Cell Death Differ. 15, 1178–1186. https://doi.org/10.1038/cdd.2008.70

Cai, J., Qi, Y., Hu, X., Tan, M., Liu, Z., Zhang, J., Li, Q., Sander, M., Qiu, M., 2005. Generation of Oligodendrocyte Precursor Cells from Mouse Dorsal Spinal Cord Independent of Nkx6 Regulation and Shh Signaling. Neuron 45.

Calvi, A., Haider, L., Prados, F., Tur, C., Chard, D., Barkhof, F., 2022. In vivo imaging of chronic active lesions in multiple sclerosis. Mult. Scler. J. 28, 683–690. https://doi.org/10.1177/https

Campanella, G.S.V., Tager, A.M., El Khoury, J.K., Thomas, S.Y., Abrazinski, T.A., Manice, L.A., Colvin, R.A., Luster, A.D., 2008. Chemokine receptor CXCR3 and its ligands CXCL9 and CXCL10 are required for the development of murine cerebral malaria. Proc. Natl. Acad. Sci. U. S. A. https://doi.org/10.1073/pnas.0801544105

Caprariello, A. V., Batt, C.E., Zippe, I., Romito-Digiacomo, R.R., Karl, M., Miller, R.H., 2015. Apoptosis of oligodendrocytes during early development delays myelination and impairs subsequent responses to demyelination. J. Neurosci. 35, 14031–14041. https://doi.org/10.1523/JNEUROSCI.1706-15.2015

Cardona, S.M., Kim, S. V., Church, K.A., Torres, V.O., Cleary, I.A., Mendiola, A.S., Saville, S.P., Watowich, S.S., Parker-Thornburg, J., Soto-Ospina, A., Araque, P., Ransohoff, R.M., Cardona, A.E., 2018. Role of the fractalkine receptor in CNS autoimmune inflammation: new approach utilizing a mouse model expressing the human CX3CR1I249/M280 variant. Front. Cell. Neurosci. 12, 1–17. https://doi.org/10.3389/fncel.2018.00365

Carlton, W., 1966. Response of mice to the chelating agents sodium diethyldithiocarbamate, alpha-benzoinoxime, and biscyclohexanone oxaldihydrazone. Toxicol. Appl. Pharmacol. 8, 512–521.

Carmignoto, G., Agarwal, A., Allen, N.J., Araque, A., Barbeito, L., Quintana, F.J., Ransohoff, R.M., Riquelme-perez, M., Robel, S., 2021. Reactive astrocyte nomenclature, definitions, and future directions. Nat. Neurosci. 24, 312–325.

Carroll, W.M., Jennings, A.R., Ironside, L.J., 1998. Identification of the adult resting progenitor cell by autoradiographic tracking of oligodendrocyte precursors in experimental CNS demyelination. Brain 121, 293–302. https://doi.org/10.1093/brain/121.2.293

Caviness, V.S., Sidman, R.L., 1973. Time of origin or corresponding cell classes in the cerebral cortex of normal and reeler mutant mice: an autoradiographic analysis. J. Comp. Neurol. 148, 141–152.

Caviness, V.S., Takahashi, T., 1995. Proliferative events in the cerebral ventricular zone. Brain Dev. 17, 159–163. https://doi.org/10.1016/0387-7604(95)00029-B

Chauhan, P., Jethwa, K., Rathawa, A., Chauhan, G., Mehra, S., 2021. The Anatomy of the Hippocampus, in: R, P. (Ed.), Cerebral Ischemia. Exon Publications, pp. 17–30. https://doi.org/10.36255/exonpublications.cerebralischemia.2021.hippocampus

Chidambaram, H., Das, R., Chinnathambi, S., 2020. Interaction of Tau with the chemokine receptor, CX3CR1 and its effect on microglial activation, migration and proliferation. Cell Biosci. 10, 1–9. https://doi.org/10.1186/s13578-020-00474-4

Chitu, V., Stanley, E.R., 2006. Colony-stimulating factor-1 in immunity and inflammation. Curr. Opin. Immunol. 18, 39–48. https://doi.org/10.1016/j.coi.2005.11.006

Christidi, F., Karavasilis, E., Velonakis, G., Ferentinos, P., Rentzos, M., Kelekis, N., Evdokimidis, I., Bede, P., 2018. The clinical and radiological spectrum of hippocampal pathology in amyotrophic lateral sclerosis. Front. Neurol. 9, 1–11. https://doi.org/10.3389/fneur.2018.00523

Clayton, B.L.L., Tesar, P.J., 2021. Oligodendrocyte progenitor cell fate and function in development and disease. Curr. Opin. Cell Biol. 73, 35–40.

https://doi.org/10.1016/j.ceb.2021.05.003

Connolly, B., Fox, S.H., 2014. Treatment of Cognitive, Psychiatric, and Affective Disorders Associated with Parkinson's Disease. Neurotherapeutics 11, 78–91. https://doi.org/10.1007/s13311-013-0238-x

Cossmann, P.H., Eggli, P.S., Christ, B., Kurz, H., 1997. Mesoderm-derived cells proliferate in the embryonic central nervous system: Confocal microscopy and three-dimensional visualization. Histochem. Cell Biol. 107, 205–213. https://doi.org/10.1007/s004180050105

Cotsapas, C., Mitrovic, M., Hafler, D., 2012. Multiple Sclerosis, in: Handbook of Clinical Neurology. pp. 723–730. https://doi.org/https://doi.org/10.1016/B978-0-444-64076-5.00046-6

Dale, J.K., Vesque, C., Lints, T.J., Sampath, T.K., Furley, A., Dodd, J., Placzek, M., 1997. Cooperation of BMP7 and SHH in the induction of forebrain ventral midline cells by prechordal mesoderm. Cell 90, 257–269. https://doi.org/10.1016/S0092-8674(00)80334-7

de Almeida, M.M.A., Watson, A.E.S., Bibi, S., Dittmann, N.L., Goodkey, K., Sharafodinzadeh, P., Galleguillos, D., Nakhaei-Nejad, M., Kosaraju, J., Steinberg, N., Wang, B.S., Footz, T., Giuliani, F., Wang, J., Sipione, S., Edgar, J.M., Voronova, A., 2023. Fractalkine enhances oligodendrocyte regeneration and remyelination in a demyelination mouse model. Stem Cell Reports. https://doi.org/10.1016/j.stemcr.2022.12.001

DeFlitch, L., Gonzalez-Fernandez, E., Crawley, I., Kang, S.H., 2022. Age and Alzheimer's Disease-Related Oligodendrocyte Changes in Hippocampal Subregions. Front. Cell. Neurosci. 16, 1–14. https://doi.org/10.3389/fncel.2022.847097

Delgado, A.C., Maldonado-Soto, A.R., Silva-Vargas, V., Mizrak, D., Von Känel, T., Tan, K.R., Paul, A., Madar, A., Cuervo, H., Kitajewski, J., Lin, C.S., Doetsch, F., 2021. Release of stem cells from quiescence reveals gliogenic domains in the adult mouse brain. Science (80-.). 372, 1205–1209. https://doi.org/10.1126/science.abg8467

Derouet, D., Rousseau, F., Alfonsi, F., Froger, J., Hermann, J., Barbier, F., Perret, D., Diveu, C., Guillet, C., Preisser, L., Dumont, A., Barbado, M., Morel, A., DeLapeyrièret, O., Gascan, H., Chevalier, S., 2004. Neuropoietin, a new IL-6-related cytokine signaling through the ciliary neurotrophic factor receptor. Proc. Natl. Acad. Sci. U. S. A. https://doi.org/10.1073/pnas.0306178101

Deverman, B.E., Patterson, P.H., 2009. Cytokines and CNS development. Neuron 64, 61–78.

Dobson, R., Giovannoni, G., 2019. Multiple sclerosis-a review. Eur. J. Neurol. 26, 27–40.

Doetsch, F., 2003. A niche for adult neural stem cells. Curr. Opin. Genet. Dev. 13, 543–550. https://doi.org/10.1016/j.gde.2003.08.012

Dutta, R., Chang, A., Doud, M.K., Kidd, G.J., Ribaudo, M. V., Young, E.A., Fox, R.J., Staugaitis, S.M., Trapp, B.D., 2011. Demyelination causes synaptic alterations in

hippocampi from multiple sclerosis patients. Ann Neurol 69, 445–454.

Dworzak, J., Renvoisé, B., Habchi, J., Yates, E. V., Combadière, C., Knowles, T.P., Dobson, C.M., Blackstone, C., Paulsen, O., Murphy, P.M., 2015. Neuronal Cx3cr1 deficiency protects against amyloid β-induced neurotoxicity. PLoS One 10, 1–25. https://doi.org/10.1371/journal.pone.0127730

Dyment, D.A., Dessa Sadnovich, A., Ebers, G.C., 1997. Genetics of multiple sclerosis. Hum. Mol. Genet. 6, 1693–1698. https://doi.org/10.1093/hmg/6.10.1693

Dziembowska, M., Tham, T.N., Lau, P., Vitry, S., Lazarini, F., Dubois-Dalcq, M., 2005. A Role for CXCR4 Signaling inSurvival and Migration of Neural andOligodendrocyte Precursors. Glia 50, 258–269.

El Khoury, J., Toft, M., Hickman, S.E., Means, T.K., Terada, K., Geula, C., Luster, A.D., 2007. Ccr2 deficiency impairs microglial accumulation and accelerates progression of Alzheimer-like disease. Nat. Med. 13, 432–438. https://doi.org/10.1038/nm1555

Eng, L.F., Ghirnikar, R.S., 1994. GFAP and Astrogliosis. Brain Pathol. 4, 229–237.

Eroglu, C., Barres, B.A., 2010. Regulation of synaptic connectivity by glia. Nature 468, 223–231. https://doi.org/10.1038/nature09612

Fasnacht, N., Müller, W., 2008. Conditional gp130 deficient mouse mutants. Semin. Cell Dev. Biol. 19, 379–384. https://doi.org/10.1016/j.semcdb.2008.07.001

Fernandes-alnemri, T., Litwacks, G., Alnemris, E.S., 1994. CPP32, a novel human apoptotic protein with homology to Caenorhabditis elegans cell death protein Ced-3 and mammalian interleukin-1 beta-converting enzyme. Biochemistry 30761–30764.

Fields, R.D., Araque, A., Johansen-Berg, H., Lim, S.S., Lynch, G., Nave, K.A., Nedergaard, M., Perez, R., Sejnowski, T., Wake, H., 2014. Glial biology in learning and cognition. Neuroscientist 20, 426–431. https://doi.org/10.1177/1073858413504465

Filiano, A.J., Xu, Y., Tustison, N.J., Marsh, R.L., Baker, W., Smirnov, I., Overall, C.C., Gadani, S.P., Turner, S.D., Weng, Z., Peerzade, S.N., Chen, H., Lee, K.S., Scott, M.M., Beenhakker, M.P., Litvak, V., Kipnis, J., 2016. Unexpected role of interferon-γ 3 in regulating neuronal connectivity and social behaviour. Nature 535, 425–429. https://doi.org/10.1038/nature18626

Floriddia, E.M., Lourenço, T., Zhang, S., van Bruggen, D., Hilscher, M.M., Kukanja, P., Gonçalves dos Santos, J.P., Altınkök, M., Yokota, C., Llorens-Bobadilla, E., Mulinyawe, S.B., Grãos, M., Sun, L.O., Frisén, J., Nilsson, M., Castelo-Branco, G., 2020. Distinct oligodendrocyte populations have spatial preference and different responses to spinal cord injury. Nat. Commun. 11, 1–15. https://doi.org/10.1038/s41467-020-19453-x

Fogarty, M., Richardson, W.D., Kessaris, N., 2005. A subset of oligodendrocytes generated from radial glia in the dorsal spinal cord. Development 132, 1951–1959.

https://doi.org/10.1242/dev.01777

Frisoni, G.B., Laakso, M.P., Beltramello, A., Geroldi, C., Bianchetti, A., Soininen, H., Trabucchi, M., 1999. Hippocampal and entorhinal cortex atrophy in frontotemporal dementia and Alzheimer's disease. Neurology 52, 91–100. https://doi.org/10.1212/wnl.52.1.91

Frohman, E.M., Racke, M.K., Raine, C.S., 2006. Multiple Sclerosis — The Plaque and Its Pathogenesis. N. Engl. J. Med. 354, 942–955. https://doi.org/10.1056/nejmra052130

Fujita, H., Tanaka, J., Toku, K., Tateishi, N., Suzuki, Y., Matsuda, S., Sakanaka, M., Maeda, N., 1996. Effects of GM-CSF and Ordinary Supplements on the Ramification of Microglia in Culture: A Morphometrical Study. Glia 18, 269–281. https://doi.org/10.1002/(SICI)1098-1136(199612)18:4<269::AID-GLIA2>3.0.CO;2-T

Furuta, Y., Piston, D.W., Hogan, B.L.M., 1997. Bone morphogenetic proteins (BMPs) as regulators of dorsal forebrain development. Development 124, 2203–2212. https://doi.org/10.1242/dev.124.11.2203

Gallagher, D., Norman, A.A., Woodard, C.L., Yang, G., Gauthier-Fisher, A., Fujitani, M., Vessey, J.P., Cancino, G.I., Sachewsky, N., Woltjen, K., Fatt, M.P., Morshead, C.M., Kaplan, D.R., Miller, F.D., 2013. Transient maternal IL-6 mediates long-lasting changes in neural stem cell pools by deregulating an endogenous self-renewal pathway. Cell Stem Cell. https://doi.org/10.1016/j.stem.2013.10.002

Galleguillos, D., Wang, Q., Steinberg, N., Zaidi, A., Shrivastava, G., Dhami, K., Daskhan, G.C., Schmidt, E.N., Dworsky-Fried, Z., Giuliani, F., Churchward, M., Power, C., Todd, K., Taylor, A., Macauley, M.S., Sipione, S., 2022. Anti-inflammatory role of GM1 and other gangliosides on microglia. J. Neuroinflammation 19, 1–18. https://doi.org/10.1186/s12974-021-02374-x

Garcia, A.D.R., Doan, N.B., Imura, T., Bush, T.G., Sofroniew, M. V., 2004. GFAP-expressing progenitors are the principal source of constitutive neurogenesis in adult mouse forebrain. Nat. Neurosci. 7, 1233–1241. https://doi.org/10.1038/nn1340

Gensert, J.A.M., Goldman, J.E., 1997. Endogenous progenitors remyelinate demyelinated axons in the adult CNS. Neuron 19, 197–203. https://doi.org/10.1016/S0896-6273(00)80359-1

Geurts, J.J.G., Bö, L., Pouwels, P.J.W., Castelijns, J.A., Polman, C.H., Barkhof, F., 2005. Cortical lesions in multiple sclerosis: Combined postmortem MR imaging and histopathology. Am. J. Neuroradiol. 26, 572–577.

Geurts, J.J.G., Bö, L., Roosendaal, S.D., Hazes, T., Daniëls, R., Barkhof, F., Witter, M.P., Huitinga, I., Van Der Valk, P., 2007. Extensive hippocampal demyelination in multiple sclerosis. J. Neuropathol. Exp. Neurol. 66, 819–827. https://doi.org/10.1097/nen.0b013e3181461f54

Ghasemi, N., Razavi, S., Nikzad, E., 2017. Multiple Sclerosis: Pathogenesis, Symptoms, Diagnoses and Cell-Based Therapy. Cell J. 19, 1–10.

Gibson, E.M., Purger, D., Mount, C.W., Goldstein, A.K., Lin, G.L., Wood, L.S., Inema, I., Miller, S.E., Bieri, G., Zuchero, J.B., Barres, B.A., Woo, P.J., Vogel, H., Monje, M., 2014. Neuronal Activity Promotes Oligodendrogenesis and Adaptive Myelination in the Mammalian Brain. Science (80-.). 344, 480–481. https://doi.org/10.1126/science.1254446

Gil, M., Gama, V., 2022. Emerging mitochondrial-mediated mechanisms involved in oligodendrocyte development. J. Neurosci. 101, 354–366.

Ginhoux, F., Greter, M., Leboeuf, M., Nandi, S., See, P., Gokhan, S., Mehler, M.F., Conway, S.J., Ng, L.G., Stanley, E.R., Samokhvalov, I.M., Merad, M., 2010. Fate Mapping Analysis Reveals That Adult Microglia Derive from Primitive Macrophages. Science (80-.). 701, 841–845.

Ginhoux, F., Lim, S., Hoeffel, G., Low, D., Huber, T., 2013. Origin and differentiation of microglia. Front. Cell. Neurosci. 7, 1–14. https://doi.org/10.3389/fncel.2013.00045

Gomes-Leal, W., 2012. Microglial physiopathology: How to explain the dual role of microglia after acute neural disorders? Brain Behav. 2, 345–356. https://doi.org/10.1002/brb3.51

Gordon, S., Lawson, L., Rabinowitz, S., Crocker, P.R., Morris, L., Perry, V.H., 1992. Antigen markers of macrophage differentiation in murine tissues. Curr. Top. Microbiol. Immunol. 181, 1–37. https://doi.org/10.1007/978-3-642-77377-8_1

Göritz, C., Frisén, J., 2012. Neural stem cells and neurogenesis in the adult. Cell Stem Cell 10, 657–659. https://doi.org/10.1016/j.stem.2012.04.005

Gosselin, D., Link, V.M., Romanoski, C.E., Fonseca, G.J., Eichenfield, D.Z., Spann, N.J., Stender, J.D., Chun, H.B., Garner, H., Geissmann, F., Glass, C.K., 2014. Environment drives selection and function of enhancers controlling tissue-specific macrophage identities. Cell 159, 1327–1340. https://doi.org/10.1016/j.cell.2014.12.024

Gosselin, D., Skola, D., Coufal, N.G., Holtman, I.R., Schlachetzki, J.C.M., Sajti, E., Jaeger, B.N., O'Connor, C., Fitzpatrick, C., Pasillas, M.P., Pena, M., Adair, A., Gonda, D.D., Levy, M.L., Ransohoff, R.M., Gage, F.H., Glass, C.K., 2017. An environment-dependent transcriptional network specifies human microglia identity. Science (80-.). 356, 1248–1259. https://doi.org/10.1126/science.aal3222

Göttle, P., Förster, M., Weyers, V., Küry, P., Rejdak, K., Hartung, H.P., Kremer, D., 2019. An unmet clinical need: Roads to remyelination in MS. Neurol. Res. Pract. 1, 1–12. https://doi.org/10.1186/s42466-019-0026-0

Göttle, P., Kremer, D., Jander, S., Odemis, V., Engele, J., Hartung, H.-P., Kury, P., 2010. Activation of CXCR7 Receptor PromotesOligodendroglial Cell Maturation. Am. Neurol. Assoc. 68, 915–924.

Gregg, C., Weiss, S., 2005. CNTF/LIF/gp130 receptor complex signaling maintains a VZ precursor differentiation gradient in the developing ventral forebrain. Development 132, 565–578. https://doi.org/10.1242/dev.01592

Guilbault, C., Saeed, Z., Downey, G.P., Radzioch, D., 2007. Cystic fibrosis mouse models. Am. J. Respir. Cell Mol. Biol. 36, 1–7. https://doi.org/10.1165/rcmb.2006-0184TR

Harrison, J.K., Barber, C.M., Lynch, K.R., 1994. cDNA cloning of a G-protein-coupled receptor expressed in rat spinal cord and brain related to chemokine receptors. Neurosci. Lett. 169, 85–89.

Harrison, J.K., Jiang, Y., Chen, S., Xia, Y., Maciejewski, D., Mcnamara, R.K., Streit, W.J., Salafranca, M.N., Adhikari, S., Thompson, D.A., Botti, P., Bacon, K.B., Feng, L., 1998. Role for neuronally derived fractalkine in mediating interactions between neurons and CX3CR1-expressing microglia. Proc. Natl. Acad. Sci. U. S. A. 95, 10896–10901. https://doi.org/10.1073/pnas.95.18.10896

Hedström, A.K., Sundqvist, E., Bäärnhielm, M., Nordin, N., Hillert, J., Kockum, I., Olsson, T., Alfredsson, L., 2011. Smoking and two human leukocyte antigen genes interact to increase the risk for multiple sclerosis. Brain 134, 653–664. https://doi.org/10.1093/brain/awq371

Herculano-Houzel, S., 2014. The glia/neuron ratio: How it varies uniformly across brain structures and species and what that means for brain physiology and evolution. Glia 62, 1377–1391. https://doi.org/10.1002/glia.22683

Heß, K., Starost, L., Kieran, N.W., Thomas, C., Vincenten, M.C.J., Antel, J., Martino, G., Huitinga, I., Healy, L., Kuhlmann, T., 2020. Lesion stage-dependent causes for impaired remyelination in MS. Acta Neuropathol. 140, 359–375. https://doi.org/10.1007/s00401-020-02189-9

Hickman, S.E., Allison, E.K., El Khoury, J., 2008. Microglial dysfunction and defective β-amyloid clearance pathways in aging alzheimer's disease mice. J. Neurosci. 28, 8354–8360. https://doi.org/10.1523/JNEUROSCI.0616-08.2008

Hickman, S.E., Kingery, N.D., Ohsumi, T.K., Borowsky, M.L., Wang, L.C., Means, T.K., El Khoury, J., 2013. The microglial sensome revealed by direct RNA sequencing. Nat. Neurosci. 16, 1896–1905. https://doi.org/10.1038/nn.3554

Hilton, B.J., Bradke, F., 2017. Can injured adult CNS axons regenerate by recapitulating development? Dev. 144, 3417–3429. https://doi.org/10.1242/dev.148312

Hiremath, M.M., Saito, Y., Knapp, G.W., Ting, J..-Y., Suzuki, K., Matsushima, G.K., 1998. Microglia/macrophage accumulation during cuprizone-induced demyelination in C57BL/6 mice.pdf. J. Neuroimmunol. 92, 38–49.

Hopperton, K.E., Mohammad, D., Trépanier, M.O., Giuliano, V., Bazinet, R.P., 2018. Markers of microglia in post-mortem brain samples from patients with Alzheimer's disease: A systematic review. Mol. Psychiatry 23, 177–198. https://doi.org/10.1038/mp.2017.246

Hoshiko, M., Arnoux, I., Avignone, E., Yamamoto, N., Audinat, E., 2012. Deficiency of the microglial receptor CX3CR1 impairs postnatal functional development of thalamocortical synapses in the barrel cortex. J. Neurosci. 32, 15106–15111.

https://doi.org/10.1523/JNEUROSCI.1167-12.2012

Hughes, E.G., Stockton, M.E., 2021. Premyelinating Oligodendrocytes: Mechanisms Underlying Cell Survival and Integration. Front. Cell Dev. Biol. 9, 1–17. https://doi.org/10.3389/fcell.2021.714169

Huxley, A.F., Stampfli, R., 1949. Evidence for saltatory conduction in peripheral myelinated nerve fibres. J. Physiol. 108, 315–339.

Imai, T., Hieshima, K., Haskell, C., Baba, M., Nagira, M., Nishimura, M., Kakizaki, M., Takagi, S., Nomiyama, H., Schall, T.J., Yoshie, O., 1997. Identification and molecular characterization of fractalkine receptor CX3CR1, which mediates both leukocyte migration and adhesion. Cell 91, 521–530. https://doi.org/10.1016/S0092-8674(00)80438-9

Jablonska, B., Aguirre, A., Raymond, M., Szabo, G., Kitabatake, Y., Sailor, K.A., Ming, G.L., Song, H., Gallo, V., 2010. Chordin-induced lineage plasticity of adult SVZ neuroblasts after demyelination. Nat. Neurosci. 13, 541–550. https://doi.org/10.1038/nn.2536

Jäkel, S., Agirre, E., Falcão, A.M., Bruggen, D. van, Lee, K.W., Knuesel, I., Malhotra, D., Ffrench-Constant, C., Williams, A., Castelo-Branco, G., 2019. Altered human oligodendrocyte heterogeneity in multiple sclerosis. Nature 566, 543–547.

Ji, J.F., He, B.P., Dheen, S.T., Tay, S.S.W., 2004. Expression of chemokine receptors CXCR4, CCR2, CCR5 and CX3CR1 in neural progenitor cells isolated from the subventricular zone of the adult rat brain. Neurosci. Lett. 355, 236–240. https://doi.org/10.1016/j.neulet.2003.11.024

Jinnou, H., Sawada, M., Kawase, K., Kaneko, N., Herranz-Pérez, V., Miyamoto, T., Kawaue, T., Miyata, T., Tabata, Y., Akaike, T., García-Verdugo, J.M., Ajioka, I., Saitoh, S., Sawamoto, K., 2018. Radial Glial Fibers Promote Neuronal Migration and Functional Recovery after Neonatal Brain Injury. Cell Stem Cell 22, 128-137.e9. https://doi.org/10.1016/j.stem.2017.11.005

Julien, J.P., Meyer, D., Flavell, D., Hurst, J., Grosveld, F., 1986. Cloning and developmental expression of the murine neurofilament gene family. Mol. Brain Res. 1, 243–250. https://doi.org/10.1016/0169-328X(86)90030-6

Jung, S., Aliberti, J., Graemmel, P., Sunshine, M.J., Kreutzberg, G.W., Sher, A., Littman, D.R., 2000. Analysis of Fractalkine Receptor CX 3 CR1 Function by Targeted Deletion and Green Fluorescent Protein Reporter Gene Insertion . Mol. Cell. Biol. 20, 4106–4114. https://doi.org/10.1128/mcb.20.11.4106-4114.2000

Kagawa, T., Ikenaka, K., Inoue, Y., Kuriyama, S., Tsujii, T., Nakao, J., Nakajima, K., Aruga, J., Okano, H., Mikoshiba, K., 1994. Glial cell degeneration and hypomyelination caused by overexpression of myelin proteolipid protein gene. Neuron 13, 427–442. https://doi.org/10.1016/0896-6273(94)90358-1

Karussis, D., 2014. The diagnosis of multiple sclerosis and the various related demyelinating

syndromes: A critical review. J. Autoimmun. https://doi.org/10.1016/j.jaut.2014.01.022

Kempermann, G., Song, H., Gage, F.H., 2015. Neurogenesis in the Adult Hippocampus. Cold Spring Harb. Perspect. Biol. 7, a018812. https://doi.org/10.1101/cshperspect.a018812

Kessaris, N., Fogarty, M., Iannarelli, P., Grist, M., Wegner, M., Richardson, W.D., 2006. Competing waves of oligodendrocytes in the forebrain and postnatal elimination of an embryonic lineage. Nat. Neurosci. https://doi.org/10.1038/nn1620

Kigerl, K.A., Vaccari, J.P. de R., Dietrich, W.D., Popovich, P.G., Keane, R.W., 2014. Pattern recognition receptors and central nervous system repair. Exp. Neurol. 258, 5–16. https://doi.org/10.1016/j.expneurol.2014.01.001.Pattern

Kim, W.K., Kim, D., Cui, J., Jang, H.H., Kim, K.S., Lee, H.J., Kim, S.U., Ahn, S.M., 2014. Secretome analysis of human oligodendrocytes derived from neural stem cells. PLoS One 9. https://doi.org/10.1371/journal.pone.0084292

Kitazawa, A., Kubo, K.I., Hayashi, K., Matsunaga, Y., Ishii, K., Nakajima, K., 2014. Hippocampal pyramidal neurons switch from a multipolar migration mode to a novel "climbing" migration mode during development. J. Neurosci. 34, 1115–1126. https://doi.org/10.1523/JNEUROSCI.2254-13.2014

Klein, R.S., Garber, C., Howard, N., 2017. Infectious immunity in the central nervous system and brain function. Nat. Immunol. 18, 132–141. https://doi.org/10.1038/ni.3656

Klein, R.S., Lin, E., Zhang, B., Luster, A.D., Tollett, J., Samuel, M.A., Engle, M., Diamond, M.S., 2005. Neuronal CXCL10 Directs CD8 + T-Cell Recruitment and Control of West Nile Virus Encephalitis . J. Virol. 79, 11457–11466. https://doi.org/10.1128/jvi.79.17.11457-11466.2005

Kornek, B., Storch, M.K., Weissert, R., Wallstroem, E., Stefferl, A., Olsson, T., Linington, C., Schmidbauer, M., Lassmann, H., 2000. Multiple sclerosis and chronic autoimmune encephalomyelitis: A comparative quantitative study of axonal injury in active, inactive, and remyelinated lesions. Am. J. Pathol. 157, 267–276. https://doi.org/10.1016/S0002-9440(10)64537-3

Kreutzberg, G.W., 1996. Microglia: A sensor for pathological events in the CNS. Trends Neurosci. 19, 312–318. https://doi.org/10.1016/0166-2236(96)10049-7

Kriegstein, A., Alvarez-Buylla, A., 2009. The Glial Nature of Embryonic and Adult Neural Stem Cells. Annu Rev Neurosci 32, 149–184. https://doi.org/10.1146/annurev.neuro.051508.135600.The

Kriegstein, A.R., Götz, M., 2003. Radial glia diversity: A matter of cell fate. Glia 43, 37–43. https://doi.org/10.1002/glia.10250

Kuhn, S., Gritti, L., Crooks, D., Dombrowski, Y., 2019. Oligodendrocytes in Development, Myelin Generation and Beyond. Cells 8, 1–23.

Laakso, M.P., Frisoni, G.B., Könönen, M., Mikkonen, M., Beltramello, A., Geroldi, C., Bianchetti, A., Trabucchi, M., Soininen, H., Aronen, H.J., 2000. Hippocampus and entorhinal cortex in frontotemporal dementia and Alzheimer's disease: A morphometric MRI study. Biol. Psychiatry 47, 1056–1063. https://doi.org/10.1016/S0006-3223(99)00306-6

Lampron, A., ElAli, A., Rivest, S., 2013. Innate Immunity in the CNS: Redefining the relationship between the CNS and its Environment. Neuron 78, 214–232. https://doi.org/10.1016/j.neuron.2013.04.005

Lampron, A., Larochelle, A., Laflamme, N., Préfontaine, P., Plante, M.M., Sánchez, M.G., Wee Yong, V., Stys, P.K., Tremblay, M.È., Rivest, S., 2015. Inefficient clearance of myelin debris by microglia impairs remyelinating processes. J. Exp. Med. 212, 481–495. https://doi.org/10.1084/jem.20141656

Lassmann, H., 2014. Multiple sclerosis: Lessons from molecular neuropathology. Exp. Neurol. 262, 2–7. https://doi.org/10.1016/j.expneurol.2013.12.003

Lavin, Y., Winter, D., Blecher-Gonen, R., David, E., Keren-Shaul, H., Merad, M., Jung, S., Amit, I., 2014. Tissue-resident macrophage enhancer landscapes are shaped by the local microenvironment. Cell 159, 1312–1326. https://doi.org/10.1016/j.cell.2014.11.018

Lawson, L.J., Perry, V.H., Dri, P., Gordon, S., 1990. Heterogeneity in the distribution and morphology of microglia in the normal adult mouse brain. Neuroscience 39, 151–170. https://doi.org/10.1016/0306-4522(90)90229-W

Lee, S., Varvel, N.H., Konerth, M.E., Xu, G., Cardona, A.E., Ransohoff, R.M., Lamb, B.T., 2010. CX3CR1 deficiency alters microglial activation and reduces beta-amyloid deposition in two Alzheimer's disease mouse models. Am. J. Pathol. 177, 2549–2562. https://doi.org/10.2353/ajpath.2010.100265

Lentferink, D.H., Jongsma, J.M., Werkman, I., Baron, W., 2018. Grey matter OPCs are less mature and less sensitive to IFNγ than white matter OPCs: Consequences for remyelination. Sci. Rep. 8, 1–15. https://doi.org/10.1038/s41598-018-19934-6

Levison, S.W., Goldman, J.E., 1993. Both oligodendrocytes and astrocytes develop from progenitors in the subventricular zone of postnatal rat forebrain. Neuron 10, 201–212. https://doi.org/10.1016/0896-6273(93)90311-E

Levitt, P., Rakic, P., 1980. Immunoperoxidase localization of glial fibrillary acidic protein in radial glial cells and astrocytes of the developing rhesus monkey brain. J. Comp. Neurol. 193, 815–840. https://doi.org/10.1002/cne.901930316

Li, X., Zhao, X., 2008. Epigenetic regulation of mammalian stem cells. Stem Cells Dev. 17, 1043–1052. https://doi.org/10.1089/scd.2008.0036

Li, Y., Dittmann, N.L., Eve, A., Watson, S., de Almeida, M.M.A., Footz, T., Voronova, A., 2022. Hepatoma Derived Growth Factor Enhances Oligodendrocyte Genesis from Subventricular

Zone Precursor Cells. ASN Neuro 14, 1–27. https://doi.org/10.1177/17590914221086340

Liao, B., Zhao, W., Beers, D.R., Henkel, J.S., Appel, S.H., 2012. Transformation from a neuroprotective to a neurotoxic microglial phenotype in a mouse model of ALS. Exp. Neurol. 237, 147–152. https://doi.org/10.1016/j.expneurol.2012.06.011

Limatola, C., Ransohoff, R.M., 2014. Modulating neurotoxicity through CX3CL1/CX3CR1 signaling. Front. Cell. Neurosci. 8, 1–8. https://doi.org/10.3389/fncel.2014.00229

Lin, S.C., Bergles, D.E., 2002. Physiological characteristics of NG2-expressing glial cells. J. Neurocytol. 31, 537–549. https://doi.org/10.1023/A:1025799816285

Lopez-Lopez, A., Gamez, J., Syriani, E., Morales, M., Salvado, M., 2014. CX3CR1 Is a Modifying Gene of Survival and Progression in Amyotrophic Lateral Sclerosis. PLoS One 9, 96528. https://doi.org/10.1371/journal.pone.0096528

López-López, A., Gelpi, E., Lopategui, D.M., Vidal-Taboada, J.M., 2018. Association of the CX3CR1-V249I Variant with Neurofibrillary Pathology Progression in Late-Onset Alzheimer's Disease. Mol. Neurobiol. 55, 2340–2349. https://doi.org/10.1007/s12035-017-0489-3

Luo, P., Chu, S. feng, Zhang, Z., Xia, C. yuan, Chen, N. hong, 2019. Fractalkine/CX3CR1 is involved in the cross-talk between neuron and glia in neurological diseases. Brain Res. Bull. 146, 12–21. https://doi.org/10.1016/j.brainresbull.2018.11.017

Ma, Y., Wang, J., Wang, Y., Yang, G.Y., 2017. The biphasic function of microglia in ischemic stroke. Prog. Neurobiol. 157, 247–272. https://doi.org/10.1016/j.pneurobio.2016.01.005

Marques, S., Bruggen, D. van, Vanichkina, D.P., Floriddia, E.M., Munguba, H., Väremo, L., Giacomello, S., Falcão, A.M., Meijer, M., Björklund, Å.K., Hjerling-Leffler, J., Taft, R.J., Castelo-Branco, G., 2018. Transcriptional Convergence of Oligodendrocyte Lineage Progenitors during Development. Dev. Cell 46, 504–517.

Marques, S., Zeisel, A., Codeluppi, S., Van Bruggen, D., Falcão, A.M., Xiao, L., Li, H., Häring, M., Hochgerner, H., Romanov, R.A., Gyllborg, D., Muñoz-Manchado, A.B., La Manno, G., Lönnerberg, P., Floriddia, E.M., Rezayee, F., Ernfors, P., Arenas, E., Hjerling-Leffler, J., Harkany, T., Richardson, W.D., Linnarsson, S., Castelo-Branco, G., 2016. Oligodendrocyte heterogeneity in the mouse juvenile and adult central nervous system. Science (80-.). 352, 1326–1329. https://doi.org/10.1126/science.aaf6463

Marrodan, M., Alessandro, L., Farez, M.F., Correale, J., 2019. The role of infections in multiple sclerosis. Mult. Scler. J. 25, 891–901. https://doi.org/10.1177/https

Matcovitch-Natan, O., Winter, D.R., Giladi, A., Aguilar, S.V., Spinrad, A., Sarrazin, S., Ben-Yehuda, H., David, E., González, F.Z., Perrin, P., Keren-Shaul, H., Gury, M., Lara-Astaiso, D., Thaiss, C.A., Cohen, M., Halpern, K.B., Baruch, K., Deczkowska, A., Lorenzo-Vivas, E., Itzkovitz, S., Elinav, E., Sieweke, M.H., Schwartz, M., Amit, I., 2016. Microglia development follows a stepwise program to regulate brain homeostasis. Science (80-.). 353.

https://doi.org/10.1126/science.aad8670

McCarthy, G.F., Leblond, C.P., 1988. Radioautographic evidence for slow astrocyte turnover and modest oligodendrocyte production in the corpus callosum of adult mice infused with 3H-thymidine. J. Comp. Neurol. 271, 589–603.

McDermott, D.H., Fong, A.M., Yang, Q., Sechler, J.M., Cupples, L.A., Merrell, M.N., Wilson, P.W.F., D'Agostino, R.B., O'Donnell, C.J., Patel, D.D., Murphy, P.M., 2003. Chemokine receptor mutant CX3CR1-M280 has impaired adhesive function and correlates with protection from cardiovascular disease in humans. J. Clin. Invest. 111, 1241–1250. https://doi.org/10.1172/JCI16790

McKenzie, I.A., Ohayon, D., Li, H., De Faria, J.P., Emery, B., Tohyama, K., Richardson, W.D., 2014. Motor skill learning requires active central myelination. Science (80-.). 346, 318–322. https://doi.org/10.1126/science.1254960

Méndez-Salcido, F.A., Torres-Flores, M.I., Ordaz, B., Peña-Ortega, F., 2022. Abnormal innate and learned behavior induced by neuron–microglia miscommunication is related to CA3 reconfiguration. Glia 70, 1630–1651. https://doi.org/10.1002/glia.24185

Mendiola, A.S., Church, K.A., Cardona, S.M., Vanegas, D., Garcia, S.A., Macklin, W., Lira, S.A., Ransohoff, R.M., Kokovay, E., Lin, C.H.A., Cardona, A.E., 2022. Defective fractalkine-CX3CR1 signaling aggravates neuroinflammation and affects recovery from cuprizone-induced demyelination. J. Neurochem. 1–14. https://doi.org/10.1111/jnc.15616

Menn, B., Garcia-Verdugo, J.M., Yaschine, C., Gonzalez-Perez, O., Rowitch, D., Alvarez-Buylla, A., 2006. Origin of oligodendrocytes in the subventricular zone of the adult brain. J. Neurosci. 26, 7907–7918. https://doi.org/10.1523/JNEUROSCI.1299-06.2006

Michel, L., 2018. Environmental factors in the development of multiple sclerosis. Rev. Neurol. (Paris). 174, 372–377. https://doi.org/10.1016/j.neurol.2018.03.010

Michelucci, A., Heurtaux, T., Grandbarbe, L., Morga, E., Heuschling, P., 2009. Characterization of the microglial phenotype under specific pro-inflammatory and anti-inflammatory conditions: Effects of oligomeric and fibrillar amyloid-β. J. Neuroimmunol. 210, 3–12. https://doi.org/10.1016/j.jneuroim.2009.02.003

Miller, F.D., Gauthier, A.S., 2007. Timing Is Everything: Making Neurons versus Glia in the Developing Cortex. Neuron 54, 357–369. https://doi.org/10.1016/j.neuron.2007.04.019

Miron, V.E., 2017. Microglia-driven regulation of oligodendrocyte lineage cells, myelination, and remyelination. J. Leukoc. Biol. 101, 1103–1108. https://doi.org/10.1189/jlb.3ri1116-494r

Miron, V.E., Boyd, A., Zhao, J.W., Yuen, T.J., Ruckh, J.M., Shadrach, J.L., Van Wijngaarden, P., Wagers, A.J., Williams, A., Franklin, R.J.M., Ffrench-Constant, C., 2013. M2 microglia and macrophages drive oligodendrocyte differentiation during CNS remyelination. Nat. Neurosci. 16, 1211–1218. https://doi.org/10.1038/nn.3469

Molyneaux, B.J., Arlotta, P., Menezes, J.R.L., Macklis, J.D., 2007. Neuronal subtype specification in the cerebral cortex. Nat. Rev. Neurosci. 8, 427–437. https://doi.org/10.1038/nrn2151

Mori, S., Leblond, C.P., 1970. Electron microscopic identification of three classes of oligodendrocytes and a preliminary study of their proliferative activity in the corpus callosum of young rats. J. Comp. Neurol. 139, 1–29. https://doi.org/10.1002/cne.901390102

Moroni, R.F., Deleo, F., Regondi, M.C., Madaschi, L., Amadeo, A., Frassoni, C., 2018. Proliferative cells in the rat developing neocortical grey matter: new insights into gliogenesis. Brain Struct. Funct. 223, 4053–4066. https://doi.org/10.1007/s00429-018-1736-8

Moser, B., Loetscher, P., 2001. Lymphocyte traffic control by chemokines. Nat. Immunol. 2, 123–128. https://doi.org/10.1038/84219

Moshinsky, M., 1994. Divergent Lineages for Oligodendrocytes and Astrocytes Originating in the Neonatal Forebrain Subventricular Zone. Glia 11, 211–226.

Mosley, M., Shah, C., Morse, K.A., Miloro, S.A., Holmes, M.M., Ahern, T.H., Forger, N.G., 2017. Patterns of cell death in the perinatal mouse forebrain. J Comp Neurol. 525, 47–64. https://doi.org/10.1002/cne.24041.Patterns

Mousa, A., Bakhiet, M., 2013. Role of cytokine signaling during nervous system development. Int. J. Mol. Sci. 14, 13931–13957. https://doi.org/10.3390/ijms140713931

MuhChyi, C., Juliandi, B., Matsuda, T., Nakashima, K., 2013. Epigenetic regulation of neural stem cell fate during corticogenesis. Int. J. Dev. Neurosci. 31, 424–433. https://doi.org/10.1016/j.ijdevneu.2013.02.006

Muzio, L., Martino, G., Furlan, R., 2007. Multifaceted aspects of inflammation in multiple sclerosis: The role of microglia. J. Neuroimmunol. 191, 39–44. https://doi.org/10.1016/j.jneuroim.2007.09.016

Nait-Oumesmar, B., Decker, L., Lachapelle, F., Avellana-Adalid, V., Bachelin, C., Evercooren, A.B.-V., 1999. Progenitor cells of the adult mouse subventricular zone proliferate, migrate and differentiate into oligodendrocytes after demyelination. J. Neurosci. 11, 4357–4366.

Nave, K.A., Werner, H.B., 2014. Myelination of the nervous system: Mechanisms and functions. Annu. Rev. Cell Dev. Biol. 30, 503–533. https://doi.org/10.1146/annurev-cellbio-100913-013101

Negi, N., Das, B.K., 2018. CNS: Not an immunoprivilaged site anymore but a virtual secondary lymphoid organ. Int. Rev. Immunol. 37, 57–68. https://doi.org/10.1080/08830185.2017.1357719

Nemes-Baran, A.D., White, D.R., DeSilva, T.M., 2020. Fractalkine-Dependent Microglial Pruning of Viable Oligodendrocyte Progenitor Cells Regulates Myelination. Cell Rep. 32.

https://doi.org/10.1016/j.celrep.2020.108047

Nielsen, N.M., Westergaard, T., Rostgaard, K., Frisch, M., Hjalgrim, H., Wohlfahrt, J., Koch-Henriksen, N., Melbye, M., 2005. Familial risk of multiple sclerosis: A nationwide cohort study. Am. J. Epidemiol. 162, 774–778. https://doi.org/10.1093/aje/kwi280

Niino, M., 2016. Neuropsychological aspects of multiple sclerosis. Neuroimmunol. Dis. 8, 123–133. https://doi.org/10.1007/978-4-431-55594-0_7

Nimmerjahn, A., Kirchhoff, F., Helmchen, F., 2005. Resting microglial cells are highly dynamic surveillants of brain parenchyma in vivo. Neuroforum 11, 95–96. https://doi.org/10.1515/nf-2005-0304

Nishiyama, A., Chang, A., Trapp, B.D., 1999. NG2+ glial cells: a novel glial cell population in the adult brain. J. Neuropathol. Exp. Neurol. 58, 1113–1124.

Nishiyama, A., Lin, X.-H., Giese, N., Heldin, C.-H., Stallcup, W.B., 1996. Co-localization of NG2 proteoglycan and PDGF α-receptor on O2A progenitor cells in the developing rat brain. J. Neurosci. Res. 43, 299–314.

Nishiyama, A., Yu, M., Drazba, J.A., Tuohy, V.K., 1997. Normal and reactive NG2+ glial cells are distinct from resting and activated microglia. J. Neurosci. Res. 48, 299–312.

Nixdorf-Bergweiler, B.E., Albrecht, D., Heinemann, U., 1994. Developmental changes in the number, size, and orientation of GFAP-positive cells in the CA1 region of rat hippocampus. Glia 12, 180–195. https://doi.org/10.1002/glia.440120304

Nowakowski, R.S., Lewin, S.B., Miller, M.W., 1989. Bromodeoxyuridine immunohistochemical determination of the lengths of the cell cycle and the DNA-synthetic phase for an anatomically defined population. J. Neurocytol. 18, 311–318. https://doi.org/10.1007/BF01190834

Okano, H., 2010. Neural stem cells and strategies for the regeneration of the central nervous system. Proc. Japan Acad. Ser. B Phys. Biol. Sci. 86, 438–450. https://doi.org/10.2183/pjab.86.438

Okano, H., Temple, S., 2009. Cell types to order: temporal specification of CNS stem cells. Curr. Opin. Neurobiol. 19, 112–119. https://doi.org/10.1016/j.conb.2009.04.003

Omari, K.M., John, G.R., Sealfon, S.C., Raine, C.S., 2005. CXC chemokine receptors on human oligodendrocytes: Implications for multiple sclerosis. Brain 128, 1003–1015. https://doi.org/10.1093/brain/awh479

Oppenheim, R.W., 1991. Cell death during development of the nervous system. Annu Rev Neurosci 14, 453–501.

Ortiz, F.C., Habermacher, C., Graciarena, M., Houry, P.Y., Nishiyama, A., Oumesmar, B.N., Angulo, M.C., 2019. Neuronal activity in vivo enhances functional myelin repair. JCI

Insight 4, 1–15. https://doi.org/10.1172/jci.insight.123434

Osanai, Y., Yamazaki, R., Shinohara, Y., Ohno, N., 2022. Heterogeneity and regulation of oligodendrocyte morphology. Front. Cell Dev. Biol. 10, 1–13. https://doi.org/10.3389/fcell.2022.1030486

Pan, Y., Lloyd, C., Zhou, H., Dolich, S., Deeds, J., Gonzalo, J.A., Vath, J., Gosselin, M., Ma, J., Dussault, B., Woolf, E., Alperin, G., Culpepper, J., Gutierrez-Ramos, J.C., Gearing, D., 1997. Neurotactin, a membrane-anchored chemokine upregulated in brain inflammation. Nature 387, 611–617. https://doi.org/10.1038/42491

Pandey, S., Shen, K., Lee, S.H., Shen, Y.A.A., Wang, Y., Otero-García, M., Kotova, N., Vito, S.T., Laufer, B.I., Newton, D.F., Rezzonico, M.G., Hanson, J.E., Kaminker, J.S., Bohlen, C.J., Yuen, T.J., Friedman, B.A., 2022. Disease-associated oligodendrocyte responses across neurodegenerative diseases. Cell Rep. 40, 1–18. https://doi.org/10.1016/j.celrep.2022.111189

Pang, C.C.C., Kiecker, C., O'Brien, J.T., Noble, W., Chang, R.C.C., 2019. Ammon's Horn 2 (CA2) of the Hippocampus: A Long-Known Region with a New Potential Role in Neurodegeneration. Neuroscientist 25, 167–180. https://doi.org/10.1177/1073858418778747

Pantazou, V., Schluep, M., Du Pasquier, R., 2015. Environmental factors in multiple sclerosis. Press. Medicale 44, e113–e120. https://doi.org/10.1016/j.lpm.2015.01.001

Paolicelli, R.C., Bisht, K., Tremblay, M.È., 2014. Fractalkine regulation of microglial physiology and consequences on the brain and behavior. Front. Cell. Neurosci. 8, 1–10. https://doi.org/10.3389/fncel.2014.00129

Paolicelli, R.C., Sierra, A., Stevens, B., 2022. Microglia states and nomenclature : A field at its crossroads. Neuron 110, 3458–3483.

Papadopoulos, D., Dukes, S., Patel, R., Nicholas, R., Vora, A., Reynolds, R., 2009. Substantial archaeocortical atrophy and neuronal loss in multiple sclerosis. Brain Pathol. 19, 238–253.

Paraschivescu, C., Barbosa, S., Van Steenwinckel, J., Gressens, P., Glaichenhaus, N., Davidovic, L., 2022. Early Life Exposure to Tumor Necrosis Factor Induces Precocious Sensorimotor Reflexes Acquisition and Increases Locomotor Activity During Mouse Postnatal Development. Front. Behav. Neurosci. 16, 1–12. https://doi.org/10.3389/fnbeh.2022.845458

Parkhurst, C.N., Yang, G., Ninan, I., Savas, J.N., Yates, J.R., Lafaille, J.J., Hempstead, B.L., Littman, D.R., Gan, W.B., 2013. Microglia promote learning-dependent synapse formation through brain-derived neurotrophic factor. Cell 155, 1596–1609. https://doi.org/10.1016/j.cell.2013.11.030

Perry, V.H., Hume, D.A., Gordon, S., 1985. Immunohistochemical localization of macrophages and microglia in the adult and developing mouse brain. Neuroscience 15, 313–326. https://doi.org/10.1016/0306-4522(85)90215-5

Pfeiffer, S.E., Warrington, A.E., Bansal, R., 1993. The oligodendrocyte and its many cellular processes. Trends Cell Biol. 3, 191–197. https://doi.org/10.1016/0962-8924(93)90213-K

Picard-Riera, N., Decker, L., Delarasse, C., Goude, K., Nait-Oumesmar, B., Liblau, R., Pham-Dinh, D., Baron-Van Evercooren, A., 2002. Experimental autoimmune encephalomyelitis mobilizes neural progenitors from the subventricular zone to undergo oligodendrogenesis in adult mice. Proc. Natl. Acad. Sci. U. S. A. https://doi.org/10.1073/pnas.192314199

Poggi, G., Boretius, S., Möbius, W., Moschny, N., Baudewig, J., Ruhwedel, T., Hassouna, I., Wieser, G.L., Werner, H.B., Goebbels, S., Nave, K.A., Ehrenreich, H., 2016. Cortical network dysfunction caused by a subtle defect of myelination. Glia 64, 2025–2040. https://doi.org/10.1002/glia.23039

Poniatowski, Ł.A., Wojdasiewicz, P., Krawczyk, M., Szukiewicz, D., Gasik, R., Kubaszewski, Ł., Kurkowska-Jastrzębska, I., 2017. Analysis of the Role of CX3CL1 (Fractalkine) and Its Receptor CX3CR1 in Traumatic Brain and Spinal Cord Injury: Insight into Recent Advances in Actions of Neurochemokine Agents. Mol. Neurobiol. 54, 2167–2188. https://doi.org/10.1007/s12035-016-9787-4

Porter, A.G., Jänicke, R.U., 1999. Emerging roles of caspase-3 in apoptosis. Cell Death Differ. 6, 99–104. https://doi.org/10.1038/sj.cdd.4400476

Praet, J., Guglielmetti, C., Berneman, Z., 2014. Cellular and molecular neuropathology of the cuprizone mouse model. Neurosci. Biobehav. Rev.

Prakash, R.S., Schirda, B., Valentine, T.R., Crotty, M., Nicholas, J.A., 2019. Emotion dysregulation in multiple sclerosis: Impact on symptoms of depression and anxiety. Mult. Scler. Relat. Disord. 36, 1–7. https://doi.org/10.1016/j.msard.2019.101399

Pringle, N.P., Richardson, W.D., 1993. A singularity of PDGF alpha-receptor expression in the dorsoventral axis of the neural tube may define the origin of the oligodendrocyte lineage. Development 117, 525–533. https://doi.org/10.1242/dev.117.2.525

Raes, G., Noël, W., Beschin, A., Brys, L., De Baetselier, P., Hassanzadeh, G.G., 2002. FIZZ1 and Ym as tools to discriminate between differentially activated macrophages. Dev. Immunol. 9, 151–159. https://doi.org/10.1080/1044667031000137629

Raine, C.S., 1994. The Dale E. McFarlin Memorial Lecture: The Immunology of the Multiple Sclerosis Lesion. Ann Neurol 36, S61–S72.

Rakic, P., 1974. Neurons in Rhesus Monkey Visual Cortex: Systematic Relation between Time of Origin and Eventual Disposition. Science (80-.). 183, 425–427.

Rakic, P., 1972. Mode of cell migration to the superficial layers of fetal monkey neocortex. J. Comp. Neurol. 145, 61–83. https://doi.org/10.1002/cne.901450105

Ramalho-Santos, M., Willenbring, H., 2007. On the Origin of the Term Calypso. Cell Stem Cell 1, 35–38. https://doi.org/10.1016/j.stem.2007.05.013

Ramesh, G., Maclean, A.G., Philipp, M.T., 2013. Cytokines and chemokines at the crossroads of neuroinflammation, neurodegeneration, and neuropathic pain. Mediators Inflamm. 2013, 1–20. https://doi.org/10.1155/2013/480739

Ransome, M.I., Renoir, T., Hannan, A.J., 2012. Hippocampal neurogenesis, cognitive Deficits and affective disorDer in huntington's disease. Neural Plast. 2012, 1–7. https://doi.org/10.1155/2012/874387

Rao, S.M., 1995. Neuropsychology of multiple sclerosis. Curr. Opin. Neurol. 8, 216–220.

Raponi, E., Agenes, F., Delphin, C., Assard, N., Baudier, J., Legraverend, C., Deloulme, J.-C., 2015. S100B expression defines a state in which GFAP-expressing cells lose their neural stem cell potential and acquire a more mature developmental stage. Sixth Rep. World Nutr. Situat. Geneva 479, 132. https://doi.org/10.1002/glia

Rasband, M.N., Peles, E., 2021. Mechanisms of node of Ranvier. Nat. Rev. Neurosci. 22, 7–20.

Rivers, L.E., Young, K.M., Rizzi, M., Jamen, F., Psachoulia, K., Wade, A., Kessaris, N., Richardson, W.D., 2008. PDGFRA/NG2 glia generate myelinating oligodendrocytes and piriform projection neurons in adult mice. Nat. Neurosci. 11, 1392–1401. https://doi.org/10.1038/nn.2220

Rocca, M.A., Barkhof, F., Luca, J. De, Geurts, J.J.G., Hulst, H.E., Sastre-garriga, J., Filippi, M., 2018. The hippocampus in multiple sclerosis. Lancet Neurol 17, 918–926.

Rogers, J.T., Morganti, J.M., Bachstetter, A.D., Hudson, C.E., Peters, M.M., Grimmig, B.A., Weeber, E.J., Bickford, P.C., Gemma, C., 2011. CX3CR1 deficiency leads to impairment of hippocampal cognitive function and synaptic plasticity. J. Neurosci. 31, 16241–16250. https://doi.org/10.1523/JNEUROSCI.3667-11.2011

Sadovnick, A.D., Baird, P.A., Ward, R.H., 1988. Multiple sclerosis: Updated risks for relatives. Am. J. Med. Genet. 29, 533–541. https://doi.org/10.1002/ajmg.1320290310

Saito, L.B., Fernandes, J.P., Smith, M.J., Doan, M.A.L., Branton, W.G., Schmitt, L.M., Wuest, M., Monaco, M.C., Major, E.O., Wuest, F., Power, C., 2021. Intranasal anti-caspase-1 therapy preserves myelin and glucose metabolism in a model of progressive multiple sclerosis. Glia 69, 216–229. https://doi.org/10.1002/glia.23896

Sampath, D., Sathyanesan, M., Newton, S.S., 2017. Cognitive dysfunction in major depression and Alzheimer's disease is associated with hippocampal–prefrontal cortex dysconnectivity. Neuropsychiatr. Dis. Treat. 13, 1509–1519. https://doi.org/10.2147/NDT.S136122

Schafer, D.P., Lehrman, E.K., Kautzman, A.G., Koyama, R., Mardinly, A.R., Yamasaki, R., Ransohoff, R.M., Greenberg, M.E., Barres, B.A., Stevens, B., 2012. Microglia Sculpt Postnatal Neural Circuits in an Activity and Complement-Dependent Manner. Neuron 74, 691–705. https://doi.org/10.1016/j.neuron.2012.03.026

Scherer, S.S., Braun, P.E., Grinspan, J., Collarini, E., Wang, D. y., Kamholz, J., 1994.

Differential regulation of the 2′,3′-cyclic nucleotide 3′-phosphodiesterase gene during oligodendrocyte development. Neuron 12, 1363–1375. https://doi.org/10.1016/0896-6273(94)90451-0

Schindelin, J., Arganda-Carreras, I., Frise, E., Kaynig, V., Longair, M., Pietzsch, T., Preibisch, S., Rueden, C., Saalfeld, S., Schmid, B., Tinevez, J.Y., White, D.J., Hartenstein, V., Eliceiri, K., Tomancak, P., Cardona, A., 2012. Fiji: An open-source platform for biological-image analysis. Nat. Methods 9, 676–682. https://doi.org/10.1038/nmeth.2019

Seibenhener, M.L., Wooten, M.C., 2015. Use of the open field maze to measure locomotor and anxiety-like behavior in mice. J. Vis. Exp. 1–6. https://doi.org/10.3791/52434

Sherafat, A., Pfeiffer, F., Reiss, A.M., Wood, W.M., Nishiyama, A., 2021. Microglial neuropilin-1 promotes oligodendrocyte expansion during development and remyelination by trans-activating platelet-derived growth factor receptor. Nat. Commun. 12, 1–17.

Sheridan, G.K., Murphy, K.J., 2013. Neuron-glia crosstalk in health and disease: Fractalkine and CX3CR1 take centre stage. Open Biol. 3, 1–14. https://doi.org/10.1098/rsob.130181

Shin, M., Kitazawa, A., Yoshinaga, S., Hayashi, K., Hirata, Y., Dehay, C., Kubo, K. ichiro, Nakajima, K., 2019. Both excitatory and inhibitory neurons transiently form clusters at the outermost region of the developing mammalian cerebral neocortex. J. Comp. Neurol. 527, 1577–1597. https://doi.org/10.1002/cne.24634

Simons, M., Nave, K.A., 2016. Oligodendrocytes: Myelination and axonal support. Cold Spring Harb. Perspect. Biol. 8, 1–16. https://doi.org/10.1101/cshperspect.a020479

Sohn, J., Orosco, L., Guo, F., Chung, S.H., Bannerman, P., Ko, E.M., Zarbalis, K., Deng, W., Pleasure, D., 2015. The subventricular zone continues to generate corpus callosum and rostral migratory stream astroglia in normal adult mice. J. Neurosci. 35, 3756–3763. https://doi.org/10.1523/JNEUROSCI.3454-14.2015

Stadelmann, C., Timmler, S., Barrantes-Freer, A., Simons, M., 2019. Myelin in the central nervous system: Structure, function, and pathology. Physiol. Rev. 99, 1381–1431. https://doi.org/10.1152/physrev.00031.2018

Stence, N., Waite, M., Dailey, M.E., 2001. Dynamics of Microglial Activation: A Confocal Time-Lapse Analysis in Hippocampal Slices. Glia 33, 256–266.

Stojković, L., Djurić, T., Stanković, A., Dinčić, E., Stančić, O., Veljković, N., Alavantić, D., Živković, M., 2012. The association of V249I and T280M fractalkine receptor haplotypes with disease course of multiple sclerosis. J. Neuroimmunol. 245, 87–92. https://doi.org/10.1016/j.jneuroim.2011.12.028

Storer, M.A., Gallagher, D., Fatt, M.P., Simonetta, J. V., Kaplan, D.R., Miller, F.D., 2018. Interleukin-6 Regulates Adult Neural Stem Cell Numbers during Normal and Abnormal Post-natal Development. Stem Cell Reports 10, 1464–1480.

Stratoulias, V., Ruiz, R., Kanatani, S., Osman, A.M., Keane, L., Armengol, J.A., Rodríguez-Moreno, A., Murgoci, A.N., García-Domínguez, I., Alonso-Bellido, I., González Ibáñez, F., Picard, K., Vázquez-Cabrera, G., Posada-Pérez, M., Vernoux, N., Tejera, D., Grabert, K., Cheray, M., González-Rodríguez, P., Pérez-Villegas, E.M., Martínez-Gallego, I., Lastra-Romero, A., Brodin, D., Avila-Cariño, J., Cao, Y., Airavaara, M., Uhlén, P., Heneka, M.T., Tremblay, M.È., Blomgren, K., Venero, J.L., Joseph, B., 2023. ARG1-expressing microglia show a distinct molecular signature and modulate postnatal development and function of the mouse brain. Nat. Neurosci. 26. https://doi.org/10.1038/s41593-023-01326-3

Stuart, M.J., Singhal, G., Baune, B.T., 2015. Systematic review of the neurobiological relevance of chemokines to psychiatric disorders. Front. Cell. Neurosci. 9, 1–15. https://doi.org/10.3389/fncel.2015.00357

Su Akdemir, E., Yu-Szu Huang, A., Deneen, B., 2020. Astrocytogenesis: where, when, and how. F1000Research 9, 1–14.

Sun, G.J., Zhou, Y., Stadel, R.P., Moss, J., Yong, J.H.A., Ito, S., Kawasaki, N.K., Phan, A.T., Oh, J.H., Modak, N., Reed, R.R., Toni, N., Song, H., Ming, G.L., 2015. Tangential migration of neuronal precursors of glutamatergic neurons in the adult mammalian brain. Proc. Natl. Acad. Sci. U. S. A. 112, 9484–9489. https://doi.org/10.1073/pnas.1508545112

Suvannavejh, G.C., Lee, H.O., Padilla, J., Dal Canto, M.C., Barrett, T.A., Miller, S.D., 2000. Divergent roles for p55 and p75 tumor necrosis factor receptors in the pathogenesis of MOG35-55-induced experimental autoimmune encephalomyelitis. Cell. Immunol. 205, 24–33. https://doi.org/10.1006/cimm.2000.1706

Suzuki, N., Sekimoto, K., Hayashi, C., Mabuchi, Y., Nakamura, T., Akazawa, C., 2017. Differentiation of Oligodendrocyte Precursor Cells from Sox10-Venus Mice to Oligodendrocytes and Astrocytes. Sci. Rep. 7, 1–11. https://doi.org/10.1038/s41598-017-14207-0

Szabo, M., Gulya, K., 2013. Development of the microglial phenotype in culture. Neuroscience 241, 280–295. https://doi.org/10.1016/j.neuroscience.2013.03.033

Taga, T., 1997. Gp130 and the Interleukin-6 Family of Cytokines. Annu. Rev. Immunol. 15, 797–819. https://doi.org/10.1146/annurev.immunol.15.1.797

Tanaka, E.M., Ferretti, P., 2009. Considering the evolution of regeneration in the central nervous system. Nat. Rev. Neurosci. 10, 713–723. https://doi.org/10.1038/nrn2707

Tanaka, H., Ma, J., Tanaka, K.F., Takao, K., Komada, M., Tanda, K., Suzuki, A., Ishibashi, T., Baba, H., Isa, T., Shigemoto, R., Ono, K., Miyakawa, T., Ikenaka, K., 2009. Mice with altered myelin proteolipid protein gene expression display cognitive deficits accompanied by abnormal neuron-glia interactions and decreased conduction velocities. J. Neurosci. 29, 8363–8371. https://doi.org/10.1523/JNEUROSCI.3216-08.2009

Temple, S., 2001. The development of neural stem cells. Nature 414, 112–117. https://doi.org/10.1038/35102174

Tepavčević, V., Lubetzki, C., 2022. Oligodendrocyte progenitor cell recruitment and remyelination in multiple sclerosis: the more, the merrier? Brain 145, 4178–4192. https://doi.org/10.1093/brain/awac307

Tham, T.N., Lazarini, F., Franceschini, I.A., Lachapelle, F., Amara, A., Dubois-Dalcq, M., 2001. Developmental pattern of expression of the alpha chemokine stromal cell-derived factor 1 in the rat central nervous system. Eur. J. Neurosci. 12, 845–856.

Thompson, M.K., Gilbert, W. V., 2017. mRNA length-sensing in eukaryotic translation: reconsidering the "closed loop" and its implications for translational control. Curr. Genet. 63, 613–620. https://doi.org/10.1007/s00294-016-0674-3

Timsit, S., Martinez, S., Allinquant, B., Peyron, F., Puelles, L., Zalc, B., 1995. Oligodendrocytes originate in a restricted zone of the embryonic ventral neural tube defined by DM-20 mRNA expression. J. Neurosci. 15, 1012–1024. https://doi.org/10.1523/jneurosci.15-02-01012.1995

Torres-Platas, S.G., Comeau, S., Rachalski, A., Bo, G.D., Cruceanu, C., Turecki, G., Giros, B., Mechawar, N., 2014. Morphometric characterization of microglial phenotypes in human cerebral cortex. J. Neuroinflammation 11. https://doi.org/10.1186/1742-2094-11-12

Tran, P.B., Miller, R.J., 2003. Chemokine receptors: Signposts to brain development and disease. Nat. Rev. Neurosci. 4, 444–455. https://doi.org/10.1038/nrn1116

Trapp, B.D., Nishiyama, A., Cheng, D., Macklin, W., 1997. Differentiation and death of premyelinating oligodendrocytes in developing rodent brain. J. Cell Biol. 137, 459–468. https://doi.org/10.1083/jcb.137.2.459

Trapp, B.D., Peterson, J., Ransohoff, R.M., Rudick, R., Mörk, S., Bö, L., 1998. Axonal Transection in the Lesions of Multiple Sclerosis. N. Engl. J. Med. 338, 278–285. https://doi.org/10.1056/nejm199801293380502

Tremblay, M.È., Stevens, B., Sierra, A., Wake, H., Bessis, A., Nimmerjahn, A., 2011. The role of microglia in the healthy brain. J. Neurosci. 31, 16064–16069. https://doi.org/10.1523/JNEUROSCI.4158-11.2011

Tripathi, R.B., Jackiewicz, M., McKenzie, I.A., Kougioumtzidou, E., Grist, M., Richardson, W.D., 2017. Remarkable Stability of Myelinating Oligodendrocytes in Mice. Cell Rep. 21, 316–323. https://doi.org/10.1016/j.celrep.2017.09.050

Ueno, M., Fujita, Y., Tanaka, T., Nakamura, Y., Kikuta, J., Ishii, M., Yamashita, T., 2013. Layer v cortical neurons require microglial support for survival during postnatal development. Nat. Neurosci. 16, 543–551. https://doi.org/10.1038/nn.3358

Valihrach, L., Matusova, Z., Zucha, D., Klassen, R., Benesova, S., Abaffy, P., Kubista, M., Anderova, M., 2022. Recent advances in deciphering oligodendrocyte heterogeneity with single-cell transcriptomics. Front. Cell. Neurosci. 16, 1–8. https://doi.org/10.3389/fncel.2022.1025012

Vallstedt, A., Klos, J.M., Ericson, J., 2005. Multiple dorsoventral origins of ols generation in the spinal cord. Neuron 45, 55–67.

Venkatesh, H.S., Johung, T.B., Caretti, V., Noll, A., Tang, Y., Nagaraja, S., Gibson, E.M., Mount, C.W., Polepalli, J., Mitra, S.S., Woo, P.J., Malenka, R.C., Vogel, H., Bredel, M., Mallick, P., Monje, M., 2015. Neuronal activity promotes glioma growth through neuroligin-3 secretion. Cell 161, 803–816. https://doi.org/10.1016/j.cell.2015.04.012

Vercellino, M., Plano, F., Votta, B., Mutani, R., Giordana, M.T., Cavalla, P., 2005. Grey matter pathology in multiple sclerosis. J Neuropathol Exp Meurol 64, 1101–1107. https://doi.org/10.1007/978-88-470-2127-3_9

Verkerke, M., Hol, E.M., Middeldorp, J., 2021. Physiological and Pathological Ageing of Astrocytes in the Human Brain. Neurochem. Res. 46, 2662–2675. https://doi.org/10.1007/s11064-021-03256-7

Voronova, A., Yuzwa, S.A., Wang, B.S., Zahr, S., Syal, C., Wang, J., Kaplan, D.R., Miller, F.D., 2017. Migrating Interneurons Secrete Fractalkine to Promote Oligodendrocyte Formation in the Developing Mammalian Brain. Neuron 94, 500-516.e9. https://doi.org/10.1016/j.neuron.2017.04.018

Wake, H., Moorhouse, A.J., Jinno, S., Kohsaka, S., Nabekura, J., 2009. Resting microglia directly monitor the functional state of synapses in vivo and determine the fate of ischemic terminals. J. Neurosci. 29, 3974–3980. https://doi.org/10.1523/JNEUROSCI.4363-08.2009

Wakselman, S., Béchade, C., Roumier, A., Bernard, D., Triller, A., Bessis, A., 2008. Developmental neuronal death in hippocampus requires the microglial CD11b integrin and DAP12 immunoreceptor. J. Neurosci. 28, 8138–8143. https://doi.org/10.1523/JNEUROSCI.1006-08.2008

Walf, A.A., Frye, C.A., 2007. The use of the elevated plus maze as an assay of anxiety-related behavior in rodents. Nat. Protoc. 2, 322–328. https://doi.org/10.1038/nprot.2007.44

Walz, A., Peveri, P., Aschauer, H., Baggiolini, M., 1987. Purification and amino acid sequencing of NAF, a novel neutrophil-activating factor produced by monocytes. Biochem. Biophys. Res. Commun. 149, 755–761. https://doi.org/10.1016/0006-291X(87)90432-3

Warf, B.C., Fok-Seang, J., Miller, R.H., 1991. Evidence for the ventral origin of oligodendrocyte precursors in the rat spinal cord. J. Neurosci. 11, 2477–2488. https://doi.org/10.1523/jneurosci.11-08-02477.1991

Watson, A.E.S., de Almeida, M.M.A., Dittmann, N.L., Li, Y., Torabi, P., Footz, T., Vetere, G., Galleguillos, D., Sipione, S., Cardona, A.E., Voronova, A., 2021. Fractalkine signaling regulates oligodendroglial cell genesis from SVZ precursor cells. Stem Cell Reports 16, 1968–1984. https://doi.org/10.1016/j.stemcr.2021.06.010

Watson, A.E.S., Goodkey, K., Footz, T., Voronova, A., 2020. Regulation of CNS precursor function by neuronal chemokines. Neurosci. Lett. 715, 134533.

https://doi.org/10.1016/j.neulet.2019.134533

Williams, J.L., Holman, D.W., Klein, R.S., 2014. Chemokines in the balance: Maintenance of homeostasis and protection at CNS barriers. Front. Cell. Neurosci. 8, 1–12. https://doi.org/10.3389/fncel.2014.00154

Witter, M.P., Naber, P.A., Van Haeften, T., Machielsen, W.C.M., Rombouts, S.A.R.B., Barkhof, F., Scheltens, P., Lopes Da Silva, F.H., 2000. Cortico-hippocampal communication by way of parallel parahippocampal-subicular pathways. Hippocampus 10, 398–410. https://doi.org/10.1002/1098-1063(2000)10:4<398::AID-HIPO6>3.0.CO;2-K

Xiao, Y., Petrucco, L., Hoodless, L.J., Portugues, R., Czopka, T., 2022. Oligodendrocyte precursor cells sculpt the visual system by regulating axonal remodeling. Nat. Neurosci. 25, 280–284. https://doi.org/10.1038/s41593-022-01023-7

Xing, Y.L., Röth, P.T., Stratton, J.A.S., Chuang, B.H.A., Danne, J., Ellis, S.L., Ng, S.W., Kilpatrick, T.J., Merson, T.D., 2014. Adult neural precursor cells from the subventricular zone contribute significantly to oligodendrocyte regeneration and remyelination. J. Neurosci. 34, 14128–14146. https://doi.org/10.1523/JNEUROSCI.3491-13.2014

Yokota, Y., Ghashghaei, H.T., Han, C., Watson, H., Campbell, K.J., Anton, E.S., 2007. Radial glial dependent and independent dynamics of interneuronal migration in the developing cerebral cortex. PLoS One 2. https://doi.org/10.1371/journal.pone.0000794

Yoshimura, T., Matsushima, K., Oppenheim, J.J., Leonard, E.J., 1987. Neutrophil chemotactic factor produced by lipopolysaccharide (LPS)-stimulated human blood mononuclear leukocytes: partial characterization and separation from interleukin 1 (IL 1). J. Immunol. 139, 788–793. https://doi.org/10.4049/jimmunol.139.3.788

Yuzwa, S.A., Borrett, M.J., Innes, B.T., Voronova, A., Ketela, T., Kaplan, D.R., Bader, G.D., Miller, F.D., 2017. Developmental Emergence of Adult Neural Stem Cells as Revealed by Single-Cell Transcriptional Profiling. Cell Rep. 21, 3970–3986. https://doi.org/10.1016/j.celrep.2017.12.017

Yuzwa, S.A., Yang, G., Borrett, M.J., Clarke, G., Cancino, G.I., Zahr, S.K., Zandstra, P.W., Kaplan, D.R., Miller, F.D., 2016. Proneurogenic Ligands Defined by Modeling Developing Cortex Growth Factor Communication Networks. Neuron 91, 988–1004. https://doi.org/10.1016/j.neuron.2016.07.037

Zarghami, A., Li, Y., Claflin, S.B., van der Mei, I., Taylor, B. V., 2021. Role of environmental factors in multiple sclerosis. Expert Rev. Neurother. 21, 1389–1408. https://doi.org/10.1080/14737175.2021.1978843

Zhan, Y., Paolicelli, R.C., Sforazzini, F., Weinhard, L., Bolasco, G., Pagani, F., Vyssotski, A.L., Bifone, A., Gozzi, A., Ragozzino, D., Gross, C.T., 2014. Deficient neuron-microglia signaling results in impaired functional brain connectivity and social behavior. Nat. Neurosci. 17, 400–406. https://doi.org/10.1038/nn.3641

Zhao, X., Moore, D.L., 2018. Neural stem cells: developmental mechanisms and disease modeling. Cell Tissue Res. 371, 1–6. https://doi.org/10.1007/s00441-017-2738-1

Zhi, J.-J., Wu, S.-L., Wu, H.-Q., Ran, Q., Gao, X., Chen, J.-F., Gu, X.-M., Li, T., Wang, F., Xiao, L., Ye, J., Mei, F., 2023. Insufficient Oligodendrocyte Turnover in Optic Nerve Contributes to Age-Related Axon Loss and Visual Deficits. J. Neurosci. 43, 1859–1870. https://doi.org/10.1523/jneurosci.2130-22.2023

Zhu, Q., Zhao, X., Zheng, K., Li, H., Huang, H., Zhang, Z., Mastracci, T., Wegner, M., Chen, Y., Sussel, L., Qiu, M., 2014. Genetic evidence that Nkx2.2 and Pdgfra are major determinants of the timing of oligodendrocyte differentiation in the developing CNS. Dev. 141, 548–555. https://doi.org/10.1242/dev.095323

Zhu, T., Zhu, M., Qiu, Y., Wu, Z., Huang, N., Wan, G., Xu, J., Song, P., Wang, S., Yin, Y., Li, P., 2021. Puerarin Alleviates Vascular Cognitive Impairment in Vascular Dementia Rats. Front. Behav. Neurosci. 15, 1–15. https://doi.org/10.3389/fnbeh.2021.717008